

Hunting BFKL in semi-hard reactions at the LHC

Francesco Giovanni Celiberto^{1, 2, 3, 4,*}

¹*Dipartimento di Fisica, Università degli Studi di Pavia, I-27100 Pavia, Italy*

²*INFN, Sezione di Pavia, I-27100 Pavia, Italy*

³*European Centre for Theoretical Studies in Nuclear Physics and Related Areas (ECT*), I-38123 Villazzano, Trento, Italy*

⁴*Fondazione Bruno Kessler (FBK), I-38123 Povo, Trento, Italy*

The agreement between calculations inspired by the resummation of energy logarithms, known as BFKL approach, and experimental data in the semi-hard sector of QCD has become manifest after a wealthy series of phenomenological analyses. However, the contingency that the same data could be concurrently portrayed at the hand of fixed-order, DGLAP-based calculations, has been pointed out recently, but not yet punctually addressed. Taking advantage of the richness of configurations gained by combining the acceptances of CMS and CASTOR detectors, we give results in the full next-to-leading logarithmic approximation of cross sections, azimuthal correlations and azimuthal distributions for three distinct semi-hard processes, each of them featuring a peculiar final-state exclusiveness. Then, making use of disjoint intervals for the transverse momenta of the emitted objects, *i.e.* κ -windows, we clearly highlight how high-energy resummed and fixed-order driven predictions for semi-hard sensitive observables can be decisively discriminated in the kinematic ranges typical of current and forthcoming analyses at the LHC. The scale-optimization issue is also introduced and explored, while the uncertainty coming from the use of different PDF and FF set is deservedly handled. Finally, a brief overview of JETHAD, a numerical tool recently developed, suited for the computation of inclusive semi-hard reactions is provided.

KEYWORDS: QCD phenomenology, NLO computations

*Electronic address: francescogiovanni.celiberto@unipv.it

Contents

1. Introductory remarks	2
2. Theoretical setup	6
2.1. Cross section in the NLA BFKL	7
2.1.1. LO and NLO BFKL kernel	8
2.1.2. LO impact factors in the (n, ν) -representation	9
2.2. High-energy DGLAP	9
2.3. Strong-coupling setting	10
2.4. PDF and FF selection	10
2.5. Jet algorithm and event selection	11
3. Phenomenology	11
3.1. Integration over the final-state phase space	11
3.1.1. Symmetric CMS configuration	12
3.1.2. Asymmetric CMS configuration	12
3.1.3. CASTOR-jet configuration	12
3.2. Final-state observables	12
3.3. Prelude: Mueller–Navelet jets at 7 TeV LHC, theory versus experiment	13
3.4. Need for scale optimization	14
3.4.1. BLM scale setting and BFKL cross section	15
3.4.2. Hadron-species analysis	19
3.5. BFKL versus DGLAP	19
3.5.1. Azimuthal correlations	19
3.5.2. Azimuthal distribution	28
3.6. Numerical strategy	29
3.6.1. JETHAD: an object-based, process-independent interface	29
3.6.2. Uncertainty estimate	30
4. Closing statements	31
Acknowledgments	32
A. Forward-hadron NLO impact factor	32
B. Forward-jet NLO impact factor	34
Bibliography	35

1. INTRODUCTORY REMARKS

The search for evidence of New Physics is in the viewfinder of current and forthcoming analyses at the Large Hadron Collider (LHC). This is the best time to shore up our knowledge of strong interactions though, the high luminosity and the record energies reachable widening the horizons of kinematic sectors uninvestigated so far. A broad class of processes, called *diffractive semi-hard* reactions [1], *i.e.* where the scale hierarchy, $s \gg \{Q^2\} \gg \Lambda_{\text{QCD}}^2$ (s is the squared center-of-mass energy, $\{Q\}$ a (set of) hard scale(s) characteristic of the

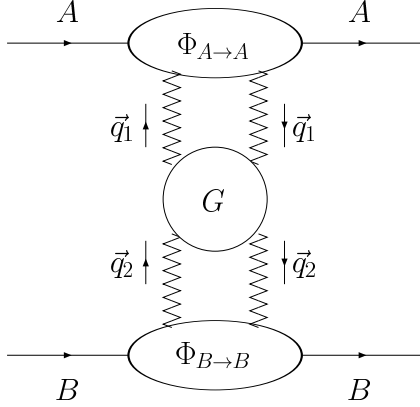


FIG. 1: Diagrammatic representation of the imaginary part of the BFKL amplitude.

process and Λ_{QCD} the QCD scale), is stringently preserved, gives us a faultless chance to test perturbative QCD (pQCD) in new and quite original ways¹.

In the kinematical regime, known as *Regge limit*, where s is much larger than the Mandelstam variable t , fixed-order calculations in pQCD based on collinear factorization fail to catch the effect of large-energy logarithmic contributions, entering the perturbative series with a power increasing with the order and thus balancing the slightness of the strong coupling, α_s . The Balitsky–Fadin–Kuraev–Lipatov (BFKL) approach [2–5] serves as the most adequate tool to perform the all-order resummation of these large-energy logarithms both in the leading approximation (LLA), namely of terms proportional to $(\alpha_s \ln s)^n$ and the next-to-leading approximation (NLA), namely of terms proportional to $\alpha_s(\alpha_s \ln s)^n$. In the BFKL formalism, the imaginary part of the amplitude of a hadronic process (thence its cross section, in the case of inclusive final states, via the *optical theorem* [6]) is elegantly expressed via a suitable convolution, pictorially depicted in Fig. 1, between two impact factors, portraying the transition from each parent particle to the final-state object(s) belonging to its *fragmentation region*, and a process-independent Green's function. The BFKL Green's function depends on energy and its evolution is regulated by an integral equation, whose kernel is known at the next-to-leading order (NLO) both for forward scattering [7, 8], *i.e.* for $t = 0$ and color singlet in the t -channel, and for any fixed (not growing with energy) t and any possible two-gluon color configuration in the t -channel [9–12]. Conversely, impact factors strictly depend on the final state and on the hard scale, but not on the energy. Thus, the number of processes which can be investigated via the BFKL resummation is shortened by the narrow list of available impact factors, just few of them being calculated at the NLO: 1) colliding-parton (quarks and gluons) impact factors [13–17], which represent the landmark for the calculation of the 2) forward-jet impact factor [18–22] and of the 3) forward charged-light hadron one [23], 4) the impact factor specific of the $(\gamma^* \rightarrow \text{LVM})$ transition [24] at leading twist, where LVM stands for light vector meson, and 5) and the one detailing the $(\gamma^* \rightarrow \gamma^*)$ subprocess [25–31].

With the aim of deepening our understanding of the high-energy regime, a notable variety of semi-hard reactions (see Ref. [32] for applications) has been proposed so far.

In particular, jet impact factors have been widely employed to describe the inclusive hadroproduction of two jets tagged with high transverse momenta and large separation in rapidity (Mueller–Navelet configuration [33]), for which several phenomenological studies have been carried out so far [34–49]. The comparison of theoretical

¹ Diffractive reactions are characterized by colorless exchanges (*i.e.* vacuum quantum numbers) in the t -channel, this leading to large, non exponentially suppressed rapidity intervals. Depending on the number and on the rapidity of final-state objects, we classify the given process as single or double diffraction (*dissociation*), central diffraction (*double-Pomeron exchange*), and so on. It is worth to note that not all semi-hard processes fall in the diffractive class. As an example, di-jet production in *ultra-peripheral* collisions of heavy ions can easily feature a semi-hard ordering and also large rapidity intervals among the recoiling hadrons and the di-jet system, but the condition of vacuum quantum numbers exchanged in the t -channel is violated. In that case, in a kinematic configuration where photons carry just a fraction of the energy of the corresponding parent nuclei, observable jet transverse momenta are much larger than Λ_{QCD} but, at the same time, much smaller than \sqrt{s} . Therefore, although this process is not diffractive, a strict semi-hard scale ordering is respected. From here on out, we will implicitly refer to diffractive scatterings when considering semi-hard production channels.

distributions on the azimuthal-angle distance between the two jets, $\varphi = \varphi_{J_1} - \varphi_{J_2} - \pi$, with experimental analyses [50] recently conducted by the Compact-Muon-Solenoid (CMS) collaboration at CERN, has addressed *projections* on azimuthal-angle observables and ratios between any two of them,

$$R_{n0} \equiv \langle \cos(n\varphi) \rangle, \quad R_{nm} \equiv \frac{\langle \cos(n\varphi) \rangle}{\langle \cos(m\varphi) \rangle}, \quad (1)$$

as very favorable observables in the search for distinct signals of the onset of BFKL dynamics.

The same impact factors, taken at the leading-order (LO) of the perturbative expansion, enter the calculation of the so-called *generalized azimuthal correlations*,

$$C_{n_1 \dots n_{N-1}} = \left\langle \prod_{k=1}^{N-1} \cos(n_k \varphi_{[k,k+1]}) \right\rangle = \int_0^{2\pi} d\varphi_1 \cdots \int_0^{2\pi} d\varphi_N \prod_{k=1}^{N-1} \cos(n_k \varphi_{[k,k+1]}) d\sigma^{N\text{-jet}} \quad (2)$$

and of their ratios, defined in the framework of the inclusive multi-jet (N -jet) hadroproduction [51–59] at LHC collision energies. In Eq. (2), $\varphi_{[k,k+1]} = \varphi_k - \varphi_{k+1} - \pi$, with φ_k the azimuthal angle of the k^{th} emitted jet, and $d\sigma^{N\text{-jet}}$ stands for the differential partonic cross section.

Then, forward-hadron impact factors allowed us for a complete NLA study of the inclusive detection of two identified hadrons (composed of light quarks and well separated in rapidity) [60–62], and of the inclusive hadron-jet hadroproduction [63–66].

The theoretical description of the $(\gamma^* \rightarrow \gamma^*)$ total cross section relies on the $(\gamma^* \rightarrow \gamma^*)$ impact factor. Although being recognized as a privileged channel for the manifestation of the BFKL dynamics, comparisons between the large number of BFKL predictions [67–73] with the only available data from the LEP2 CERN experiment were ineffective due to the relatively low center-of-mass energy and the limited accuracy of the detector. Quite recently [74, 75], the amplitude for the light-by-light elastic scattering via a single-quark loop was calculated in the so-called *double-logarithmic* approximation (DLA). This approach² accounts for the resummation of those contributions proportional to $(\alpha_s \ln s \ln s)^n$ that, at variance with gluon interactions in the BFKL ladder, appear in the quark-antiquark exchange [86–89], giving rise to a different asymptotic behavior in the power of s with respect to the single-logarithmic trend of the BFKL Pomeron (for more details, see Refs. [90, 91]).

The exclusive leptoproduction of two LVMs was investigated by encoding the $(\gamma^* \rightarrow \text{LVM})$ impact factors in the definition of the BFKL amplitude. In particular, first studies at Born level were done in Ref. [92] with longitudinally polarized virtual photons, and in Ref. [93] by accounting also for the photon transverse polarization. Then, a LLA treatment supplemented by improvements of the LO BFKL kernel was proposed in Ref. [94], while a full NLA analysis was performed in Refs. [95, 96].

LO impact factors for the production of forward heavy-quark pairs [97, 98] represent the key ingredients for phenomenological analyses with partial NLA resummation effects, by including next-to-leading logarithmic corrections to the BFKL Green's function, of the heavy-quark di-jet photo- [99, 100] and hadroproduction [98, 100], tracing the path towards a prospective NLA BFKL treatment of heavy-flavored-meson production channels. With the same accuracy, J/Ψ -jet [101], Higgs-jet [102] and heavy-light di-jet [103] correlations have been proposed, while a full LLA description, together with consistency-inspired collinear improvements [104] to the BFKL kernel, of the forward Drell-Yan dilepton production plus a backward jet has been recently conducted [105].

All the possibilities presented above fall into a distinctive family of reactions, where at least two final-state particles are always emitted with large mutual separation in rapidity, together (in the inclusive channel) with a secondary, undetected gluon system. Another interesting subclass of semi-hard processes is represented by those final states featuring the tag of a single forward object in lepton-proton or proton-proton scatterings.

² As a meaningful remark, we note that *sub-eikonal* corrections, inevitably neglected by BFKL, are instead genuinely included in DLA-based calculations. Thus, DLA resummation comes out as a powerful tool to investigate polarization effects in the high-energy/small- x regime. In this context, the Bartels-Ermolaev-Ryskin (BER) approach permits us to calculate flavor non-singlet [76] and singlet contributions [77] to the g_1 helicity structure function in the Deep Inelastic Scattering (DIS) at small- x . Another way to resum double-logarithmic powers in the definition of small- x polarized parton densities is represented by the Kovchegov-Pitonyak-Sievert (KPS) formalism [78–82], whose evolution equations are built in terms of (polarized) *Wilson lines* [83] and account for saturation effects. Originally aimed at the study of quark and gluon helicity distributions, the KPS scheme was then extended to valence-quark transversity [84] and orbital angular momentum [85] in the small- x limit.

This engaging configuration offers the chance to define an unintegrated, *transverse-momentum-dependent* gluon distribution (UGD) in the proton. This scheme is known as *high-energy factorization*³. In its standard definition, the analytic structure of the UGD is given in terms of a convolution between the BFKL gluon Green's function and a soft proton impact factor. Being a non-perturbative quantity, the UGD is not well known and several parametrizations have been developed so far (see, for instance, Refs. [108–129]).

A phenomenological UGD, incorporating NLA BFKL contributions together with a relatively simple model for the proton impact factor, was originally employed in the analysis of DIS structure functions [121] and then in the study of single bottom-quark hadroproduction [130] and of quarkonium-state (J/Ψ or Υ) photoproduction [131, 132]. The same model allowed us to improve the description of the inclusive forward Drell–Yan dilepton production at the LHC [133], previously investigated with LLA accuracy and in the dipole formalism with saturation corrections [134–139]. On the other hand, in Refs. [140–143] it was highlighted how comparisons with HERA data on helicity-dependent observables for the forward polarized ρ -meson electroproduction permit to constrain the κ -shape of the UGD (pioneering studies on the diffractive production of ρ mesons in the high-energy factorization can be found in Refs. [144–147]). Quite recently [148], the study of helicity-conserving amplitudes and cross sections was extended to the case of the single forward ϕ -meson emission, gauging the effect of the inclusion of effective strange-quark masses and calculating the ($\gamma^* \rightarrow \phi$) massive impact factor [149] in the light-cone wave-function approach [150–156].

Not enough high center-of-mass energies, leading to insufficiently large rapidity distances among the final-state detected particles, had been so far the weakness point in the search for unambiguous signals of the high-energy resummation. In addition, too inclusive observables were considered⁴. The current and forthcoming record energies, together with the superior azimuthal-angle resolution of detectors provided by the LHC, offer us a peerless opportunity to disentangle the BFKL dynamics from other resummation mechanisms.

The first analysis on azimuthal-angle decorrelations in the Mueller–Navelet channel, conducted by the CMS collaboration at $\sqrt{s} = 7$ TeV [50], gave a valid indication that the considered kinematic domain lies *in between* the sectors described by the BFKL and the Dokshitzer–Gribov–Lipatov–Altarelli–Parisi (DGLAP) [159–163] evolution, whereas clearer manifestations of high-energy signatures are expected to be more definite at increasing collision energies. Then, in a recent pioneering study [44, 45], it was pointed out how the pure adoption of partially *asymmetric* configurations for the transverse momenta of the two tagged jets allows for a clear separation between BFKL-resummed and fixed-order predictions. More in general, the use of κ -asymmetric windows has various benefits. On the one side, it allows to dampen the Born contribution, thus heightening effects of the additional undetected hard-gluon radiation. This enhances the imprints of BFKL with respect to the DGLAP ones in the cross section, suppressing at the same time possible instabilities observed in fixed-order calculations at the NLO [164, 165]. On the other side, violation of the energy-momentum conservation in the NLA is definitely quenched with respect to what happens in the LLA (see Ref. [40]).

The aim of this paper is to improve and extend the analysis previously discussed, setting a common framework for the description of inclusive semi-hard reactions and studying the rapidity-behavior of azimuthal correlations and distributions for a selection of three of them, namely: a) Mueller–Navelet jet, b) hadron-jet and c) di-hadron production at the LHC (Fig. 2). Our choice falls into a subclass of those, hadron-initiated processes, for which the theoretical description can be afforded with full NLA accuracy. Each kind of final-state object brings with itself some unique and distinctive features. On the one hand, jet emissions can be detected either in the barrel and in the endcap CMS calorimeters or in the CASTOR very-backward detector (the acronym stands for “Centauro And Strange Object Research”), allowing for a wider rapidity range. They also permit to compare different parametrizations for parton distribution functions (PDFs) and for jet algorithms. On the other hand, hadron detection is feasible only inside the barrel calorimeter of CMS, this leading to a significant

³ Some ambiguities on the definition of the high-energy factorization, also known as κ -factorization, arose in the literature over the course of time. Originally developed in Refs. [106, 107], it consists in a scheme, valid in the high-energy limit, where amplitudes (or cross sections) factorize into a convolution among off-shell matrix elements and transverse-momentum-dependent parton distribution functions. Then, in the BFKL approach, the matrix element corresponds to the forward impact factor describing the emission of the final-state particle, while the parton content, almost entirely driven by gluon evolution, is embodied by the UGD.

⁴ An astonishing example is the growth with energy of DIS structure functions at small- x , where a fair agreement with HERA data was obtained both by BFKL predictions [157] and by fixed-order based calculations. On the other side, strong statements have been made in Ref. [158], highlighting how a BFKL-like resummation, encoded in the evolution of collinear parton distributions, clearly improves the description of HERA data, in comparison with a pure fixed-order approach.

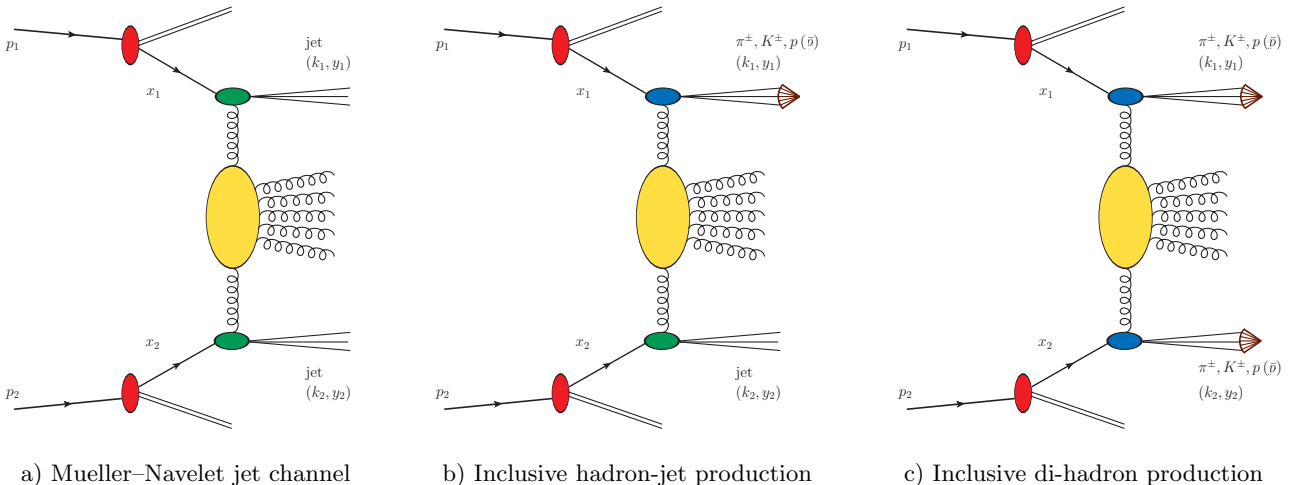


FIG. 2: Diagrammatic representation of the three semi-hard processes investigated. The BFKL gluon Green’s function is schematically represented in yellow, while the hard factor of the jet (hadron) impact factor is portrayed by the green (blue) blob. Collinear PDFs describing the incoming partons are given in red, whereas the final-state hadron FFs are pictorially expressed through the bordeaux arrowheads.

reduction in rapidity with respect to jets. It gives the possibility, however, to probe and constrain not only PDFs, but also fragmentation functions (FFs) entering the expression of the hadronic cross section. The limiting acceptances imposed by the hadron identification can be compensated by considering the concurrent emission of a forward (backward) hadron and a backward (forward) jet, as recently proposed in a first work on hadron-jet correlations [63]. Thus, in our study we take advantage of the window of opportunities offered by all the possible final-state combinations given in Fig. 2, shaped on CMS and CASTOR acceptances.

Imposing disjoint intervals for final-state emissions in the transverse-momentum plane (κ -windows) to shed light on the transition region between the two resummations, we provide indisputable evidence that the onset of BFKL dynamics can be disentangled from DGLAP-sensitive contaminations at current energies and kinematic configurations of prospective experimental studies at the LHC.

At the same time, we address the issue related to the “optimal” value for the renormalization scale (together with a supplementary analysis on single hadron-species detection) and gauge the effect of the uncertainty coming from the use of different PDF and FF parametrizations.

Finally, we present the main features of JETHAD, an object-based interface we have been developing, pursuing the goal to provide the scientific community with a common reference software for the phenomenological study of inclusive semi-hard processes.

The paper reads as follows: in Section 2 a general framework for the three considered reactions is set; in Section 3 results for observables of interest are presented and discussed; Section 4 brings our conclusions.

2. THEORETICAL SETUP

A comprehensive expression of the processes under exam reads (see panels of Fig. 2):

$$\text{proton}(p_1) + \text{proton}(p_2) \rightarrow O_1(k_1, y_1) + X + O_2(k_2, y_2), \quad (3)$$

where $O_{i=1,2} = \{\text{hadron}, \text{jet}\}$ are the final-state objects⁵, emitted with high transverse momenta, $|\vec{k}_{1,2}| \equiv \kappa_{1,2} \gg \Lambda_{\text{QCD}}$, and large rapidity separation, $Y \equiv y_1 - y_2$, while X is a secondary, undetected hadronic

⁵ In the case of hadron emission, the *sum* over charged-light hadrons, $\pi^\pm, K^\pm, p(\bar{p})$, is intended. A complementary analysis, focused on the effect of the scale choice for single hadron-species detection, is given in Section 3.4.2.

system. The protons' momenta, $p_{1,2}$ are taken as Sudakov vectors satisfying $p_{1,2}^2 = 0$ and $(p_1 p_2) = s/2$, allowing for a suitable decomposition of the momenta of the produced objects:

$$k_{1,2} = x_{1,2} p_{1,2} + \frac{\vec{k}_{1,2}^2}{x_{1,2}s} p_{2,1} + k_{1,2\perp}, \quad k_{1,2\perp}^2 = -\vec{k}_{1,2}^2 \equiv -\kappa_{1,2}^2. \quad (4)$$

In the center-of-mass system, the final-state longitudinal momentum fractions, $x_{1,2}$, are related to the respective rapidities through the expressions $y_{1,2} = \pm \frac{1}{2} \ln \frac{x_{1,2}s}{\kappa_{1,2}^2}$, so that $dy_{1,2} = \pm \frac{dx_{1,2}}{x_{1,2}}$, and $Y = y_1 - y_2 = \ln \frac{x_1 x_2 s}{\kappa_1 \kappa_2}$, here the space part of the four-vector p_1 parallel to the beam axis being taken positive.

We can present a general formula for the processes under consideration (Eq. (3)), making use of collinear factorization:

$$\frac{d\sigma}{dx_1 dx_2 d^2 \vec{k}_1 d^2 \vec{k}_2} = \sum_{\alpha, \beta = q, \bar{q}, g} \int_0^1 dx_1 \int_0^1 dx_2 f_\alpha(x_1, \mu_{F1}) f_\beta(x_2, \mu_{F2}) \frac{d\hat{\sigma}_{\alpha, \beta}(\hat{s}, \mu_{F1,2})}{dx_1 dx_2 d^2 \vec{k}_1 d^2 \vec{k}_2}, \quad (5)$$

where the (α, β) indices run over the parton types (quarks $q = u, d, s, c, b$; antiquarks $\bar{q} = \bar{u}, \bar{d}, \bar{s}, \bar{c}, \bar{b}$; or gluon g), $f_{\alpha, \beta}(x, \mu_{F1,2})$ are the initial proton PDFs; $x_{1,2}$ stand for the longitudinal fractions of the partons involved in the hard subprocess, whereas μ_{F1} (μ_{F2}) is the factorization scale characteristic of the fragmentation region of the upper (lower) parent proton in panels of Fig. 2; $d\hat{\sigma}_{\alpha, \beta}(\hat{s}, \mu_{F1,2})$ denotes the partonic cross section and $\hat{s} \equiv x_1 x_2 s$ is the squared center-of-mass energy of the partonic collision.

2.1. Cross section in the NLA BFKL

We can decompose the cross section (see Ref. [36] for further details) into a suitable Fourier expansion of the azimuthal coefficients, \mathcal{C}_n , getting so:

$$\frac{d\sigma}{dy_1 dy_2 d\kappa_1 d\kappa_2 d\varphi_1 d\varphi_2} = \frac{1}{(2\pi)^2} \left[\mathcal{C}_0 + 2 \sum_{n=1}^{\infty} \cos(n\varphi) \mathcal{C}_n \right], \quad (6)$$

where $\varphi \equiv \varphi_1 - \varphi_2 - \pi$, with $\varphi_{1,2}$ the azimuthal angles of the tagged objects, $O_{1,2}$, and the Jacobian for the change of variables has been taken into account. The zeroth coefficient, $\mathcal{C}_{n=0}$, gives the φ -averaged contribution to the cross section, while the other ones, $\mathcal{C}_{n \neq 0}$, are simply called *azimuthal-correlation* coefficients. It is known that various expressions for \mathcal{C}_n , equivalent in the NLA BFKL approximation, exist (for an extensive study of them and of their peculiarities, see Ref. [41]). For the purposes of the analysis proposed in this work, it is sufficient to consider just one representation, the so-called *exponentiated* one, where the following global formula for the $\mathcal{C}_n \equiv \mathcal{C}_n^{\text{NLA}}$ coefficients holds with NLA BFKL accuracy:

$$\begin{aligned} \mathcal{C}_n^{\text{NLA}} &\equiv \int_0^{2\pi} d\varphi_1 \int_0^{2\pi} d\varphi_2 \cos(n\varphi) \frac{d\sigma}{dy_1 dy_2 d\kappa_1 d\kappa_2 d\varphi_1 d\varphi_2} \\ &= \frac{x_1 x_2}{\kappa_1 \kappa_2} \int_{-\infty}^{+\infty} d\nu e^{\bar{\alpha}_s(\mu_R) \{ \chi(n, \nu) + \bar{\alpha}_s(\mu_R) [\bar{\chi}(n, \nu) + \beta_0/(8N_c) \chi(n, \nu) [-\chi(n, \nu) + 10/3 + 4 \ln(\mu_R/\sqrt{\kappa_1 \kappa_2})]] \}} \\ &\quad \times \alpha_s^2(\mu_R) c_1(n, \nu, \kappa_1, x_1) [c_2(n, \nu, \kappa_2, x_2)]^* \\ &\quad \times \left\{ 1 + \alpha_s(\mu_R) \left[\frac{\hat{c}_1(n, \nu, \kappa_1, x_1)}{c_1(n, \nu, \kappa_1, x_1)} + \left[\frac{\hat{c}_2(n, \nu, \kappa_2, x_2)}{c_2(n, \nu, \kappa_2, x_2)} \right]^* + \bar{\alpha}_s(\mu_R) Y \frac{\beta_0}{4\pi} \chi(n, \nu) f(\nu) \right] \right\}, \end{aligned} \quad (7)$$

with n is an integer larger than one and $\bar{\alpha}_s(\mu_R) \equiv \alpha_s(\mu_R) N_c / \pi$, where N_c is the color number and β_0 the first coefficient of the QCD β -function, responsible for running-coupling effects (Eq. (19)). Details on the BFKL kernel and on the impact factors can be found in Sections 2.1.1 and 2.1.2, respectively. It is worth to remark that

the formula given in Eq. (7) is obtained in the so-called (n, ν) -representation, *i.e.* taking the projection onto the eigenfunctions of the *LO BFKL kernel* (for more details, see Refs. [95, 96]). For the sake of completeness, we give the expression for the azimuthal coefficients in the LLA BFKL approximation:

$$\mathcal{C}_n^{\text{LLA}} = \frac{x_1 x_2}{\kappa_1 \kappa_2} \int_{-\infty}^{+\infty} d\nu e^{\bar{\alpha}_s(\mu_R) \chi(n, \nu)} \alpha_s^2(\mu_R) c_1(n, \nu, \kappa_1, x_1) [c_2(n, \nu, \kappa_2, x_2)]^*. \quad (8)$$

All these formulae for the azimuthal coefficients are obtained in the $\overline{\text{MS}}$ renormalization scheme. Corresponding expressions in the MOM scheme and with scale-optimization setting will be given in Section 3.4.1.

2.1.1. LO and NLO BFKL kernel

The expression in Eq. (7) for the LO BFKL characteristic function or *LO BFKL kernel* is

$$\chi(n, \nu) = 2\psi(1) - \psi\left(\frac{n}{2} + \frac{1}{2} + i\nu\right) - \psi\left(\frac{n}{2} + \frac{1}{2} - i\nu\right), \quad (9)$$

with $\psi(z) \equiv \Gamma'(z)/\Gamma(z)$ the logarithmic derivative of the Gamma function, while $\bar{\chi}(n, \nu)$, calculated in Ref. [166] (see also Ref. [167]), stands for the *NLO correction* to the BFKL kernel, handily represented in the form:

$$\begin{aligned} \bar{\chi}(n, \nu) = & -\frac{1}{4} \left\{ \frac{\pi^2 - 4}{3} \chi(n, \nu) - 6\zeta(3) - \chi''(n, \nu) + 2\phi(n, \nu) + 2\phi(n, -\nu) \right. \\ & \left. + \frac{\pi^2 \sinh(\pi\nu)}{2\nu \cosh^2(\pi\nu)} \left[\left(3 + \left(1 + \frac{n_f}{N_c^3} \right) \frac{11 + 12\nu^2}{16(1 + \nu^2)} \right) \delta_{n0} - \left(1 + \frac{n_f}{N_c^3} \right) \frac{1 + 4\nu^2}{32(1 + \nu^2)} \delta_{n2} \right] \right\}, \end{aligned} \quad (10)$$

where n_f is the flavor number, and

$$\begin{aligned} \phi(n, \nu) = & - \int_0^1 dx \frac{x^{-1/2+i\nu+n/2}}{1+x} \left\{ \frac{1}{2} \left(\psi'\left(\frac{n+1}{2}\right) - \zeta(2) \right) + \text{Li}_2(x) + \text{Li}_2(-x) \right. \\ & \left. + \ln x \left[\psi(n+1) - \psi(1) + \ln(1+x) + \sum_{k=1}^{\infty} \frac{(-x)^k}{k+n} \right] + \sum_{k=1}^{\infty} \frac{x^k}{(k+n)^2} [1 - (-1)^k] \right\} \\ = & \sum_{k=0}^{\infty} \frac{(-1)^{k+1}}{k + (n+1)/2 + i\nu} \left\{ \psi'(k+n+1) - \psi'(k+1) \right. \\ & \left. + (-1)^{k+1} [\beta_\psi(k+n+1) + \beta_\psi(k+1)] - \frac{\psi(k+n+1) - \psi(k+1)}{k + (n+1)/2 + i\nu} \right\}, \end{aligned} \quad (11)$$

$$\beta_\psi(z) = \frac{1}{4} \left[\psi'\left(\frac{z+1}{2}\right) - \psi'\left(\frac{z}{2}\right) \right], \quad (12)$$

$$\text{Li}_2(z) \equiv \int_0^z du \frac{\ln(1-u)}{-u}. \quad (13)$$

2.1.2. LO impact factors in the (n, ν) -representation

Two kinds of LO impact factors, generically indicated in Eq. (7) as $c_i(n, \nu, \kappa_i, x_i) \equiv \{c^{(H)}(n, \nu), c^{(J)}(n, \nu)\}$, where the labels (H) and (J) refer to the jet and the hadron case, respectively, will be considered.

The LO forward-hadron impact factor, $c^{(H)}(n, \nu)$, consists in the convolution over the parton longitudinal fraction x between the quark/antiquark/gluon PDFs and the FFs portraying the detected hadron:

$$c^{(H)}(n, \nu, \kappa_H, x_H) = 2\sqrt{\frac{C_F}{C_A}}(\kappa_H^2)^{i\nu-1/2} \int_{x_H}^1 \frac{dx}{x} \left(\frac{x}{x_H}\right)^{2i\nu-1} \times \left[\frac{C_A}{C_F} f_g(x) D_g^h \left(\frac{x_H}{x}\right) + \sum_{\alpha=q,\bar{q}} f_\alpha(x) D_\alpha^h \left(\frac{x_H}{x}\right) \right], \quad (14)$$

with $C_F = (N_c^2 - 1)/(2N_c)$ and $C_A \equiv N_c$ the Casimir factors connected to gluon emission from a quark and from a gluon, respectively. Correspondingly, $c^{(J)}(n, \nu)$ is the LO forward-jet impact factor in the (n, ν) -representation:

$$c^{(J)}(n, \nu, \kappa_J, x_J) = 2\sqrt{\frac{C_F}{C_A}}(\kappa_J^2)^{i\nu-1/2} \left(\frac{C_A}{C_F} f_g(x_J) + \sum_{\alpha=q,\bar{q}} f_\alpha(x_J) \right), \quad (15)$$

and the $f(\nu)$ function in the last term of Eq. (7) reads

$$f(\nu) = \frac{i}{2} \left[\frac{d}{d\nu} \ln \left(\frac{c_1(n, \nu)}{[c_2(n, \nu)]^*} \right) + \ln (\kappa_1^2 \kappa_2^2) \right], \quad (16)$$

after fixing the final state, *i.e.* having selected one of the processes in Fig. 2. The remaining objects are NLO corrections to impact factors, $\hat{c}_i(n, \nu, \kappa_i, x_i) \equiv \{\hat{c}^{(H)}(n, \nu), \hat{c}^{(J)}(n, \nu)\}$, their expressions being given in Appendix A (hadron) and in Appendix B (jet).

2.2. High-energy DGLAP

With the aim of providing a systematic comparison between BFKL-inspired predictions and fixed-order calculations, we derive a DGLAP-like general formula, valid for all the considered processes (Fig. 2), where the $\mathcal{C}_n^{\text{DGLAP}}$ azimuthal coefficients are introduced as truncation to the $\mathcal{O}(\alpha_s^3)$ order of the corresponding NLA BFKL ones, $\mathcal{C}_n^{\text{NLA}}$, up to the inclusion of terms beyond the LO accuracy. This allows us to catch the leading-power asymptotic features of a genuine NLO DGLAP description, neglecting at the same time those factors which are quenched by inverse powers of the energy of the partonic subprocess. Although being an alternative (and approximated) way to the standard, fixed-order DGLAP analysis, such procedure results to be adequate in the region of high-rapidity distance, Y , investigated in this work, as well as easy and flexible to implement.

Starting from Eq. (7), one gets the DGLAP limit by expanding the exponentiated BFKL kernel up to the first order in α_s , and keeping impact factors at NLO. Our DGLAP master formula reads

$$\begin{aligned} \mathcal{C}_n^{\text{DGLAP}} &\equiv \frac{x_1 x_2}{\kappa_1 \kappa_2} \int_{-\infty}^{+\infty} d\nu \alpha_s^2(\mu_R) c_1(n, \nu, \kappa_1, x_1) [c_2(n, \nu, \kappa_2, x_2)]^* \\ &\times \left\{ 1 + \alpha_s(\mu_R) \left[Y \frac{C_A}{\pi} \chi(n, \nu) + \frac{\hat{c}_1(n, \nu, \kappa_1, x_1)}{c_1(n, \nu, \kappa_1, x_1)} + \left[\frac{\hat{c}_2(n, \nu, \kappa_2, x_2)}{c_2(n, \nu, \kappa_2, x_2)} \right]^* \right] \right\}, \end{aligned} \quad (17)$$

where the BFKL exponentiated kernel has been replaced by its expansion up to terms proportional to $\alpha_s(\mu_R)$.

We stress that, although the ν -integral in Eq. (17) leads to distributions in the transverse-momentum space rather than ordinary functions, final expressions for the DGLAP azimuthal coefficients become regular when integrated over the final-state phase space, as in Eq. (22). This allows us to safely calculate them via a multidimensional strategy, where ν and phase-space integration are simultaneously performed (for more details, see Section 3.6).

2.3. Strong-coupling setting

We use a two-loop running-coupling setup with $\alpha_s(M_Z) = 0.11707$ and five quark flavors, n_f , active. Its expression in the $\overline{\text{MS}}$ scheme reads:

$$\alpha_s(\mu_R) \equiv \alpha_s^{(\overline{\text{MS}})}(\mu_R) = \frac{\pi}{\beta_0 \lambda(\mu_R)} \left(4 - \frac{\beta_1}{\beta_0^2} \frac{\ln \lambda(\mu_R)}{\lambda(\mu_R)} \right), \quad (18)$$

where

$$\lambda(\mu_R) = 2 \ln \frac{\mu_R}{\Lambda_{\text{QCD}}} , \quad \beta_0 = 11 - \frac{2}{3} n_f , \quad \beta_1 = 102 - \frac{38}{3} n_f . \quad (19)$$

It is possible to obtain the corresponding expression for the strong coupling in the MOM scheme, whose definition is related to the 3-gluon vertex (an essential ingredient in the BFKL framework), by performing the following finite renormalization:

$$\alpha_s^{(\overline{\text{MS}})} = \alpha_s^{(\text{MOM})} \left(1 + \frac{T^\beta + T^{\text{conf}}}{\pi} \alpha_s^{(\text{MOM})} \right) , \quad (20)$$

with

$$T^\beta = -\frac{\beta_0}{2} \left(1 + \frac{2}{3} I \right) ,$$

$$T^{\text{conf}} = \frac{C_A}{8} \left[\frac{17}{2} I + \frac{3}{2} (I-1) \xi + \left(1 - \frac{1}{3} I \right) \xi^2 - \frac{1}{6} \xi^3 \right] , \quad (21)$$

where $I = -2 \int_0^1 du \frac{\ln(u)}{u^2 - u + 1} \simeq 2.3439$ and ξ is a gauge parameter, fixed at zero in the following.

The infrared improvement of the running coupling via well-known procedures, as the Webber parametrization [168], here is not needed, since energy scales are always in the perturbative region. They are strictly related to transverse-momentum ranges (see Section 3.2), their large values protecting us from a region where the *diffusion pattern* [169] (see also Refs. [170, 171]) becomes relevant.

2.4. PDF and FF selection

Potential sources of uncertainty are expected to arise from the choice of particular PDF and FF sets, rather than other ones. While preliminary tests done using the three most popular NLO PDF parametrizations (MMHT 2014 [172], CT 2014 [173] and NNPDF3.0 [174]) have shown no significant discrepancy in the kinematic regions of our interest, this does not hold anymore for FFs, where the selection of distinct sets leads to non-negligible effects. This feature was pointed out in a first phenomenological analysis [60] on φ -averaged cross sections for the inclusive di-hadron production, with the hadrons' ranges tailored on the acceptances of the CMS detector, and then confirmed also for azimuthal correlations (*i.e.* ratios of phase-space integrated azimuthal coefficients, as explained in Section 3.2) in the case of inclusive hadron-jet emission [63], when the jet is tagged inside the CASTOR backward detector. The simplest strategy to address this issue is in line with the recommendations suggested by the PDF4LHC community [176] for Standard Model phenomenology, and consists in selecting an individual PDF set and taking its convolution with a given FF. This method will be stringently applied in our analysis on the scale optimization (Section 3.4) and on our results for azimuthal distributions (Section 3.5.2), where we will give predictions for the MMHT 2014 [172] NLO PDF together with the NNFF1.0 [175] NLO FF. Conversely, we will adopt a more extensive solution when gauging the effect discussed above for the comparison of our BFKL results with fixed-order DGLAP calculations, which is actually the main outcome of this paper (Section 3.5.1). On the one hand, as for the PDFs, we will choose the NLO PDF4LHC15_100 parametrization [176], which represents a statistical combination of the three sets mentioned before [172–174]. On the other hand, we will build our own combination for the FFs by merging predictions obtained with the four following NLO parametrizations: AKK 2008 [177], DSS 2007 [178, 179], HKNS 2007 [180] and NNFF1.0 [175]. It is worth to

remark that our prescription refers to the average of final results for our observables, while no new FF set has been created. A higher-level analysis, based on the so-called *bootstrap replica method* (see Ref. [181] for a combined study including fit procedures inspired by neural-network techniques), is employed just in one case, namely our *theory-versus-experiment* study for azimuthal correlations in the Mueller–Navelet channel at $\sqrt{s} = 7$ TeV (Section 3.3). We make use of a sample of 100 replicas of the central value of the PDF4LHC15_100 set. This collection of replicas is obtained by randomly altering the central value with a Gaussian background featuring the original variance. The extensive application of the replica method to all the considered observables goes beyond our scope and is left to further investigations which will include all the systematic effects.

2.5. Jet algorithm and event selection

Several types of reconstruction algorithms can be implemented in the definition of the (NLO) jet impact factor, although the choice of a particular one instead of the others seems not to produce a crucial effect on semi-hard typical observables, as pointed out in Section 2.3 of Ref [37]. The most popular jet-reconstruction functions essentially belong to two distinct classes (for further details, see *e.g.*, Refs. [182, 183] and Refs. therein): *cone-type* and *sequential-clustering* algorithms (the well known (*anti-*) κ_\perp kind [184, 185] falls into this last family). We will adopt a simpler version, *infrared-safe* up to NLO perturbative accuracy and suited to numerical calculations, given in Ref. [21] in terms of the so-called “small-cone” approximation (SCA) [186, 187], *i.e.* for small-jet cone aperture in the rapidity-azimuthal angle plane (see Ref. [22] for a detailed study on different jet algorithms and their small-cone, approximated versions).

A potential issue, highlighted first [41] in the case of Mueller–Navelet jet production (left panel of Fig. 2) but present in any process featuring jet emission in the final state, is related with the experimental event selection in a situation when more than one jet is tagged in a single event. As an example, let us consider events with three objects in the final state, two of them being jets emitted in the forward region (with large positive rapidities, $y_{J,1} > y_{J,2} > 0$), and the third one being a backward object (hadron or jet, in our analyses), with negative rapidity, $y_O < 0$. Traditionally, as in the current CMS analysis, such event would be classified as a unique one, with a single forward jet plus another, backward particle detected, the largest rapidity interval being, $Y = y_{J,1} - y_O$. This selection criterion is suited to experimental analyses, but it does not match the theoretical definition in NLA BFKL calculations. Examining the derivation of the NLO jet impact factor [18, 20], it follows that our calculation describes an *inclusive*, forward-in-rapidity jet production in the fragmentation region of the parent hadron, whereas possible additional parton radiation is attributed to the inclusive hadron system, X (Eq. (3)). The issue may be clarified either from the experimental side, by adapting the jet-selection paradigm, or from the theoretical side, by improving the NLO calculation, as proposed in Ref. [188].

3. PHENOMENOLOGY

3.1. Integration over the final-state phase space

Starting from Eqs. (7) and (17), we consider the *integrated* coefficients over the phase space for the two emitted objects, $O_{1,2}(\kappa_{1,2}, y_{1,2})$, while their rapidity distance, $Y = y_1 - y_2$, is kept fixed:

$$C_n^{[\text{resum}]}(s, Y) = \int_{\kappa_1^{\min}}^{\kappa_1^{\max}} d\kappa_1 \int_{\kappa_2^{\min}}^{\kappa_2^{\max}} d\kappa_2 \int_{y_1^{\min}}^{y_1^{\max}} dy_1 \int_{y_2^{\min}}^{y_2^{\max}} dy_2 \delta(Y - (y_1 - y_2)) \mathcal{C}_n^{[\text{resum}]}, \quad (22)$$

where the superscript [resum] stands indistinctly for LLA, NLA or DGLAP. This allows us to impose and study different ranges in transverse momenta and rapidities, based on realistic kinematic configurations used in experimental analyses at the LHC. Let us introduce the following representation for final-state particles, which will facilitate us to distinguish, process by process, the considered ranges:

- a) Mueller–Navelet: $O_1(\kappa_1, y_1) + X + O_2(\kappa_2, y_2) \equiv \text{jet}(\kappa_{J,1}, y_{J,1}) + X + \text{jet}(\kappa_{J,2}, y_{J,2}) ;$
- b) hadron-jet: $O_1(\kappa_1, y_1) + X + O_2(\kappa_2, y_2) \equiv \text{hadron}(\kappa_H, y_H) + X + \text{jet}(\kappa_J, y_J) ;$
- c) di-hadron: $O_1(\kappa_1, y_1) + X + O_2(\kappa_2, y_2) \equiv \text{hadron}(\kappa_{H,1}, y_{H,1}) + X + \text{hadron}(\kappa_{H,2}, y_{H,2}) .$

Here labels a), b) and c) refer to the respective panels in Fig. 2, while a slight, process-suitable change of notation in the final-state variables has been made. For all the considered reactions, the maximum values for the transverse momenta are determined by general requirements, based on kinematics. On the one side, in the case of CMS (di-)hadron emission, κ_H^{\max} is constrained by the lower cutoff of the used FF set and is always fixed at $\kappa_{H,\text{CMS}}^{\max} \simeq 21.5$ GeV. On the other side, when (at least) a jet is tagged inside CMS or CASTOR, the value for the upper cutoff, κ_J^{\max} , follows from the given bounds in rapidity, at fixed center-of-mass energy, \sqrt{s} and will be individually discussed for each kinematic configuration introduced below. The rapidity interval, Y , is everywhere taken positive: $0 < Y \leq y_1^{\max} - y_2^{\min}$.

3.1.1. Symmetric CMS configuration

The first kinematic configuration we take into account, namely the ***symmetric CMS*** choice, prescribes that both final-state particles, $O_{1,2}$, are tagged in the CMS detector, their transverse momenta and rapidities confined in symmetric ranges, characteristic of the experimental studies recently conducted [50]:

- a) Mueller–Navelet: $35 \text{ GeV} < \kappa_{J,1,2} < \kappa_J^{\max}$ and $|y_{J,1,2}| < 4.7$, $Y < 9.4$.

We will give results in this configuration just for Mueller–Navelet jet production (left panel of Fig. 2), comparing LLA and NLA BFKL predictions with experimental data at $\sqrt{s} = 7$ TeV and for $\kappa_J^{\max} \equiv \kappa_{J,\text{(CMS)}}^{\max} = 60$ GeV.

3.1.2. Asymmetric CMS configuration

The second range we include in our study is the ***asymmetric CMS*** configuration and consists in requiring the emitted objects, $O_{1,2}$, to be detected in disjoint intervals for the transverse momenta, *i.e.* κ -windows. In the hadron-jet production case (central panel in Fig. 2), the final-state asymmetry is further enriched by the distinct rapidity ranges which characterize the hadron and the jet, respectively. So one has:

- a) Mueller–Navelet: $35 \text{ GeV} < \kappa_{J,1} < 45 \text{ GeV} < \kappa_{J,2} < \kappa_J^{\max}$ and $|y_{J,1,2}| < 4.7$, $Y < 9.4$;
- b) hadron-jet: $5 \text{ GeV} < \kappa_H < \kappa_H^{\max} < 35 \text{ GeV} < \kappa_J < \kappa_J^{\max}$ and $|y_H| < 2.4$, $|y_J| < 4.7$, $Y < 7.1$;
- c) di-hadron: $5 \text{ GeV} < \kappa_{H,1} < 10 \text{ GeV} < \kappa_{H,2} < \kappa_H^{\max}$ and $|y_{H,1,2}| < 2.4$, $Y < 4.8$.

We will perform our analysis for $\sqrt{s} = 13$ TeV, $\kappa_H^{\max} \equiv \kappa_{H,\text{CMS}}^{\max} \simeq 21.5$ GeV and $\kappa_J^{\max} \equiv \kappa_{J,\text{CMS}}^{\max} = 60$ GeV. This last value has been kept equal with respect to the symmetric case at $\sqrt{s} = 7$ TeV (Section 3.1.1).

3.1.3. CASTOR-jet configuration

This peculiar ***CASTOR-jet*** range selection [189], valid only for Muller–Navelet and hadron-jet production (first two panels of Fig. 2), introduces the possibility to tag a backward jet inside the CASTOR (CST) calorimeter, together with another object (jet or hadron) detected by CMS. This peculiar configuration allows one to reach the largest values for the rapidity separation, Y , taking advantage of the very backward rapidity range provided by CASTOR:

- a) Mueller–Navelet: $10 \text{ GeV} < \kappa_{J,2} < \kappa_{J,\text{CST}}^{\max} < 20 \text{ GeV} < \kappa_{J,1} < \kappa_{J,\text{CMS}}^{\max}$ and $|y_{J,1}| < 4.7$, $-6.6 < y_{J,2} < -5.2$, $Y < 11.3$;
- b) hadron-jet: $5 \text{ GeV} < \kappa_H < 10 \text{ GeV} < \kappa_J < \kappa_{J,\text{CST}}^{\max}$ and $|y_H| < 2.4$, $-6.6 < y_J < -5.2$, $Y < 9$.

Results will be shown for $\sqrt{s} = 13$ TeV, $\kappa_{J,\text{CST}}^{\max} \simeq 17.68$ GeV and $\kappa_{J,\text{CMS}}^{\max} = 60$ GeV.

3.2. Final-state observables

The phenomenological observables of our interest fall into the following three classes:

1. φ -averaged cross section, C_0 , and the ratio, $R_0^{\text{NLA/LLA}}$, between C_0 calculated in the full NLA BFKL accuracy and its counterpart in the LLA BFKL approximation;
2. Azimuthal-correlation moments (or simply *azimuthal correlations*), $R_{nm} \equiv C_n/C_m$, with the ratios of the form R_{n0} among them having the immediate physical interpretation of averaged values of the cosine of n -multiples of φ , $\langle \cos(n\varphi) \rangle$;
3. *Azimuthal distribution* of the two emitted objects, which actually represents one of the most directly accessible observables in experimental analyses:

$$\frac{1}{\sigma} \frac{d\sigma}{d\varphi} = \frac{1}{2\pi} \left\{ 1 + 2 \sum_{n=1}^{\infty} \cos(n\varphi) \langle \cos(n\varphi) \rangle \right\} \equiv \frac{1}{2\pi} \left\{ 1 + 2 \sum_{n=1}^{\infty} \cos(n\varphi) R_{n0} \right\}. \quad (24)$$

On the one side, azimuthal distributions are very favorable observables to be compared with experimental analyses, even more than the azimuthal-correlation moments. This stems from the fact that, since measured distributions cannot cover the whole (2π) range of azimuthal angle due to detector limitations, observables differential on φ permit us to dampen the descending accuracy loss. On the other side, numeric calculations of Eq. (24) are not easy to perform, due to the large number of azimuthal coefficients required and due to instabilities in the ν -integration that progressively increase with n . This requires sizeable effort from the numerical side (see Section 3.6.1).

3.3. Prelude: Mueller–Navelet jets at 7 TeV LHC, theory versus experiment

In this Section predictions for different azimuthal correlations, $R_{nm} \equiv C_n/C_m$, are given for the Mueller–Navelet jet production channel (left panel of Fig. 2) in the *symmetric CMS* configuration (see Section 3.1.1) and compared with recent CMS data at $\sqrt{s} = 7$ TeV [50]. We actually improve the analysis conducted in Ref. [41], by implementing the “exact”, numeric BLM scale-optimization method instead of using the two approximated, analytic ones (we are advisedly anticipating details on the scale-optimization issue, discussed in detail in Section 3.4.1). At variance with the previous work [41], where the MSTW 2008 [190] NLO PDF set (precursor of the MMHT 2014 one [172]) was employed, we adopt the NLO PDF4LHC15_100 parametrization [176]

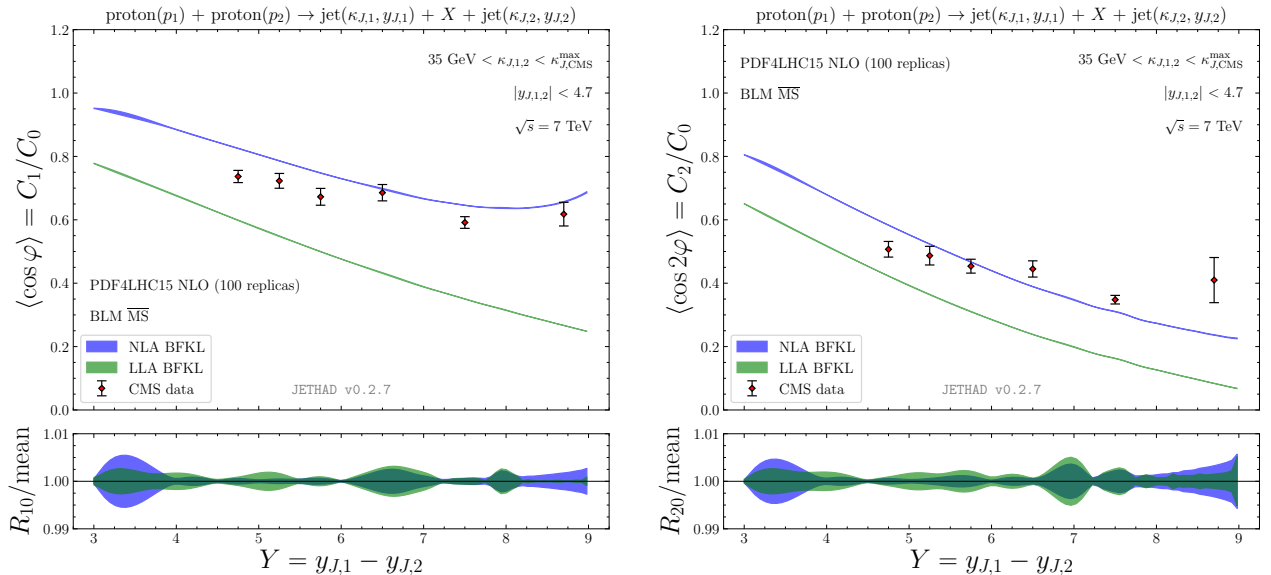


FIG. 3: Y -dependence of $R_{10} \equiv C_1/C_0$ and $R_{20} \equiv C_2/C_0$ of the Mueller–Navelet jet production (left panel of Fig. 2) for $\mu_{F1,2} = \mu_R = \mu_R^{\text{BLM}}$ and $\sqrt{s} = 7$ TeV (*symmetric CMS* configuration). Calculations are done in the $\overline{\text{MS}}$ renormalization scheme. Ancillary plots below primary panels show the reduced azimuthal correlations, *i.e.* the envelope of R_{nm} replicas’ results divided by their mean value.

and we estimate the uncertainty of our predictions by calculating the standard deviation at the hand of the replica method (see Section 2.4 for further details). As in Ref. [41], final calculations are done in the $\overline{\text{MS}}$ renormalization scheme. We remind that it is possible to recover the analytic expression for the azimuthal coefficients, C_n , in the $\overline{\text{MS}}$ scheme from the corresponding ones, given in the MOM one (Eq. (28)), by making the substitutions (note that the value of the renormalization scale is left unchanged)

$$T^{\text{conf}} \rightarrow -T^\beta, \quad \alpha_s^{(\text{MOM})} \rightarrow \alpha_s^{(\overline{\text{MS}})},$$

with T^{conf} , T^β , $\alpha_s^{(\overline{\text{MS}})}$ and $\alpha_s^{(\text{MOM})}$ given in Section 2.3. The two factorization scales and the renormalization one are set equal to the one provided, as outcome for each value of Y , by the BLM procedure: $\mu_{F1,2} = \mu_R = \mu_R^{\text{BLM}}$.

Results for R_{10} and R_{20} , reported in Fig. 3, unambiguously highlight that the pure LLA calculations overestimate by far the decorrelation between the two tagged jets, whereas the agreement with experimental data definitely improves, when NLA BFKL corrections, together with the BLM prescription, are included. For this process and for the considered transverse-momentum kinematics, the uncertainty coming from the numerical multidimensional integration over the final-state phase space is very small. Therefore, error bands strictly refer to the uncertainty hailing from the use of different PDF members inside the PDF4LHC15_100 collection of 100 replicas. As expected, its effect is very small when ratios of azimuthal coefficients are taken. Ancillary plots below primary panels of Fig. 3 clearly indicate that the relative standard deviation of the replicas' results is smaller than 1% in all cases. Here, nodal points bring information on uncertainty oscillations inherited from the collinear-PDF parametrization.

3.4. Need for scale optimization

It is widely recognized that calculations purely based on the BFKL resummation suffer from large higher-order corrections both in the kernel of the gluon Green's function and in the non-universal impact factors. *Inter alia*, NLA BFKL contributions to the zeroth conformal spin come up with roughly the same order of the corresponding LLA predictions, but with opposite sign. The primary manifestation of this instability lies in the large uncertainties arising from the renormalization (and factorization) scale choice, which hamper any genuine attempt at high-precision calculations. All that calls for some “stabilizing” procedure of the perturbative series, which can consist in:

- (i) the inclusion of next-to-NLA terms (*a priori* unknown), such as those ones prescribed by the renormalization group, as in the all-order [39, 191–203] or in the consistency-condition [104] *collinear-improvement* procedures, or by energy-momentum conservation [204];
- (ii) the restriction of undetected-radiation activity to only allow final-state gluons separated by a minimum distance in rapidity (*rapidity-veto* approach [48, 205, 206]);
- (iii) an “optimal” choice of the values of the energy and renormalization scales, which, though arbitrary within the NLA, can have a sizeable numerical impact through subleading terms.

As for the case (iii), the most common *optimization* methods are those ones inspired by: the *principle of minimum sensitivity* (PMS) [207, 208], the *fast apparent convergence* (FAC) [209–211], and the *Brodsky–Lepage–Mackenzie method* (BLM) [212–216]. Even though the selection of one or the other optimization procedure should not consistently affect the prediction of physical observables, it produces, *de facto*, a non-negligible impact. Thus, as pointed out in Ref. [41], preference to a particular method should be assigned by grading the agreement with experimental data in a given setup and, consequently, assumed to apply also in other configurations. Predictions derived with BLM turned to be in fair agreement [38, 41] with the only kinematic configuration for which experimental analyses are to date performed, *i.e.* *symmetric CMS* cuts in the Mueller–Navelet channel (for a detailed comparison of the three listed methods, see the Discussion Section of Ref. [41]). In view of this outcome, the use of the BLM scheme was extended in time to the study of other semi-hard reactions.

In Section 3.4.1 we briefly introduce the key features of BLM, which relies on the removal of the renormalization scale ambiguity by absorbing the non-conformal β_0 -terms into the running coupling. Then, we apply it to the cases of our interest and present results for BLM optimal scale values and cross sections.

3.4.1. BLM scale setting and BFKL cross section

The *BLM-optimized* renormalization scale, μ_R^{BLM} , is the value of μ_R that makes the non-conformal, β_0 -dependent terms entering the expression of the observable of interest vanish. The inspection of the analytic structure of semi-hard observables shows that two groups of non-conformal contribution exist⁶. The first one originates from the NLA BFKL kernel, while the second one from the NLO impact-factor corrections. This makes μ_R^{BLM} non-universal, but dependent on the energy of the process.

In order to apply the BLM procedure, a finite renormalization from the $\overline{\text{MS}}$ to the physical MOM scheme needs to be executed (see Section 2.3). Then, the condition for the BLM scale setting for a given azimuthal coefficient, C_n , is determined by solving the following integral equation:

$$C_n^{(\beta)}(s, Y) = \int_{\kappa_1^{\min}}^{\kappa_1^{\max}} d\kappa_1 \int_{\kappa_2^{\min}}^{\kappa_2^{\max}} d\kappa_2 \int_{y_1^{\min}}^{y_1^{\max}} dy_1 \int_{y_2^{\min}}^{y_2^{\max}} dy_2 \delta(Y - (y_1 - y_2)) \mathcal{C}_n^{(\beta)} = 0, \quad (25)$$

where

$$\begin{aligned} \mathcal{C}_n^{(\beta)} &\propto \int_{-\infty}^{\infty} d\nu e^{Y \bar{\alpha}_s^{\text{MOM}}(\mu_R^{\text{BLM}}) \chi(n, \nu)} c_1(n, \nu, \kappa_1, x_1) [c_2(n, \nu, \kappa_2, x_2)]^* \\ &\times \left[\hat{f}(\nu) + \bar{\alpha}_s^{\text{MOM}}(\mu_R^{\text{BLM}}) Y \frac{\chi(n, \nu)}{2} \left(-\frac{\chi(n, \nu)}{2} + \hat{f}(\nu) \right) \right], \end{aligned} \quad (26)$$

with

$$\hat{f}(\nu) = f(\nu) + \frac{5}{3} + 2 \ln \frac{\mu_R^{\text{BLM}}}{\mu_N} - 2 - \frac{4}{3} I. \quad (27)$$

It is convenient to introduce the ratio of the BLM to the *natural* scale suggested by the kinematic of the process, *i.e.* $\mu_N \equiv \sqrt{\kappa_1 \kappa_2}$, so that $C_{\mu_R} \equiv \mu_R^{\text{BLM}} / \mu_N$, and hunt for those values of C_{μ_R} which solve Eq. (25).

As a last step, the value of the scale given by the procedure is plugged into expressions for the integrated coefficients, getting the following definition, valid in the NLA BFKL accuracy and in the MOM scheme:

$$\begin{aligned} C_n^{\text{NLA}} &= \int_{\kappa_1^{\min}}^{\kappa_1^{\max}} d\kappa_1 \int_{\kappa_2^{\min}}^{\kappa_2^{\max}} d\kappa_2 \int_{y_1^{\min}}^{y_1^{\max}} dy_1 \int_{y_2^{\min}}^{y_2^{\max}} dy_2 \delta(Y - (y_1 - y_2)) \\ &\times \int_{-\infty}^{+\infty} d\nu \frac{e^Y}{s} e^{Y \bar{\alpha}_s^{\text{MOM}}(\mu_R^{\text{BLM}}) [\chi(n, \nu) + \bar{\alpha}_s^{\text{MOM}}(\mu_R^{\text{BLM}}) (\bar{\chi}(n, \nu) + \frac{T^{\text{conf}}}{3} \chi(n, \nu))]} c_1(n, \nu, \kappa_1, x_1) [c_2(n, \nu, \kappa_2, x_2)]^* \\ &\times (\alpha_s^{\text{MOM}}(\mu_R^{\text{BLM}}))^2 \left\{ 1 + \alpha_s^{\text{MOM}}(\mu_R^{\text{BLM}}) \left[\frac{\bar{c}_1(n, \nu, \kappa_1, x_1)}{c_1(n, \nu, \kappa_1, x_1)} + \left[\frac{\bar{c}_2(n, \nu, \kappa_2, x_2)}{c_2(n, \nu, \kappa_2, x_2)} \right]^* + \frac{2T^{\text{conf}}}{\pi} \right] \right\}, \end{aligned} \quad (28)$$

where $\bar{c}_i(n, \nu, \kappa_i, x_i)$ are the NLO impact-factor corrections after the *subtraction* of those terms, entering their expressions, which are proportional to β_0 and can be universally expressed through the LO impact factors:

$$\bar{c}_i(n, \nu, \kappa_i, x_i) = \hat{c}_i(n, \nu, \kappa_i, x_i) - \frac{\beta_0}{4N_c} \left[i \frac{d}{d\nu} \ln c_i(n, \nu, \kappa_i, x_i) + \left(\ln \mu_R^2 + \frac{5}{3} \right) c_i(n, \nu, \kappa_i, x_i) \right]. \quad (29)$$

The analogous BLM-MOM expression for the DGLAP case in the high-energy limit reads:

$$C_n^{\text{DGLAP}} = \int_{\kappa_1^{\min}}^{\kappa_1^{\max}} d\kappa_1 \int_{\kappa_2^{\min}}^{\kappa_2^{\max}} d\kappa_2 \int_{y_1^{\min}}^{y_1^{\max}} dy_1 \int_{y_2^{\min}}^{y_2^{\max}} dy_2 \delta(Y - (y_1 - y_2))$$

⁶ We refer the reader to Ref. [43] for a complete treatment of the application of the BLM procedure to semi-hard reactions.

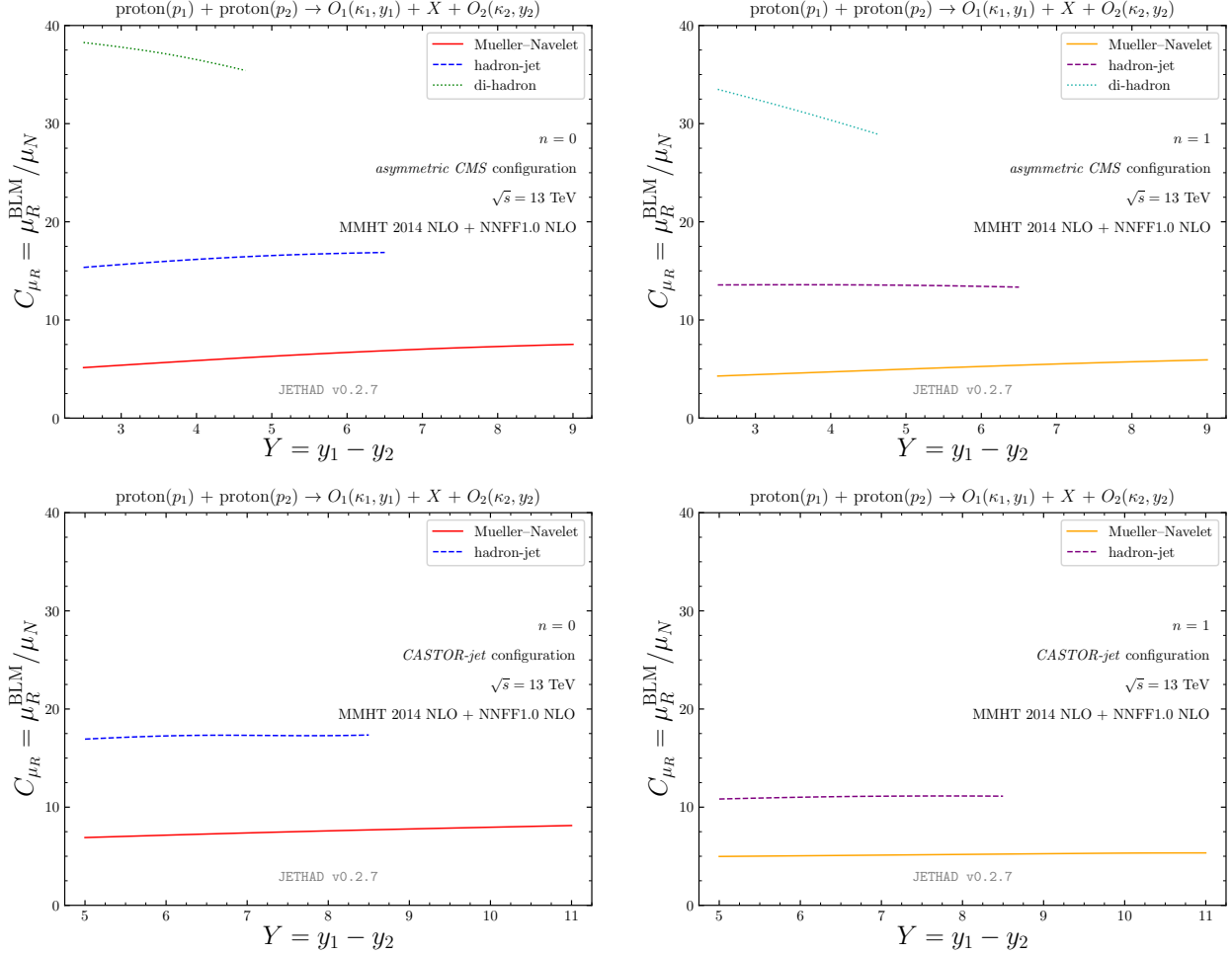


FIG. 4: BLM scales for the three considered reactions (Fig. 2) versus the final-state rapidity interval, Y , for the φ -averaged cross section C_0 (left) and the azimuthal coefficient C_1 (right). Both the factorization scales, $\mu_{F1,2}$, have been set equal to $\mu_R^{\text{BLM}} \equiv C_{\mu_R} \mu_N$. Results for $\sqrt{s} = 13$ TeV in the *asymmetric CMS* (*CASTOR-jet*) configuration are given in upper (lower) panels. Hadron emissions, when considered, are described in terms of NNFF1.0 [175] NLO FF parametrizations (see Section 2.4 for further details).

$$\begin{aligned} & \times \int_{-\infty}^{+\infty} d\nu \frac{e^Y}{s} c_1(n, \nu, \kappa_1, x_1) [c_2(n, \nu, \kappa_2, x_2)]^* (\alpha_s^{\text{MOM}}(\mu_R^{\text{BLM}}))^2 \\ & \times \left\{ 1 + \alpha_s^{\text{MOM}}(\mu_R^{\text{BLM}}) \left[Y \frac{C_A}{\pi} \chi(n, \nu) + \frac{\bar{c}_1(n, \nu, \kappa_1, x_1)}{c_1(n, \nu, \kappa_1, x_1)} + \left[\frac{\bar{c}_2(n, \nu, \kappa_2, x_2)}{c_2(n, \nu, \kappa_2, x_2)} \right]^* + \frac{2T^{\text{conf}}}{\pi} \right] \right\}. \end{aligned} \quad (30)$$

Finally, a valid formula for the azimuthal coefficients in the pure LLA BFKL accuracy can be obtained by making in Eq. (8) the substitution (note that the functional form of the strong coupling and the value of the renormalization scale are simultaneously varied)

$$\alpha_s^{(\overline{\text{MS}})}(\mu_R) \rightarrow \alpha_s^{(\text{MOM})}(\mu_R^{\text{BLM}}).$$

Eq. (25) requires a numerical solution, whose algorithm is implemented in JETHAD (see Section 3.6.1 for further details) and universally holds for any semi-hard final state. Before the advent of JETHAD, some analytic, approximate BLM methods were developed. In those cases (see Eqs. (42)-(46) of Ref. [43]), the BLM scale is treated as a function of the variable ν and is fixed in order to make vanish either the NLO impact-factor β_0 -dependent terms, the NLA BFKL kernel ones, or the whole integrand of Eq. (25).

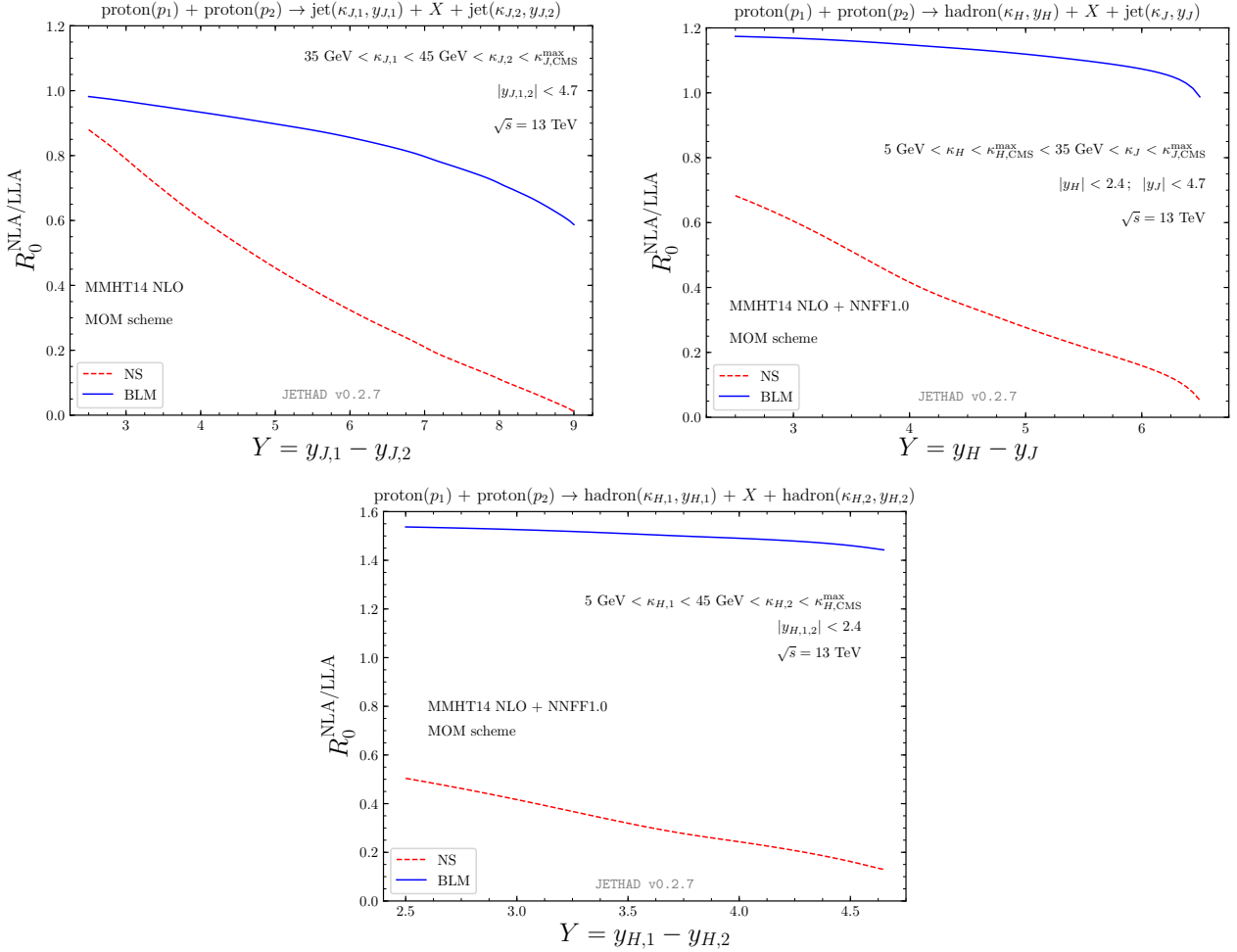


FIG. 5: Y -dependence of the $R_0^{\text{NLA/LLA}}$ ratio for the three considered reactions (Fig. 2) in the *asymmetric CMS* configuration and for $\sqrt{s} = 13$ TeV. Hadron emissions, when considered, are described in terms of `NNFF1.0` [175] NLO FF parametrizations (see Section 2.4 for further details).

In all the calculations of this work the two factorization scales, $\mu_{F1,2}$, are set equal to the renormalization scale μ_R , as assumed by most of the PDF parametrizations. All results are obtained in the MOM renormalization scheme (except for the ones presented in Section 3.3, where the $\overline{\text{MS}}$ scheme is selected).

Values of the BLM scales for C_0 and C_1 , for all the three considered production channels (Fig. 2), are presented in Fig. 4. At fixed rapidity distance, Y , the C_{μ_R} ratio definitely increases with the number of charged-light hadrons emitted in the final state, up to around $30 \div 40$ units of natural scales. This phenomenon, already observed in previous analyses on the inclusive di-hadron production [60, 62], could be controlled by the behavior of collinear FFs as functions of μ_F . More in particular, when FFs are convoluted with PDFs in our LO impact factors (Eq. (14)), the dominant contribution to PDFs in the kinematic sector of our interest is given by the gluon, and thus only the behavior of the gluon FF plays a role. Preliminary studies on FF parametrizations depicting the emissions of different hadron species, including heavy-flavored ones [217], have highlighted how the μ_F -dependence of (gluon) FFs can enhance or worsen the stability of our azimuthal coefficients. Smooth-behaved, non-decreasing gluon FF functions, characteristic of heavy-flavored bound states (see, *e.g.*, parametrizations for Λ_c baryons [218], charged D^* mesons [219–221] and b -flavored hadrons [222, 223]), have a stabilizing effect. This situation is in some aspects closer to jet emissions, where no FFs are employed. Conversely, light-flavored FF sets, typical of the study presented in this work, lead to an increased sensitivity of predictions on energy scales, as well as to a stronger discrepancy between LLA and NLA. Thus, in our case, the larger scales prescribed by the BLM method come out as a technical consequence of the stability requirement. In addition, the function

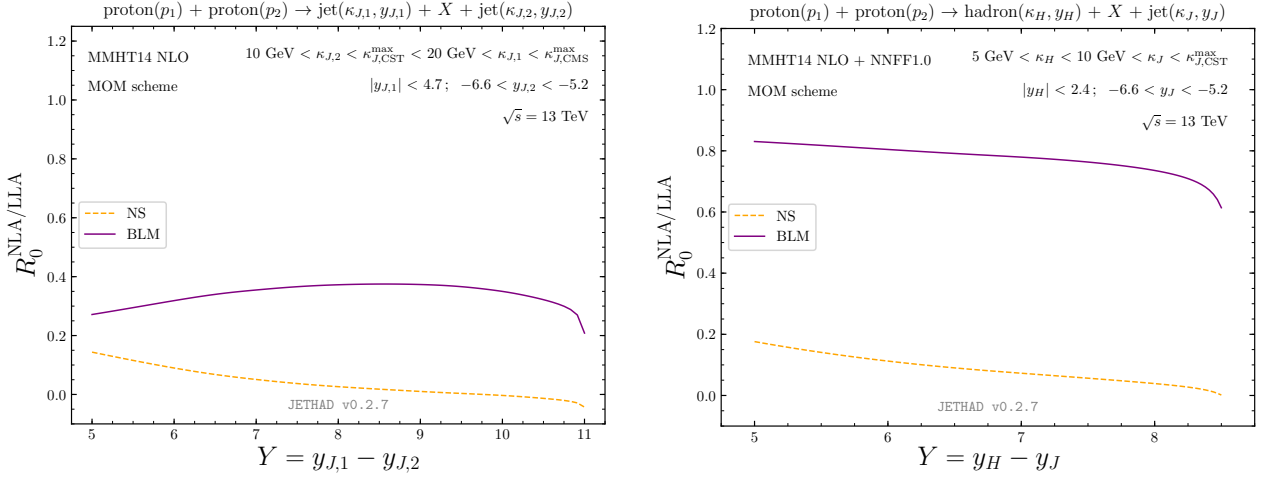


FIG. 6: Y -dependence of the $R_0^{\text{NLA/LLA}}$ ratio for the three considered reactions (Fig. 2) in the *CASTOR-jet* configuration and for $\sqrt{s} = 13$ TeV. Hadron emissions, when considered, are described in terms of NNFF1.0 [175] NLO FF parametrizations (see Section 2.4 for further details).

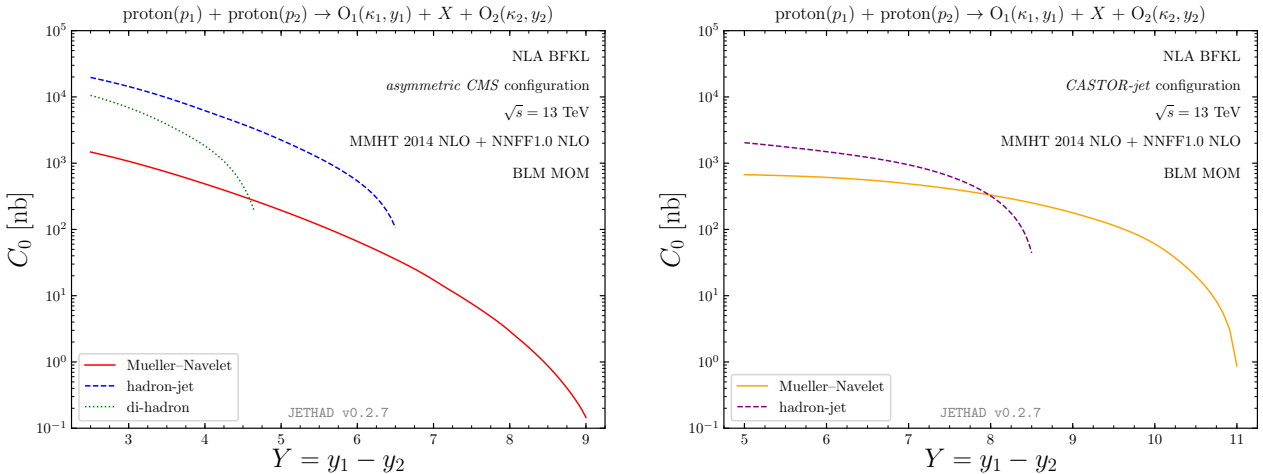


FIG. 7: Y -dependence of the φ -averaged cross section, C_0 , for the three considered reactions (Fig. 2) in the NLA BFKL accuracy. Results for $\sqrt{s} = 13$ TeV in the *asymmetric CMS* (*CASTOR-jet*) configuration are given in the left (right) panel. Hadron emissions, when considered, are described in terms of NNFF1.0 [175] NLO FF parametrizations (see Section 2.4 for further details).

$f(\nu)$ entering the expression given in Eq. (27), is zero in the Mueller–Navelet channel and non-zero in the hadron-tag case. This radically changes the analytic structure of the BLM equation (26). Finally, a side study (Section 3.4.2) on single hadron-species emission(s) addresses the potential presence of intrinsic contributions to the BLM-scale values coming from the FFs.

In Figs. 5 and 6 we compare predictions for the ratio, $R_0^{\text{NLA/LLA}} \equiv C_0^{\text{NLA}} / C_0^{\text{LLA}}$, obtained with BLM optimization to the corresponding ones calculated at *natural scales*, *i.e.* $\mu_R = \mu_N \equiv \sqrt{\kappa_1 \kappa_2}$ and $\mu_{F1,2} = \kappa_{1,2}$, after having checked that the alternative choice for $\mu_{F1,2}$, $\mu_{F1} = \mu_{F2} = \mu_N$, produces almost the same results with respect to the previous one. In particular, Fig. 5 shows the Y -dependence of the $R_0^{\text{NLA/LLA}}$ ratio for the three considered reactions (Fig. 2) in the *asymmetric CMS* configuration. We notice that NLA corrections, generally with opposite sign with respect LLA results, become larger and larger in absolute value at increasing rapidity interval, thus making the $R_0^{\text{NLA/LLA}}$ smaller and smaller (we stress that the label “NLA” in our plots *always* stands for LLA plus higher-order terms, and not just the latter ones). This is an expected phenomenon in the

BFKL approach which, however, becomes milder when scales are optimized. The adoption of the BLM method leads to a scale choice that permits to mimic the most relevant subleading terms, thus stabilizing the perturbative series. From the operational point of view, this results in a reduction of the distance between the LLA and the NLA, namely it raises the $R_0^{\text{NLA/LLA}}$ ratio in our plots, making it ideally close to one. This is exactly what happens in the Mueller–Navelet case (upper left panel of Fig. 5), while its value at BLM scales exceeds one in the case of hadron detection (remaining panels). The explanation for this, apparently odd behavior, has not to be hunted in the use of BLM, but rather in a combination of two distinct effects, already present in the expression for C_0 given in Eq. (28) and therefore independent from the scale choice. On the one side, going from the $\overline{\text{MS}}$ to the MOM renormalization scheme generates a non-exponentiated, positive extra factor proportional to T^{conf} . On the other side, it is easy to prove that the C_{gg} coefficient in Eq. (A2) gives a large and positive contribution to the hadron NLO impact-factor correction. All that makes C_0 at the NLA larger than the corresponding LLA one *before* switching any eventual scale-optimization procedure on. For the sake of completeness, the Y -dependence of the $R_0^{\text{NLA/LLA}}$ ratio for the di-jet and the hadron jet case (first two panels of Fig. 2) in the *CASTOR-jet* configuration is presented in Fig. 6.

Ultimately, the Y -dependence of the NLA φ -averaged cross section, C_0 , for all the considered reactions is examined. Final-state configurations molded on the *asymmetric CMS (CASTOR-jet)* event selection are presented in the left (right) panel of Fig. 7. Here, a definite hierarchy among them is stringently respected, except for values of Y close to the upper bound given by the kinematics: hadron detections dominate in statistics with respect to jet tags.

3.4.2. Hadron-species analysis

In this Section we hunt for possible contributions to the optimal scale values intrinsically coming from the description of the parton-to-hadron fragmentation. Predictions for single hadron-species detections (π^\pm , K^\pm , $p(\bar{p})$) are matched to the standard case, where the *sum* over all species is intended. For the sake of simplicity, we take the inclusive hadron-jet production (central panel of Fig. 2) as reference reaction and consider both the *asymmetric CMS* and the *CASTOR-jet* final-state configurations.

The inspection of results of the BLM scales (Fig. 8) for values of the conformal spin, $n = 0$ and $n = 1$, indicates that π^\pm emissions lead to larger scales which are, however, of the same order of the other single-species cases and of the *sum* one. Therefore, no clues of FF intrinsic effects emerge from our analysis. This can be due to the fact that, while FFs depend on the mass, M_H , of the corresponding light-flavored hadron, H , the hard subprocess is mass-independent. Thus, residual logarithmic contributions in M_H can survive, generating a mild sensitivity of the scale-choice procedure to the given hadron species.

For completeness of presentation, the Y -dependence of the $R_0^{\text{NLA/LLA}}$ ratio with BLM optimization is shown in Fig. 9, whereas the φ -averaged NLA BLM cross section is given in Fig. 10.

3.5. BFKL versus DGLAP

In this Section we present and discuss features of the core results of our work. The examination of azimuthal-correlation moments, given in Section 3.5.1, is extended and accompanied by the analysis of azimuthal distributions, portrayed in Section 3.5.2.

3.5.1. Azimuthal correlations

NLA BFKL predictions for the azimuthal ratios, $R_{nm} \equiv C_n/C_m$, in the Mueller–Navelet channel (left panel of Fig. 2) are compared in Fig. 11 with the corresponding high-energy DGLAP ones in the (*asymmetric CMS* configuration) for $\sqrt{s} = 13$ TeV. This extends and completes the study conducted in Refs. [44, 45], where a sharp distance between BFKL-resummed and fixed-order calculations came out in the inclusive di-jet hadroproduction with *partially asymmetric* configurations in the κ -plane, namely $35 \text{ GeV} < \kappa_{J,1} < 60 \text{ GeV}$ and $45, 50 \text{ GeV} < \kappa_{J,2} < 60 \text{ GeV}$, and for $|y_{J,1,2}| < 4.7$, at $\sqrt{s} = 7 \text{ TeV}$. Here, besides the use of *fully asymmetric* transverse-momentum cuts (disjoint κ -windows), the main improvement (panels of Fig. 11 correspond to the

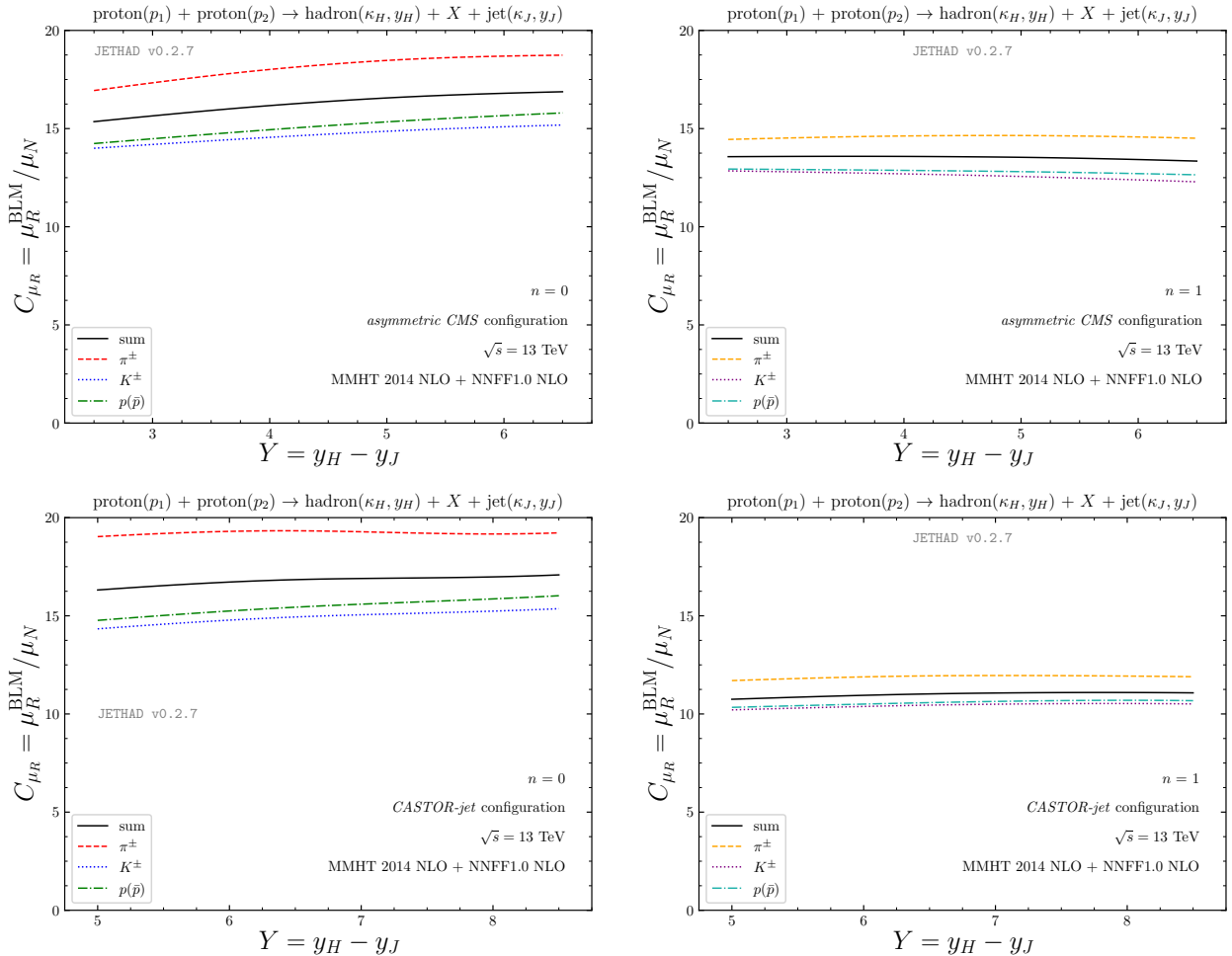


FIG. 8: BLM scales for the inclusive hadron-jet production (central panel in Fig. 2) versus the final-state rapidity interval, Y , for the φ -averaged cross section C_0 (left) and the azimuthal coefficient C_1 (right), for $\sqrt{s} = 13$ TeV in the *asymmetric CMS* configuration. Predictions for single hadron-species emissions (π^\pm , K^\pm , $p(\bar{p})$) are compared with the standard case, where the *sum* over all species is taken. Both the factorization scales, $\mu_{F1,2}$, have been set equal to $\mu_R^{\text{BLM}} \equiv C_{\mu_R} \mu_N$. Results for $\sqrt{s} = 13$ TeV in the *asymmetric CMS* (*CASTOR-jet*) configuration are given in upper (lower) panels.

respective ones in Figs. 2 and 3 of Ref. [44]) stands in the adoption of the “exact” BLM scale-optimization procedure (see Section 3.4.1) instead of approximated, semi-analytic BLM choices, and in a fair reduction of the numeric uncertainty. Analogous results for the di-jet correlations in the more exclusive, *CASTOR-jet* range, are displayed in Fig. 12. In both the cases, the pattern of the NLA BFKL R_{n0} series presents a *plateau* at large rapidity distance, Y , more emphasized in the *CASTOR-jet* configuration, which visibly evolves into a *turn-up* for R_{10} (upper left panel of Fig. 11 and of Fig. 12). The main reason for this behavior is that the increase of Y values moves the parton longitudinal fractions towards the so-called *threshold* region, where the energy of the di-jet system approaches the value of the center-of-mass energy, \sqrt{s} . Hence, PDFs are sounded in ranges close to the end-points of their definitions, where they exhibit large scaling violations and uncertainties⁷. In these configurations, our formalism misses the sizeable effect of threshold double logarithms which enter the perturbative series and have to be resummed to all orders. We note that error bands in the DGLAP case are larger with respect to the resummed ones. This originates from the highly-oscillatory behavior of the ν -integrand

⁷ When the struck-parton longitudinal-momentum fraction approaches one, the effect of *target-mass* corrections [224–234] becomes relevant and must be necessarily taken into account.

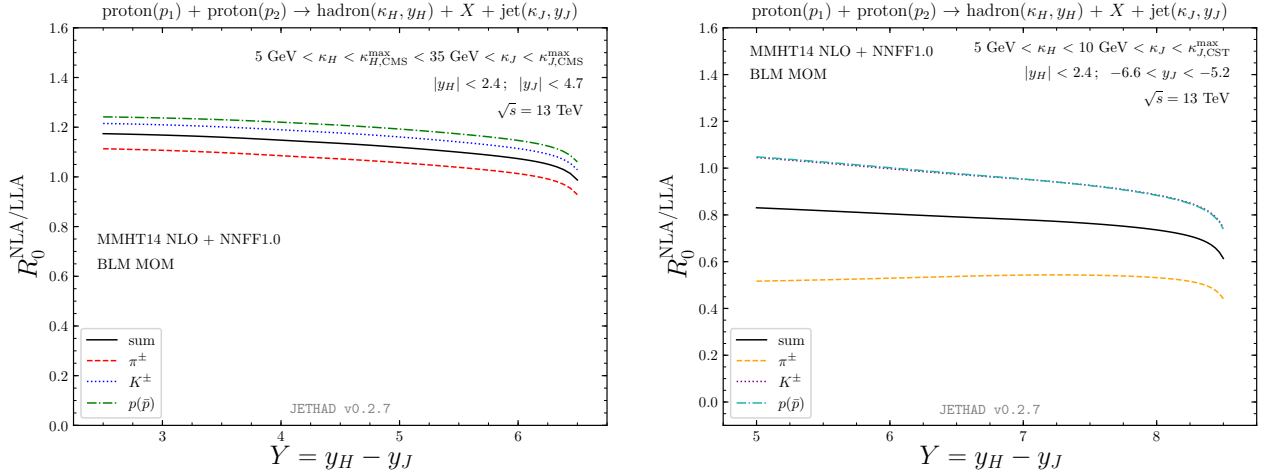


FIG. 9: Y -dependence of the $R_0^{\text{NLA/LLA}}$ ratio for the inclusive hadron-jet production (central panel in Fig. 2) in the *asymmetric CMS* (left) and in the *CASTOR-jet* (right) configuration, for $\sqrt{s} = 13$ TeV. Predictions for single hadron-species emissions ($\pi^\pm, K^\pm, p(\bar{p})$) are compared with the standard case, where the *sum* over all species is taken.

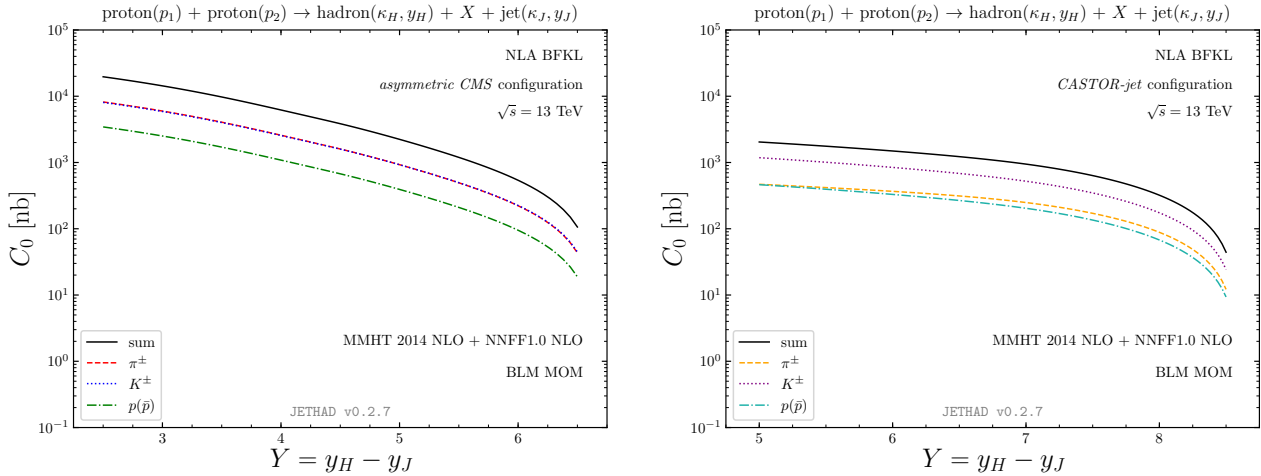


FIG. 10: Y -dependence of the φ -averaged cross section, C_0 , for inclusive hadron-jet production (central panel in Fig. 2) in the NLA BFKL accuracy, in the *asymmetric CMS* (left) and in the *CASTOR-jet* (right) configuration, and for $\sqrt{s} = 13$ TeV. Predictions for single hadron-species emissions ($\pi^\pm, K^\pm, p(\bar{p})$) are compared with the standard case, where the *sum* over all species is taken.

in Eq. (17), not anymore faded by the exponential factor as in the NLA BFKL case, in Eq. (7) (we refer the interested reader to Section 3.6.2 for more details on the numerical-uncertainty estimate of all the presented results).

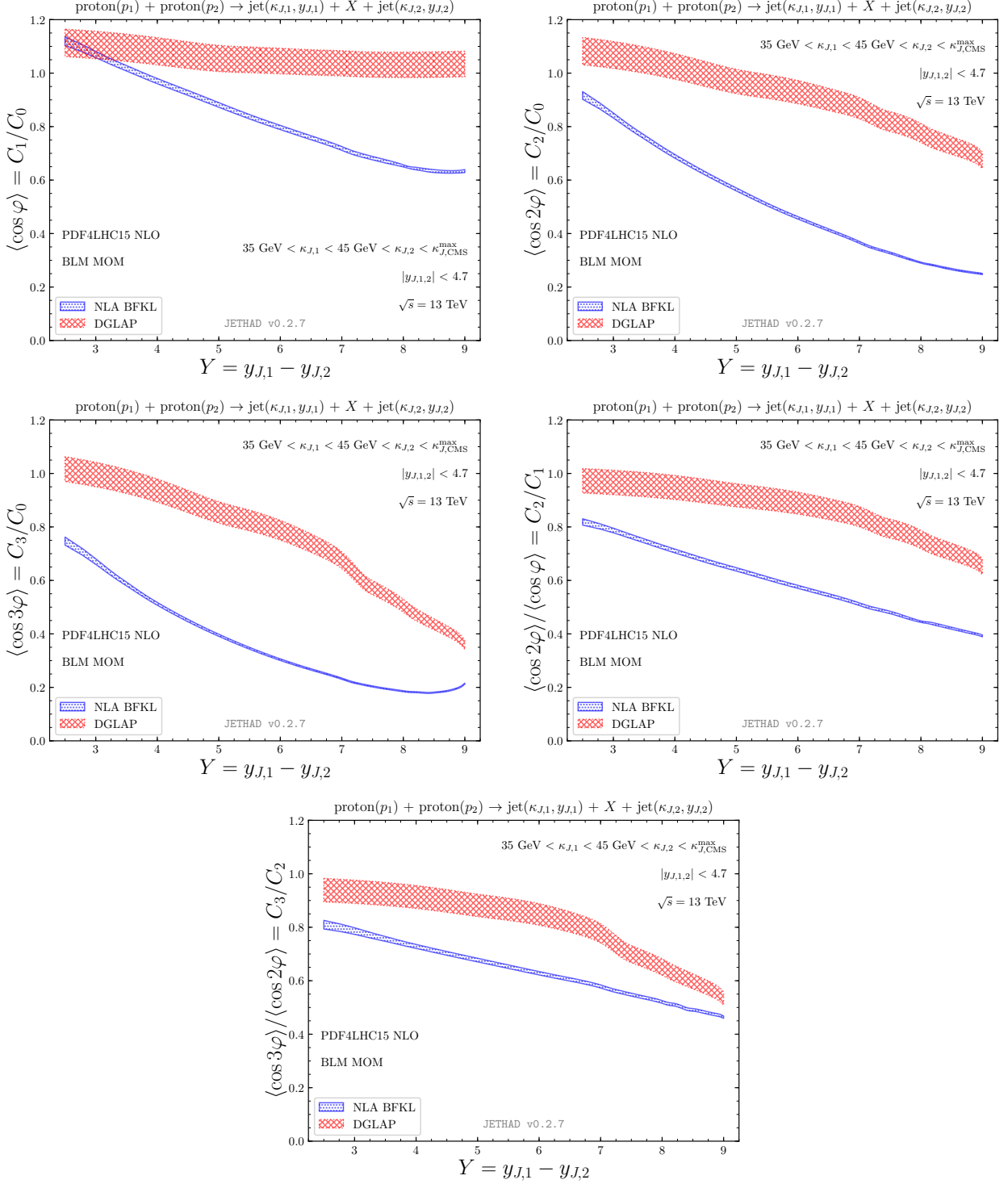


FIG. 11: Y -dependence of several azimuthal correlations, $R_{nm} \equiv C_n/C_m$, of the Mueller–Navelet jet production (left panel of Fig. 2) for $\mu_{F1,2} = \mu_R = \mu_R^{\text{BLM}}$ and $\sqrt{s} = 13$ TeV (*asymmetric CMS* configuration). Full NLA BFKL predictions are compared with the respective ones in the high-energy DGLAP limit.

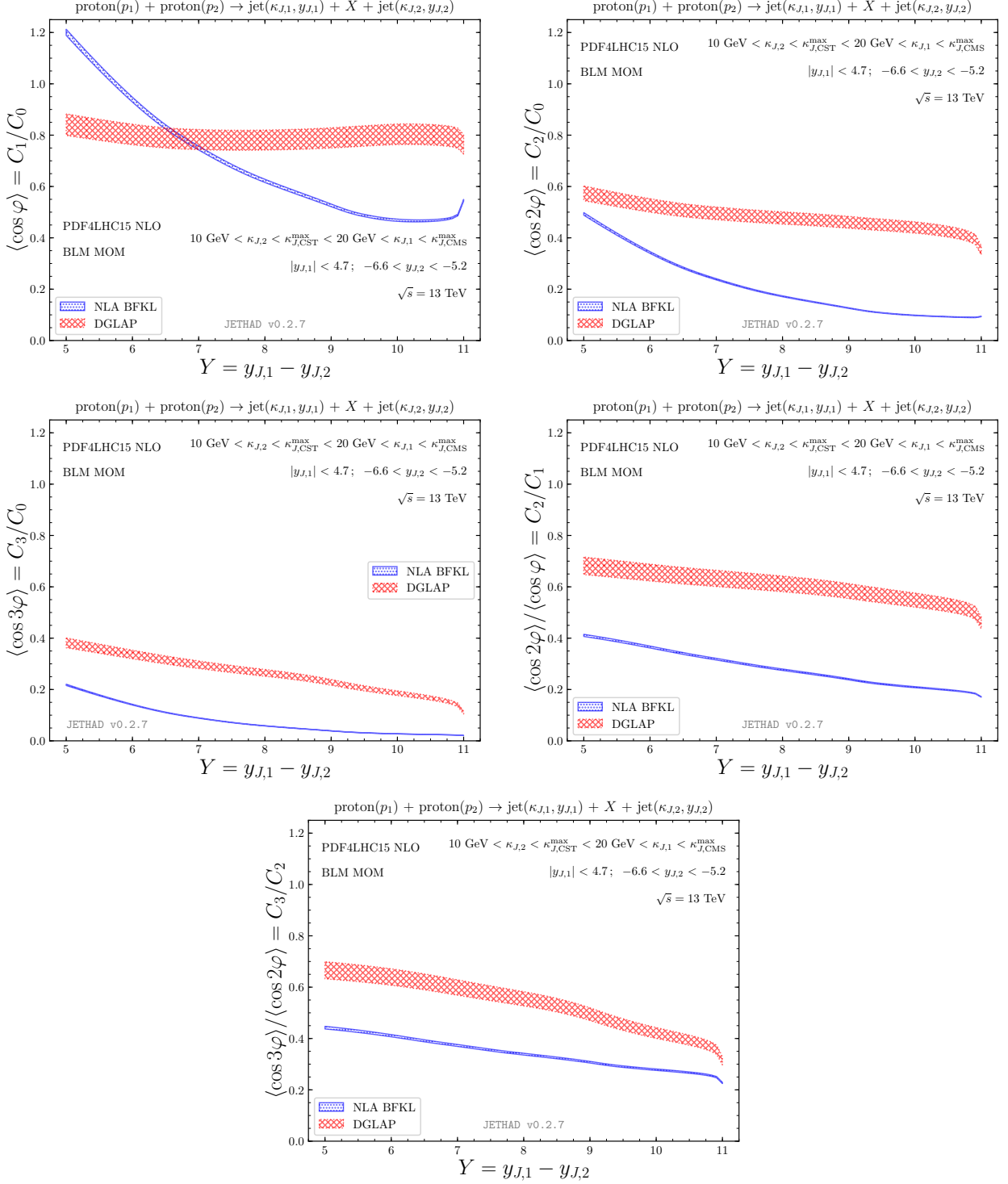


FIG. 12: Y -dependence of several azimuthal correlations, $R_{nm} \equiv C_n/C_m$, of the Mueller–Navelet jet production (left panel of Fig. 2) for $\mu_{F1,2} = \mu_R = \mu_R^{\text{BLM}}$ and $\sqrt{s} = 13 \text{ TeV}$ (*CASTOR-jet* configuration). Full NLA BFKL predictions are compared with the respective ones in the high-energy DGLAP limit.

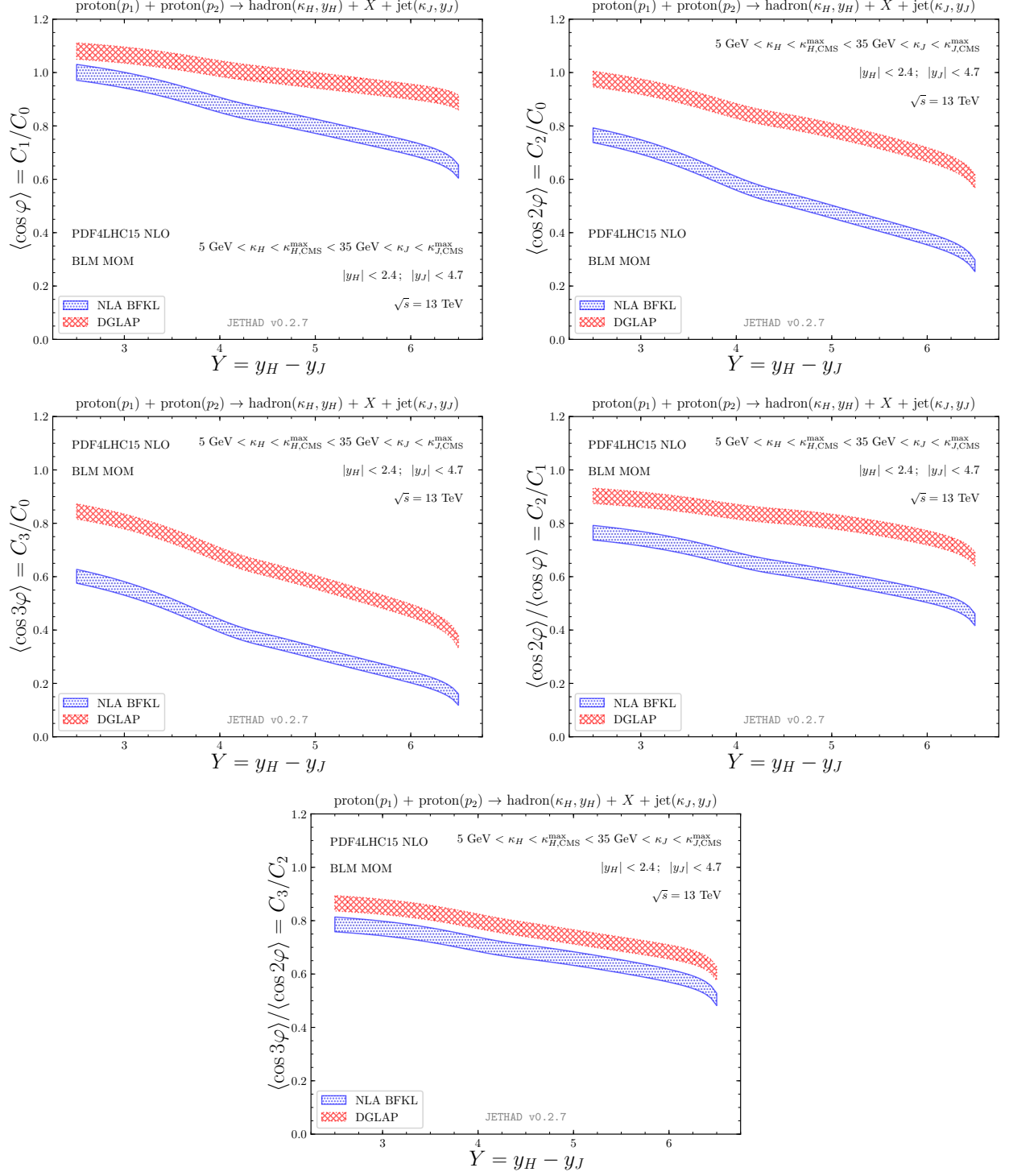


FIG. 13: Y -dependence of several azimuthal correlations, $R_{nm} \equiv C_n/C_m$, of the inclusive hadron-jet production (central panel of Fig. 2) for $\mu_{F1,2} = \mu_R = \mu_R^{\text{BLM}}$ and $\sqrt{s} = 13$ TeV (*asymmetric CMS configuration*). Full NLA BFKL predictions are compared with the respective ones in the high-energy DGLAP limit.

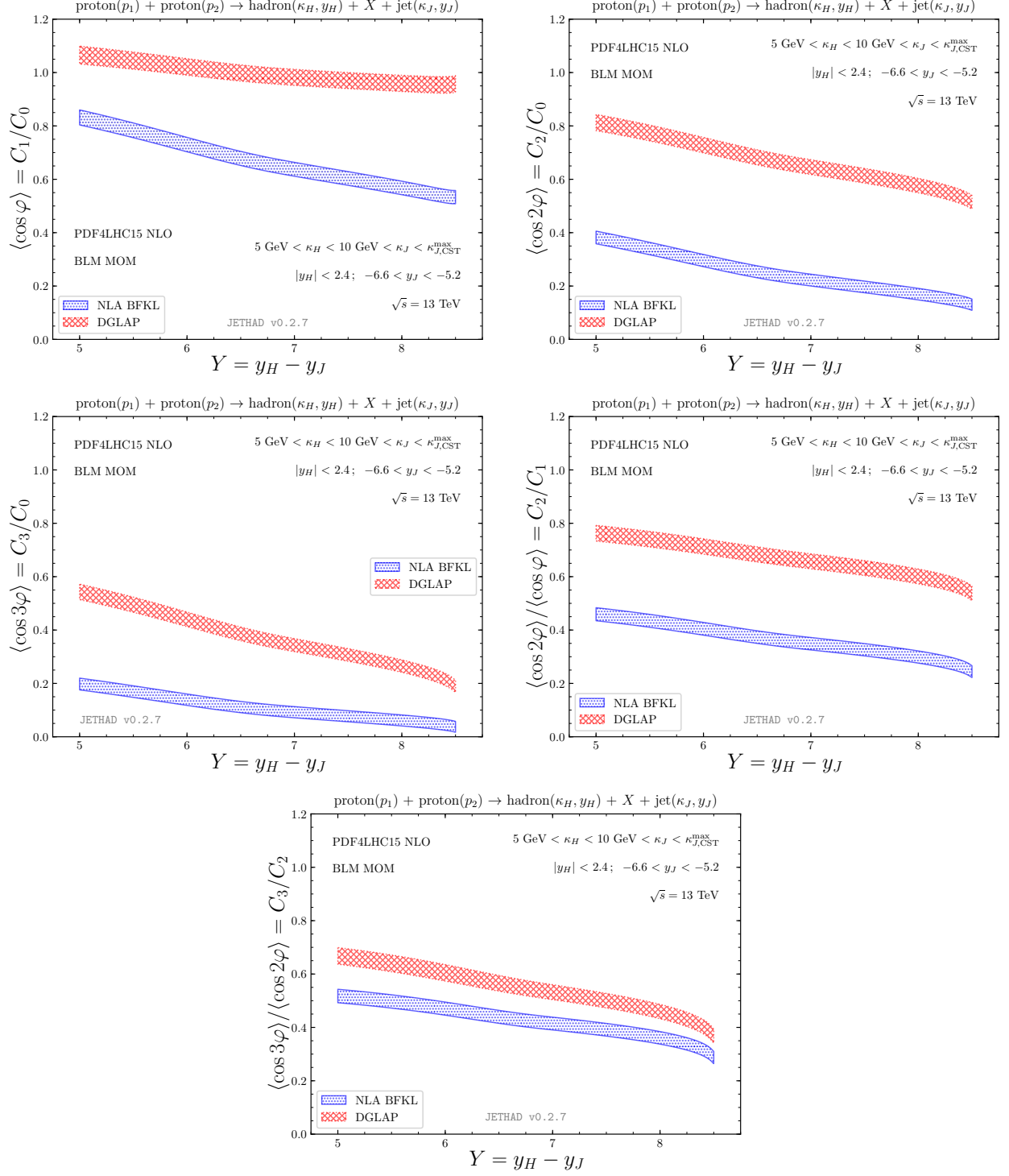


FIG. 14: Y -dependence of several azimuthal correlations, $R_{nm} \equiv C_n/C_m$, of the inclusive hadron-jet production (central panel of Fig. 2) for $\mu_{F1,2} = \mu_R = \mu_R^{\text{BLM}}$ and $\sqrt{s} = 13 \text{ TeV}$ (*CASTOR-jet* configuration). Full NLA BFKL predictions are compared with the respective ones in the high-energy DGLAP limit.

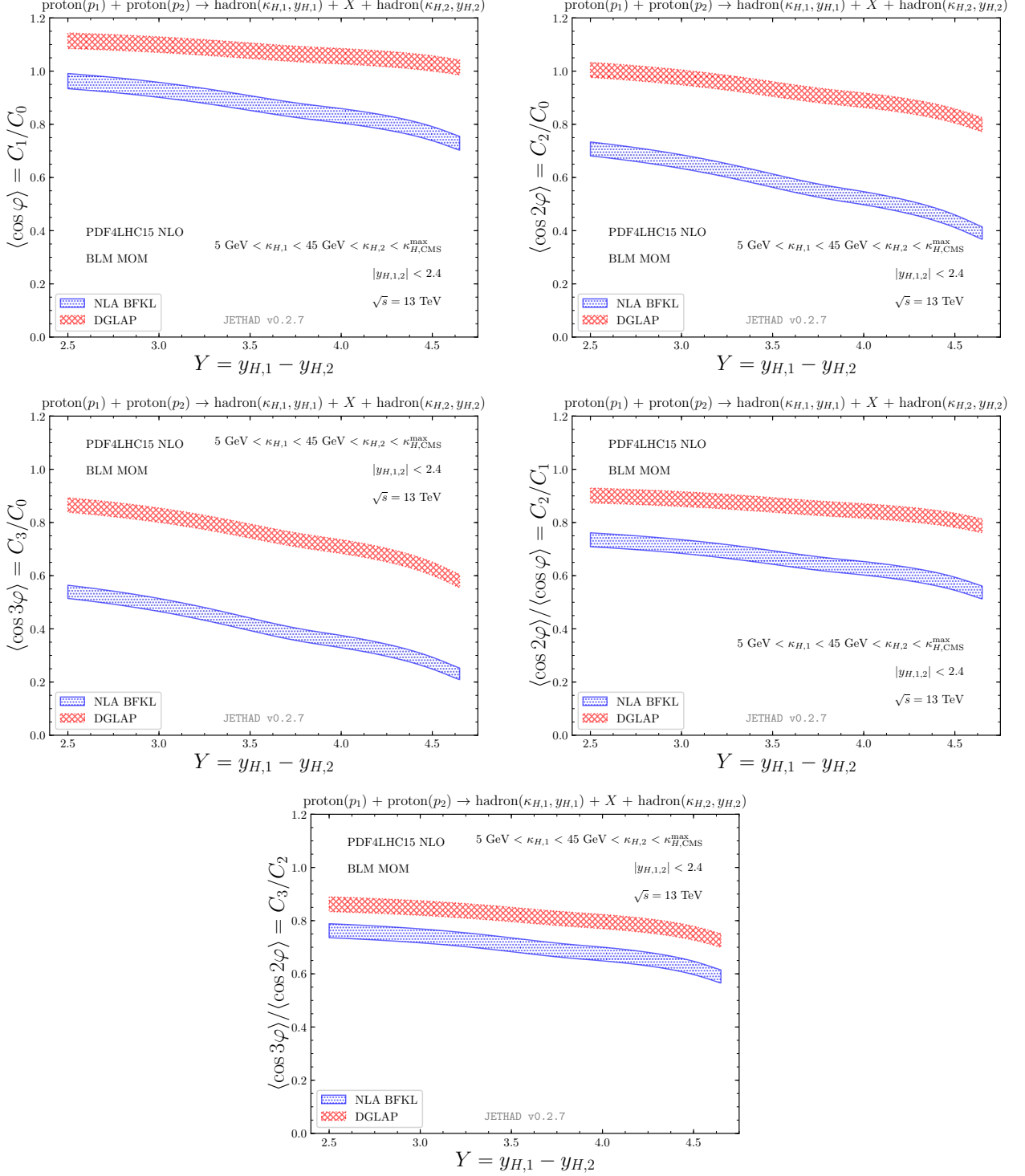


FIG. 15: Y -dependence of several azimuthal correlations, $R_{nm} \equiv C_n/C_m$, of the inclusive di-hadron production (right panel of Fig. 2) for $\mu_{F1,2} = \mu_R = \mu_R^{\text{BLM}}$ and $\sqrt{s} = 13 \text{ TeV}$ (*asymmetric CMS* configuration). Full NLA BFKL predictions are compared with the respective ones in the high-energy DGLAP limit.

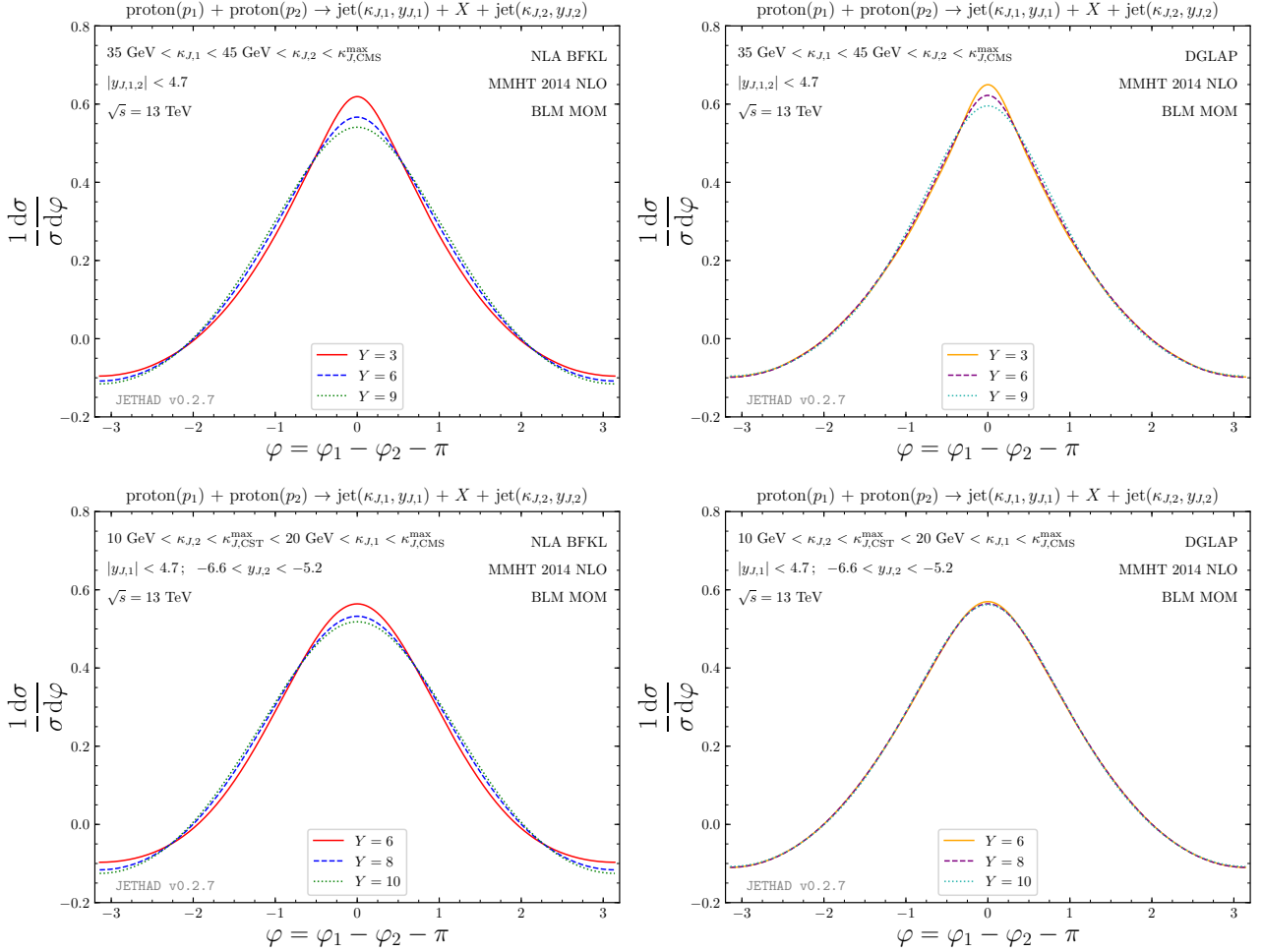


FIG. 16: NLA BFKL (left) and high-energy DGLAP (right) predictions for the azimuthal distribution of the Mueller–Navelet jet production (left panel of Fig. 2), for three distinct values of the final-state rapidity interval, Y , and $\sqrt{s} = 13$ TeV. Results in the *asymmetric CMS* (*CASTOR-jet*) configuration are given in upper (lower) panels.

We show predictions for the R_{nm} ratios in the hadron-jet channel (central panel of Fig. 2) in Fig. 13 (*asymmetric CMS*) and in Fig. 14 (*CASTOR-jet*), whereas analogous results for the di-hadron production (right panel of Fig. 2) are given in Fig. 15 (*asymmetric CMS*). Here, presence of identified hadrons in the final state has a dual impact. On the one part, the effect of further splittings (of parton momenta) entering the definition of hadron FFs prevails over the azimuthal recorrelation of the emitted objects at large Y , thus shadowing the turn-up tail observed in the Mueller–Navelet case. On the other part, the convolution between PDFs and FFs in the LO/NLO hadron impact factor(s) (Eqs. (14) and (A1)) stabilizes the oscillations of the ν -integrand, thus reducing the numeric uncertainty in the calculation of the high-energy DGLAP series, whose error bands are now of the same magnitude of the NLA BFKL ones.

The unphysical effect that brings R_{10} above one for small values of the rapidity interval, Y , is well known in the context of semi-hard reactions and has a straightforward explanation. In this kinematic limit, the hard-subprocess energy, $\sqrt{\hat{s}}$, is small and the employment of BFKL resummation, which systematically neglects terms damped by powers of \hat{s} , becomes inadequate. The fact that, in the DGLAP case, values of R_{10} larger than one are still present for larger Y -values originates from the nature of our approach. Being it, *de facto*, an high-energy calculation where the NLA resummation is truncated to a given order in the running coupling (see Section 2.2), *collinear contaminations*, which are largely present at low values of the conformal spin and at small- Y , may survive and manifest themselves also in the remaining part of the Y -range.

The overall outcome of the analysis conducted in this Section is a clear separation between BFKL and DGLAP predictions on azimuthal correlations of the two detected objects. This effects holds for all the considered

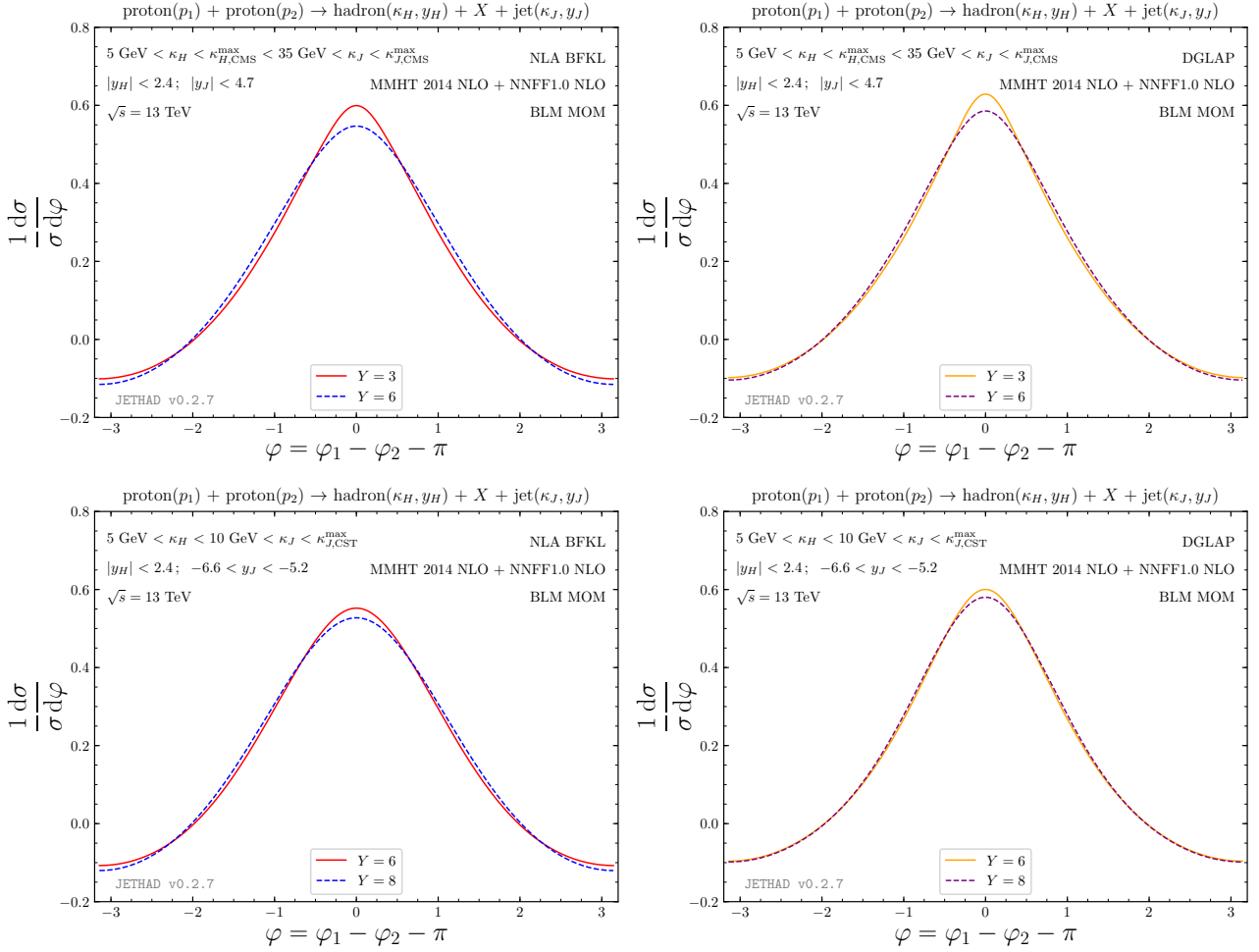


FIG. 17: NLA BFKL (left) and high-energy DGLAP (right) predictions for the azimuthal distribution of the inclusive hadron-jet production (central panel of Fig. 2), for two distinct values of the final-state rapidity interval, Y , and $\sqrt{s} = 13$. Results in the *asymmetric CMS (CASTOR-jet)* configuration are given in upper (lower) panels.

reactions and becomes more and more evident as the rapidity interval, Y , raises. The found pattern matches *in toto* the farsighted idea of Mueller and Navelet [33], namely that the wealth of undetected gluons radiated in the final state, theoretically described at the hand of the high-energy resummation, markedly heighten the decorrelation in the azimuthal plane between the emitted particles. This makes a substantial difference with respect to the DGLAP case, where only a limited number of gluon emissions, fixed by the truncation order of the perturbative series, is allowed. The adoption of asymmetric cuts for the transverse momenta in the final state fades the Born contribution, thus spotlighting the discrepancy between the two approaches.

3.5.2. Azimuthal distribution

Here we give predictions for azimuthal distributions, which, as anticipated, are directly accessible observables in the experimental studies. The first examination of these quantities was performed few years ago [37] in the context of the Mueller–Navelet jet production, for symmetric ranges of transverse momenta, and with partial and full NLA BFKL accuracy.

Results for the azimuthal distribution in the di-jet channel are shown with NLA BFKL (high-energy DGLAP) accuracy in the left (right) panels of Fig. 16, for three distinct values of the rapidity interval, Y . Predictions in the *asymmetric CMS* configuration are given in upper panels, while the lower ones refer to the *CASTOR-jet*

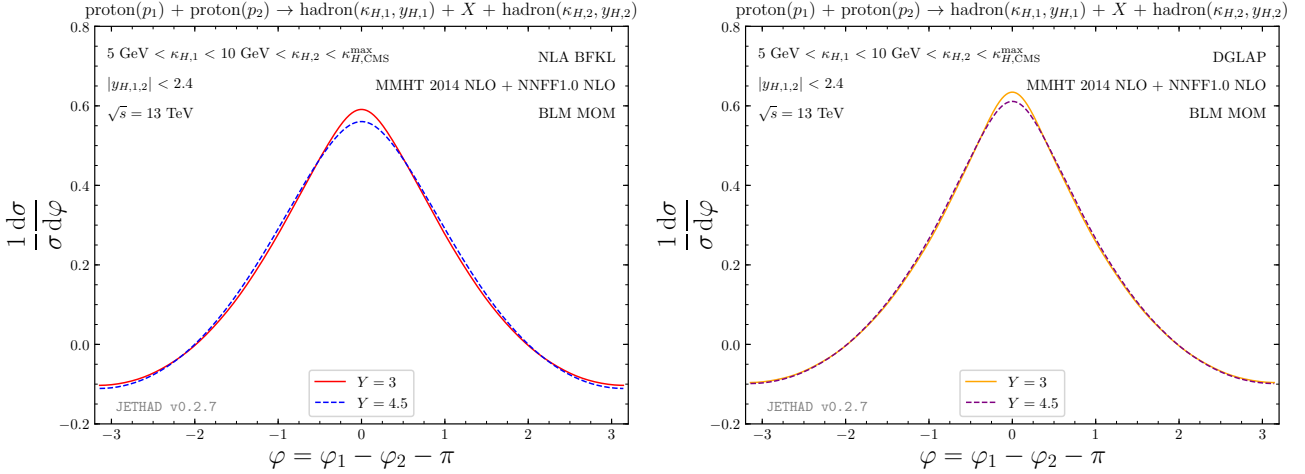


FIG. 18: NLA BFKL (left) and high-energy DGLAP (right) predictions for the azimuthal distribution of the inclusive di-hadron production (right panel of Fig. 2), for two distinct values of the final-state rapidity interval, Y , and $\sqrt{s} = 13$. Results are given in the *asymmetric CMS* configuration.

selection. Fig. 17 shows, in the same way, the azimuthal distribution in the hadron-jet emission for two distinct values of Y , whereas plots of Fig. 18 correspond to the di-hadron distribution with *asymmetric CMS* cuts, for two distinct values of Y .

The peculiar shape of our series represent a further manifestation of the BFKL-versus-DGLAP “dichotomy”. All distributions feature a clear peak in correspondence of the value of the azimuthal-angle difference, $\varphi \equiv \varphi_1 - \varphi_2 - \pi$, for which the two final-state objects are emitted back-to-back, *i.e.* $\varphi = 0$. Let us start by considering, for each panel, the first entry, which corresponds to the lower value of Y among the selected ones. Both in the BFKL and in the DGLAP cases, this peak dominates over the larger- Y ones, the DGLAP being narrower in comparison to the BFKL one. Then, when one moves towards the larger values of Y , peaks visibly shrink and widths moderately widen in the BFKL case, while that switch is much less evident for the DGLAP series. This means that, when the rapidity interval grows, the number of back-to-back events predicted by BFKL decreases, while it remains relatively unchanged according to DGLAP. Our outcome is in perfect agreement with the main statement raised in Section 3.5.1.

As a side consideration, we notice that trends obtained in the *CASTOR-jet* ranges always show a slightly larger decorrelation with respect to *asymmetric CMS* patterns (lower panels versus upper ones in Figs. 16 and 17). The added value of the more exclusive kinematic configurations offered by tagging a jet in the CASTOR ultra-backward detector translates in an intrinsic decorrelation gained by the final state.

All these features brace the message that kinematic configurations suitable to heighten high-energy effects in the context of the LHC phenomenology exist and have been effectively detected.

3.6. Numerical strategy

3.6.1. JETHAD: an object-based, process-independent interface

All numerical calculations were performed using JETHAD, a hybrid FORTRAN2008/PYTHON3 modular code we recently developed, suited for the computation of cross sections and related observables for inclusive semi-hard reactions. Natively equipped with performance acceleration, by making extensive use of parallel computing techniques, and interfaced with the most advanced (multi)dimensional integration routines, JETHAD allowed us to dynamically select the best integration algorithm, depending on the behavior of the considered integrand. *Monte-Carlo* inspired integrators with variance reduction via *importance sampling*, like the *Vegas* routine [235] as given in its concurrent version via the *Cuba* package 4.2 [236, 237], were primarily selected to perform multidimensional integrations needed to calculate the C_n^{DGLAP} coefficients (Eq. (17)) in the Mueller–Navelet

channel (left panel of Fig. 2). Conversely, *adaptive-quadrature* based functions, like `DADMUL` and `WGauss` as implemented in the last version of CERN program libraries [238], were mainly preferred for the computation of all observables related to (di-)hadron emission (central and right panels of Fig. 2) and for the one-dimensional integration over the longitudinal momentum fraction, ζ , entering the expression for the NLO hadron/jet impact factors (Eqs. (A1) and (B1)), respectively. All PDF parametrizations, as well as the NNFF1.0 FF set, were calculated through the Les Houches Accord PDF interpolator (LHAPDF) 6.2.1 [239], while native routines for the remaining FFs were directly linked to the corresponding module in our code. In order to dynamically select the considered reaction through a common interface, a *structure-based* smart-management system, where physical final-state particles are described in terms of *object* prototypes (*i.e.*, FORTRAN structures), was incorporated inside JETHAD. Particle objects carry all information about basic and kinematic properties of their physical counterparts, from mass and charge, to kinematic ranges and rapidity tag. They are first loaded by the JETHAD user routine from the master database through a specific *particle generator* routine (custom-particle generation is allowed too). Then, they are *cloned* to the final-state object array and thus *injected* from the integrand routine, differential on the final-state variables, to the respective impact-factor module through the *impact-factor controller*. To the strong flexibility in the final-state generation, a wide choice for the initial-state selection corresponds. Thanks to a peculiar *particle-ascendancy* structure attribute, JETHAD is able indeed to recognize if an object is hadroproduced or emitted as subproduct of a leptonic interaction, and automatically determines which modules need to be initialized (PDFs, FFs, unintegrated densities, etc...), breaking down computing-time lags. Hence, JETHAD comes as an object-based interface, completely independent on the reaction being investigated. While inspired by the BFKL phenomenology, it is possible to perform calculations of the same observables in different approaches, by creating new, customized routines, which can be linked to the core structure of the code through a native *point-to-routine* system, thus making JETHAD a general, HEP-purposed tool. We pursue, as a medium-term goal, to release a first public version soon, providing the scientific community with a standard software for the analysis of inclusive semi-hard processes. Another code, LExA, based on the same framework and suited to the study of exclusive semi-hard reactions, is currently at an early-development stage.

A robust improvement of our technology would consist in successfully interfacing these codes with already existing software, suited to high-energy/small- x studies. An incomplete list includes: novel software for NLA studies [240–243] of Mueller–Tang (*alias* jet-gap-jet) configurations [244], the BFKLex Monte Carlo [245–247], designed to investigate the high-energy jet production in the *multi-Regge* limit, the KaTie generator [248] of off-shell matrix elements, and the TMDlib library [249], where different models of the small- x UGD are collected.

3.6.2. Uncertainty estimate

The most relevant uncertainty comes from the numerical 4-dimensional integration over the transverse momenta, $\kappa_{1,2}$, of the two final-state objects, the rapidity, $y_{1/2}$, of one of them (the other one is fixed by the condition $Y = y_1 - y_2$ enforced in the definition of the integrated azimuthal coefficients (22)), and over ν . Its effect was directly estimated and given as output by master integrator routines. Further, secondary sources of uncertainty, are respectively: the one-dimensional integration over the parton longitudinal fraction, x , needed to perform the convolution between PDFs and, eventually, FFs in the LO/NLO hadron impact factors (Eq. (14)) for LO, Eq. (A1), the one-dimensional integration over the longitudinal momentum fraction, ζ , in the NLO impact factor corrections (Eq. (A1) for hadrons, Eq. (B1) for jets), and the upper cutoff in the numerical integral over ν . While the first two ones turn out to be negligible with respect to the multidimensional integration, the last one deserves particular attention. As pointed out in Section 3.3 of Ref. [44], the C_n^{DGLAP} coefficients are expected to exhibit a stronger sensitivity to the upper cutoff of the ν -integration, ν^{\max} , due to the fact that oscillations rising in the ν -integrand in Eq. (17) are not quenched by the exponential factor as in the NLA and LLA BFKL expressions (Eqs. (7) and (8), respectively). This turns to be particularly true in the Mueller–Navalet channel (left panel of Fig. 2), while the peculiar structure of the x -integrand in the LO hadron impact factor (Eq. (14)) generates, as the net result, a significant damping of the ν -associated oscillations both in the DGLAP and in the NLA/LLA BFKL cases, allowing us to use smaller values of ν^{\max} in hadron-jet and di-hadron production (central and right panels of Fig. 2) with respect to the di-jet case. Values for ν^{\max} , given below (Tab. I), have been taken after checking that the uncertainty on the R_{nm} ratios, coming from raising them by a value of 10, is negligible if compared to the valued error of the multidimensional integration.

Error bands of all predictions presented in this work are given in terms of the uncertainty on the final-state

integration, combined, in case of hadron emission (central and right panels of Fig. 2), with the one coming from averaging over different FF sets (see Section 2.4 for further details). An exception is represented by the *theory-versus-experiment* analysis in the Mueller–Navelet channel (Section 3.3), where error bands in the two panels of Fig. 3 show the standard deviation of predictions for the R_{nm} ratios calculated via the replica method.

TABLE I: Values of the upper cutoff, ν^{\max} , on the numerical ν -integration of the C_n coefficients in the NLA/LLA BFKL accuracy ((Eqs. (7) and (8)) and in the high-energy DGLAP limit (Eq. (17)), for all considered reactions (Fig. 2).

ν^{\max}	Mueller–Navelet	hadron-jet	di-hadron
NLA/LLA	30	10	10
DGLAP	50	10	10

4. CLOSING STATEMENTS

We brought evidence that distinctive signals of the high-energy resummation emerge in the NLA description of different semi-hard reactions. Taking advantage of the record energies and of the exclusive kinematic configurations provided by the LHC, their effects can be effectively disengaged from the ones arising from (pure) fixed-order, DGLAP-inspired calculations. In this direction, the use of (completely) asymmetric intervals for the transverse momenta of the detected objects plays a crucial role and definitely needs to be taken into account in the forthcoming experimental analyses on forward/backward final-state emissions. Among them, stringent measurements of the azimuthal-angle averaged cross section, C_0 , turn out to be essential not only in the discrimination of BFKL from other theoretical approaches, but also in the assessment of the intrinsic ambiguities of the given approach.

With the goal of providing, in the medium-term future, comparisons with genuine fixed-order calculations, the combined effect of a selection of potential uncertainties was gauged. Our preference fell on those uncertainties which are typically included in collinear-physics phenomenology, but they turn out to be novel in the semi-hard one. More in particular, we studied the sensitivity of azimuthal-correlation moments on PDF uncertainty via the so-called replica method [181] (this was done for the Mueller–Navelet channel at $\sqrt{s} = 7$ TeV (Section 3.3)) and on FF uncertainty, by averaging among four distinct FF sets. A detailed analysis of all the potential sources of uncertainty is postponed to future studies, when data for our disjoint κ -windows will be available. Then, two complementary paths should be traced and concurrently treated in the context of our studies.

Pursuing the goal of dealing with more exclusive final states, the investigation of heavy-flavored emissions has been taken into account in our program [98–100], with the medium-term target of including the case of quarkonia (for a recent work on the inclusive J/ψ -plus-jet hadroproduction, see Ref. [101]). Here, the ultimate task relies upon a profound examination of the theoretical production mechanism [250–252] for these quark-bound states, which has not yet been completely outlined, and on the grading of the most popular models proposed so far [253–255]. Various benefits can be gained from considering single forward emissions. First, the experimental statistics appreciably increases. Second, it allows us to probe different frameworks for the unintegrated gluon distribution (UGD), including the ones [256, 257] whose definition suitably embodies non-perturbative inputs driven by the *transverse-momentum-dependent* (TMD) factorization (see, *e.g.*, Refs. [129, 258, 259] and references therein for an overview on the general framework, Refs. [260–287] for quite recent applications) together with effective small- x effects.

The analysis of more differential distributions covering broader kinematic ranges requires an ineluctable effort into the enhancement of our formalism to accommodate other resummation mechanisms. A major outcome of a recent work on the inclusive hadroproduction of a Higgs boson and a jet well separated in rapidity [102] is that an exhaustive study of the Higgs transverse-momentum distribution lies on the exploration of neighboring kinematic regions, each of them representing a preferred channel to probe a specific resummation. That calls for a net overhaul of our framework (first from the analytic and then from the numeric point of view) which would not anymore rely *only* on the pure BFKL approach, but should rather evolve into an underlying *staging* where distinct resummations are *plugged-in* and play their part.

One step forward is represented by the Altarelli–Ball–Forte (ABF) formalism [288–294], where DGLAP and BFKL inputs are combined to improve the perturbative accuracy of the resummed series, by imposing

consistency conditions (duality aspects), symmetrizing the BFKL kernel in the (anti-)collinear phase-space regions, and incorporating those contributions to running coupling which affect the small- x divergences. Thence, the interplay between collinear and high-energy factorization allows us to perform the resummation of coefficient functions, whereas the resummation of splitting functions is endowed by enforcing the consistency between the two evolution equations. The first determination of proton PDFs where NLO and next-to-NLO fixed-order calculations are supplemented by the NLA small- x resummation has been recently realized [158, 295, 296], by making use of the `HELL` [297, 298] numerical code interfaced to the `APFEL` [299–301] PDF-evolution library.

Another intriguing possibility is represented by the Catani–Ciafaloni–Fiorani–Marchesini (CCFM) *branching* scheme [302–305]. Enforcing angular ordering (*coherence*) of soft-parton emission from the large- x to the small- x kinematic ranges, the CCFM framework provides with a unified evolution pattern for unintegrated gluon densities. In the totally inclusive configuration, this evolution interpolates between the DGLAP equation at moderate- x and the BFKL one at small- x . For large values of x and for high virtualities, CCFM dynamics matches DGLAP evolution, whereas in the asymptotic-energy limit it *almost* corresponds to BFKL (see Refs. [306–308]). It essentially builds on the sum of ladder diagrams with angular ordering along the chain. Parton transverse momentum is generated via the genuine recoil effect due to gluon radiation controlling the UGD evolution. The direct employment of CCFM to evolution equations for parton distributions was proposed by Jan Kwieciński [309] through the so-called CCFM–K equations. The CCFM formalism was then generalized [310] in order to account for *non-linear* effects in the gluon evolution, thus giving us a chance to gauge the impact of parton saturation on exclusive observables. On the phenomenological side, a description of the Drell–Yan production at the hand of CCFM–K-evolved distributions was recently proposed [311].

We strongly believe the scientific community would largely benefit from a *multi-lateral* formalism in which several approaches (as the high-energy resummation, the threshold resummation at fixed transverse momentum [312–314], the transverse-momentum resummation [315–331] and the resummation of Sudakov-type logarithms emerging when almost back-to-back final-state configurations occur in the small- x limit [332–337]) coexist and can be concurrently employed in the description of an increasing number of hadronic and lepto-hadronic reactions at the LHC as well as at new-generation colliding machines, as NICA-SPD [338], HL-LHC [339] and the EIC [340].

Acknowledgments

This work was supported by the Italian Foundation “Angelo Della Riccia” and by the Italian Ministry of Education, Universities and Research under the FARE grant “3DGLUE” (n. R16XKPHL3N).

The author would like to express his gratitude to Alessandro Papa, Dmitry Yu. Ivanov and Valerio Bertone for a critical reading of the manuscript, for useful suggestions and for encouragement.

The author thanks Alessandro Bacchetta, Joachim Bartels, Chiara Bissolotti, Andrée Dafne Bolognino, Giuseppe Bozzi, Stanley Brodsky, Francesco Caporale, Grigorios Chachamis, Victor S. Fadin, Michael Fucilla, Krzysztof J. Golec-Biernat, David Gordo Gómez, Krzysztof Kutak, Leszek Motyka, Mohammed M.A. Mohammed, Beatrice Murdaca, Barbara Pasquini, Fulvio Piacenza, Marco Radici, Christophe Royon, Douglas A. Ross, Deniz Sunar Cerci, Pieter Taels, Agustín Sabio Vera, Antoni Szczurek and Lech Szymanowski for inspiring discussions and for stimulating conversations.

Feynman diagrams in this work were realized via the `JaxoDraw` 2.0 interface [341].

Appendix A: Forward-hadron NLO impact factor

We give below the analytic formula for the NLO impact-factor correction for the forward-hadron production:

$$\hat{c}^{(H)}(n, \nu, \kappa_H, x_H) = 2\sqrt{\frac{C_F}{C_A}} (\kappa_H^2)^{i\nu - \frac{1}{2}} \frac{1}{2\pi} \int_{x_H}^1 \frac{dx}{x} \int_{\frac{x_H}{x}}^1 \frac{d\zeta}{\zeta} \left(\frac{x\zeta}{x_H}\right)^{2i\nu-1} \quad (\text{A1})$$

$$\begin{aligned} & \times \left[\frac{C_A}{C_F} f_g(x) D_g^h \left(\frac{x_H}{x\zeta} \right) C_{gg}(x, \zeta) + \sum_{\alpha=q\bar{q}} f_\alpha(x) D_\alpha^h \left(\frac{x_H}{x\zeta} \right) C_{qq}(x, \zeta) \right. \\ & \left. \times D_g^h \left(\frac{x_H}{x\zeta} \right) \sum_{\alpha=q\bar{q}} f_\alpha(x) C_{qg}(x, \zeta) + \frac{C_A}{C_F} f_g(x) \sum_{\alpha=q\bar{q}} D_\alpha^h \left(\frac{x_H}{x\zeta} \right) C_{gq}(x, \zeta) \right], \end{aligned}$$

$$C_{gg}(x, \zeta) = P_{gg}(\zeta) (1 + \zeta^{-2\gamma}) \ln \left(\frac{\kappa_H^2 x^2 \zeta^2}{\mu_F^2 x^2} \right) - \frac{\beta_0}{2} \ln \left(\frac{\kappa_H^2 x^2 \zeta^2}{\mu_R^2 x^2} \right) \quad (\text{A2})$$

$$\begin{aligned} & + \delta(1 - \zeta) \left[C_A \ln \left(\frac{s_0 x^2}{\kappa_H^2 x^2} \right) \chi(n, \gamma) - C_A \left(\frac{67}{18} - \frac{\pi^2}{2} \right) + \frac{5}{9} n_f \right. \\ & \left. + \frac{C_A}{2} \left(\psi' \left(1 + \gamma + \frac{n}{2} \right) - \psi' \left(\frac{n}{2} - \gamma \right) - \chi^2(n, \gamma) \right) \right] + C_A \left(\frac{1}{\zeta} + \frac{1}{(1 - \zeta)_+} - 2 + \zeta \bar{\zeta} \right) \\ & \times \left(\chi(n, \gamma) (1 + \zeta^{-2\gamma}) - 2(1 + 2\zeta^{-2\gamma}) \ln \zeta + \frac{\bar{\zeta}^2}{\zeta^2} \mathcal{I}_2 \right) \\ & + 2 C_A (1 + \zeta^{-2\gamma}) \left(\left(\frac{1}{\zeta} - 2 + \zeta \bar{\zeta} \right) \ln \bar{\zeta} + \left(\frac{\ln(1 - \zeta)}{1 - \zeta} \right)_+ \right), \end{aligned}$$

$$C_{gq}(x, \zeta) = P_{gq}(\zeta) \left(\frac{C_F}{C_A} + \zeta^{-2\gamma} \right) \ln \left(\frac{\kappa_H^2 x^2 \zeta^2}{\mu_F^2 x^2} \right) \quad (\text{A3})$$

$$+ 2 \zeta \bar{\zeta} T_R \left(\frac{C_F}{C_A} + \zeta^{-2\gamma} \right) + P_{gq}(\zeta) \left(\frac{C_F}{C_A} \chi(n, \gamma) + 2\zeta^{-2\gamma} \ln \frac{\bar{\zeta}}{\zeta} + \frac{\bar{\zeta}}{\zeta} \mathcal{I}_3 \right),$$

$$C_{qq}(x, \zeta) = P_{qq}(\zeta) \left(\frac{C_A}{C_F} + \zeta^{-2\gamma} \right) \ln \left(\frac{\kappa_H^2 x^2 \zeta^2}{\mu_F^2 x^2} \right) \quad (\text{A4})$$

$$+ \zeta (C_F \zeta^{-2\gamma} + C_A) + \frac{1 + \bar{\zeta}^2}{\zeta} \left[C_F \zeta^{-2\gamma} (\chi(n, \gamma) - 2 \ln \zeta) + 2 C_A \ln \frac{\bar{\zeta}}{\zeta} + \frac{\bar{\zeta}}{\zeta} \mathcal{I}_1 \right],$$

$$C_{qq}(x, \zeta) = P_{qq}(\zeta) (1 + \zeta^{-2\gamma}) \ln \left(\frac{\kappa_H^2 x^2 \zeta^2}{\mu_F^2 x_H^2} \right) - \frac{\beta_0}{2} \ln \left(\frac{\kappa_H^2 x^2 \zeta^2}{\mu_R^2 x_H^2} \right) \quad (\text{A5})$$

$$+ \delta(1 - \zeta) \left[C_A \ln \left(\frac{s_0 x_H^2}{\kappa_H^2 x^2} \right) \chi(n, \gamma) + C_A \left(\frac{85}{18} + \frac{\pi^2}{2} \right) - \frac{5}{9} n_f - 8 C_F \right.$$

$$\left. + \frac{C_A}{2} \left(\psi' \left(1 + \gamma + \frac{n}{2} \right) - \psi' \left(\frac{n}{2} - \gamma \right) - \chi^2(n, \gamma) \right) \right] + C_F \bar{\zeta} (1 + \zeta^{-2\gamma})$$

$$\begin{aligned}
& + (1 + \zeta^2) \left[C_A (1 + \zeta^{-2\gamma}) \frac{\chi(n, \gamma)}{2(1 - \zeta)_+} + (C_A - 2 C_F (1 + \zeta^{-2\gamma})) \frac{\ln \zeta}{1 - \zeta} \right] \\
& + \left(C_F - \frac{C_A}{2} \right) (1 + \zeta^2) \left[2(1 + \zeta^{-2\gamma}) \left(\frac{\ln(1 - \zeta)}{1 - \zeta} \right)_+ + \frac{\bar{\zeta}}{\zeta^2} \mathcal{I}_2 \right] ,
\end{aligned}$$

where s_0 is an artificial normalization scale to be suitably fixed. We define $\bar{\zeta} = 1 - \zeta$ and $\gamma = i\nu - 1/2$, while $P_{ij}(\zeta)$ are LO DGLAP kernels:

$$\begin{aligned}
P_{gq}(z) &= C_F \frac{1 + (1 - z)^2}{z} , \\
P_{qq}(z) &= T_R [z^2 + (1 - z)^2] , \\
P_{qg}(z) &= C_F \left(\frac{1 + z^2}{1 - z} \right)_+ = C_F \left[\frac{1 + z^2}{(1 - z)_+} + \frac{3}{2} \delta(1 - z) \right] , \\
P_{gg}(z) &= 2C_A \left[\frac{1}{(1 - z)_+} + \frac{1}{z} - 2 + z(1 - z) \right] + \left(\frac{11}{6} C_A - \frac{n_f}{3} \right) \delta(1 - z) .
\end{aligned} \tag{A6}$$

As for the $\mathcal{I}_{1,2,3}$ functions, one can write:

$$\begin{aligned}
\mathcal{I}_2 &= \frac{\zeta^2}{\bar{\zeta}^2} \left[\zeta \left(\frac{{}_2F_1(1, 1 + \gamma - \frac{n}{2}, 2 + \gamma - \frac{n}{2}, \zeta)}{\frac{n}{2} - \gamma - 1} - \frac{{}_2F_1(1, 1 + \gamma + \frac{n}{2}, 2 + \gamma + \frac{n}{2}, \zeta)}{\frac{n}{2} + \gamma + 1} \right) \right. \\
&\quad \left. + \zeta^{-2\gamma} \left(\frac{{}_2F_1(1, -\gamma - \frac{n}{2}, 1 - \gamma - \frac{n}{2}, \zeta)}{\frac{n}{2} + \gamma} - \frac{{}_2F_1(1, -\gamma + \frac{n}{2}, 1 - \gamma + \frac{n}{2}, \zeta)}{\frac{n}{2} - \gamma} \right) \right. \\
&\quad \left. + (1 + \zeta^{-2\gamma}) (\chi(n, \gamma) - 2 \ln \bar{\zeta}) + 2 \ln \zeta \right] ,
\end{aligned} \tag{A7}$$

$$\mathcal{I}_1 = \frac{\bar{\zeta}}{2\zeta} \mathcal{I}_2 + \frac{\zeta}{\bar{\zeta}} \left[\ln \zeta + \frac{1 - \zeta^{-2\gamma}}{2} (\chi(n, \gamma) - 2 \ln \bar{\zeta}) \right] , \tag{A8}$$

$$\mathcal{I}_3 = \frac{\bar{\zeta}}{2\zeta} \mathcal{I}_2 - \frac{\zeta}{\bar{\zeta}} \left[\ln \zeta + \frac{1 - \zeta^{-2\gamma}}{2} (\chi(n, \gamma) - 2 \ln \bar{\zeta}) \right] . \tag{A9}$$

In Eqs. (A2) and (A5) the *plus-prescription* is introduced:

$$\int_a^1 d\zeta \frac{F(\zeta)}{(1 - \zeta)_+} = \int_a^1 d\zeta \frac{F(\zeta) - F(1)}{(1 - \zeta)} - \int_0^a d\zeta \frac{F(1)}{(1 - \zeta)} , \tag{A10}$$

with $F(\zeta)$ a generic function, regular at $\zeta = 1$.

Appendix B: Forward-jet NLO impact factor

In the (n, ν) -representation, the expression for the NLO correction to the forward-jet impact factor in the small-cone limit reads (see Ref. [36] for further details):

$$\hat{c}^{(J)}(n, \nu, \kappa_J, x_J) = \frac{1}{\pi} \sqrt{\frac{C_F}{C_A}} (\kappa_J^2)^{i\nu - 1/2} \int_{x_J}^1 \frac{d\zeta}{\zeta} \zeta^{-\bar{\alpha}_s(\mu_R) \chi(n, \nu)} \tag{B1}$$

$$\begin{aligned}
& \left\{ \sum_{\alpha=q,\bar{q}} f_\alpha \left(\frac{x_J}{\zeta} \right) \left[\left(P_{qq}(\zeta) + \frac{C_A}{C_F} P_{gq}(\zeta) \right) \ln \frac{\kappa_J^2}{\mu_F^2} - 2\zeta^{-2\gamma} \ln R \{ P_{qq}(\zeta) + P_{gq}(\zeta) \} - \frac{\beta_0}{2} \ln \frac{\kappa_J^2}{\mu_R^2} \delta(1-\zeta) \right. \right. \\
& \quad \left. \left. + C_A \delta(1-\zeta) \left(\chi(n, \gamma) \ln \frac{s_0}{\kappa_J^2} + \frac{85}{18} + \frac{\pi^2}{2} + \frac{1}{2} \left(\psi' \left(1+\gamma + \frac{n}{2} \right) - \psi' \left(\frac{n}{2} - \gamma \right) - \chi^2(n, \gamma) \right) \right) \right. \right. \\
& \quad \left. \left. + (1+\zeta^2) \left\{ C_A \left(\frac{(1+\zeta^{-2\gamma}) \chi(n, \gamma)}{2(1-\zeta)_+} - \zeta^{-2\gamma} \left(\frac{\ln(1-\zeta)}{1-\zeta} \right)_+ \right) + \left(C_F - \frac{C_A}{2} \right) \left[\frac{\bar{\zeta}}{\zeta^2} \mathcal{I}_2 - \frac{2 \ln \zeta}{1-\zeta} + 2 \left(\frac{\ln(1-\zeta)}{1-\zeta} \right)_+ \right] \right\} \right. \right. \\
& \quad \left. \left. + \delta(1-\zeta) \left(C_F \left(3 \ln 2 - \frac{\pi^2}{3} - \frac{9}{2} \right) - \frac{5n_f}{9} \right) + C_A \zeta + C_F \bar{\zeta} \right. \right. \\
& \quad \left. \left. + \frac{1+\bar{\zeta}^2}{\zeta} \left(C_A \frac{\bar{\zeta}}{\zeta} \mathcal{I}_1 + 2C_A \ln \frac{\bar{\zeta}}{\zeta} + C_F \zeta^{-2\gamma} (\chi(n, \gamma) - 2 \ln \bar{\zeta}) \right) \right] + f_g \left(\frac{x_J}{\zeta} \right) \frac{C_A}{C_F} \left[\left(P_{gg}(\zeta) + 2n_f \frac{C_F}{C_A} P_{gq}(\zeta) \right) \ln \frac{\kappa_J^2}{\mu_F^2} \right. \right. \\
& \quad \left. \left. - 2\zeta^{-2\gamma} \ln R (P_{gg}(\zeta) + 2n_f P_{gq}(\zeta)) - \frac{\beta_0}{2} \ln \frac{\kappa_J^2}{4\mu_R^2} \delta(1-\zeta) + C_A \delta(1-\zeta) \left(\chi(n, \gamma) \ln \frac{s_0}{\kappa_J^2} + \frac{1}{12} + \frac{\pi^2}{6} \right. \right. \\
& \quad \left. \left. + \frac{1}{2} \left(\psi' \left(1+\gamma + \frac{n}{2} \right) - \psi' \left(\frac{n}{2} - \gamma \right) - \chi^2(n, \gamma) \right) \right) + 2C_A (1-\zeta^{-2\gamma}) \left(\left(\frac{1}{\zeta} - 2 + \zeta \bar{\zeta} \right) \ln \bar{\zeta} + \frac{\ln(1-\zeta)}{1-\zeta} \right) \right. \right. \\
& \quad \left. \left. + C_A \left[\frac{1}{\zeta} + \frac{1}{(1-\zeta)_+} - 2 + \zeta \bar{\zeta} \right] \left((1+\zeta^{-2\gamma}) \chi(n, \gamma) - 2 \ln \zeta + \frac{\bar{\zeta}^2}{\zeta^2} \mathcal{I}_2 \right) \right. \right. \\
& \quad \left. \left. + n_f \left[2\zeta \bar{\zeta} \frac{C_F}{C_A} + (\zeta^2 + \bar{\zeta}^2) \left(\frac{C_F}{C_A} \chi(n, \gamma) + \frac{\bar{\zeta}}{\zeta} \mathcal{I}_3 \right) - \frac{1}{12} \delta(1-\zeta) \right] \right] \right\} ,
\end{aligned}$$

with R the jet-cone radius, s_0 an artificial normalization scale whose value needs to be appropriately chosen, $\bar{\zeta} = 1 - \zeta$ and $\gamma = i\nu - 1/2$. $P_{ij}(\zeta)$ are LO DGLAP kernels defined in Eq. (A6), the $\mathcal{I}_{1,2,3}$ functions are given in Eqs. (A7)-(A9) and the plus-prescription is written in Eq. (A10).

Bibliography

- [1] L.V. Gribov, E.M. Levin, M.G. Ryskin, *Semihard Processes in QCD*, Phys. Rept. **100** (1983) 1. doi:[10.1016/0370-1573\(83\)90022-4](https://doi.org/10.1016/0370-1573(83)90022-4) (Cited on page 2.)
- [2] V.S. Fadin, E. Kuraev, L.N. Lipatov, *On the Pomeranchuk Singularity in Asymptotically Free Theories*, Phys. Lett. B **60**, (1975) 50 doi:[10.1016/0370-2693\(75\)90524-9](https://doi.org/10.1016/0370-2693(75)90524-9). (Cited on page 3.)
- [3] E. Kuraev, L.N. Lipatov, V.S. Fadin, *Multi-reggeon processes in the Yang-Mills theory*, Zh. Eksp. Teor. Fiz. **71** (1976) 840 [Sov. Phys. JETP **44**, (1976) 443]. (Cited on page 3.)
- [4] E. Kuraev, L.N. Lipatov, V.S. Fadin, *The Pomeranchuk Singularity in Nonabelian Gauge Theories*, Zh. Eksp. Teor. Fiz. **72** (1976) 377 [Sov. Phys. JETP **45**, (1977) 199]. (Cited on page 3.)
- [5] I. Balitsky, L.N. Lipatov, *The Pomeranchuk Singularity in Quantum Chromodynamics*, Sov. J. Nucl. Phys. **28**, (1978) 822. (Cited on page 3.)
- [6] R.G. Newton, *Optical theorem and beyond*, Am. J. Phys. **44** (1976) 639 doi:[10.1119/1.10324](https://doi.org/10.1119/1.10324). (Cited on page 3.)
- [7] V.S. Fadin, L.N. Lipatov, *BFKL pomeron in the next-to-leading approximation*, Phys. Lett. B **429** (1998) 127 doi:[10.1016/S0370-2693\(98\)00473-0](https://doi.org/10.1016/S0370-2693(98)00473-0) [hep-ph/9802290]. (Cited on page 3.)

- [8] M. Ciafaloni, G. Camici, *Energy scale(s) and next-to-leading BFKL equation*, Phys. Lett. B **430** (1998) 349 doi:[10.1016/S0370-2693\(98\)00551-6](https://doi.org/10.1016/S0370-2693(98)00551-6) [hep-ph/9803389]. (Cited on page 3.)
- [9] V.S. Fadin, R. Fiore, A. Papa, *The Quark part of the nonforward BFKL kernel and the 'bootstrap' for the gluon Reggeization*, Phys. Rev. D **60** (1999) 074025 doi:[10.1103/PhysRevD.60.074025](https://doi.org/10.1103/PhysRevD.60.074025) [hep-ph/9812456]. (Cited on page 3.)
- [10] V.S. Fadin, D.A. Gorbachev, *Nonforward color octet BFKL kernel*, JETP Lett. **71** (2000) 222 [Pisma Zh. Eksp. Teor. Fiz. **71** (2000) 322] [Yad. Fiz. **63** (12) (2000) 1] doi:[10.1134/1.568320](https://doi.org/10.1134/1.568320). (Cited on page 3.)
- [11] V.S. Fadin, R. Fiore, *Non-forward BFKL pomeron at next-to-leading order*, Phys. Lett. B **610** (2005) 61 Erratum: [Phys. Lett. B **621** (2005) 320] doi:[10.1016/j.physletb.2005.06.074](https://doi.org/10.1016/j.physletb.2005.06.074), doi:[10.1016/j.physletb.2005.01.062](https://doi.org/10.1016/j.physletb.2005.01.062) [hep-ph/0412386]. (Cited on page 3.)
- [12] V.S. Fadin, R. Fiore, *Non-forward NLO BFKL kernel*, Phys. Rev. D **72** (2005) 014018 doi:[10.1103/PhysRevD.72.014018](https://doi.org/10.1103/PhysRevD.72.014018) [hep-ph/0502045]. (Cited on page 3.)
- [13] *The Gluon Impact Factors*, V.S. Fadin, R. Fiore, M.I. Kotsky, A. Papa, Phys. Rev. D **61** (2000) 094005 doi:[10.1103/PhysRevD.61.094005](https://doi.org/10.1103/PhysRevD.61.094005) [arXiv:9908264 [hep-ph]]. (Cited on page 3.)
- [14] *The Quark Impact Factors*, V.S. Fadin, R. Fiore, M.I. Kotsky, A. Papa, Phys. Rev. D **61** (2000) 094006 doi:[10.1103/PhysRevD.61.094006](https://doi.org/10.1103/PhysRevD.61.094006) [arXiv:9908265 [hep-ph]]. (Cited on page 3.)
- [15] M. Ciafaloni, *Energy scale and coherence effects in small x equations*, Phys. Lett. B **429**, (1998) 363 doi:[10.1016/S0370-2693\(98\)00249-4](https://doi.org/10.1016/S0370-2693(98)00249-4) [hep-ph/9801322]. (Cited on page 3.)
- [16] M. Ciafaloni, D. Colferai, *K factorization and impact factors at next-to-leading level*, Nucl. Phys. B **538**, (1999) 187 doi:[10.1016/S0550-3213\(98\)00621-X](https://doi.org/10.1016/S0550-3213(98)00621-X) [hep-ph/9806350]. (Cited on page 3.)
- [17] M. Ciafaloni, G. Rodrigo, *Heavy quark impact factor at next-to-leading level*, JHEP **0005** (2000) 042 doi:[10.1088/1126-6708/2000/05/042](https://doi.org/10.1088/1126-6708/2000/05/042) [hep-ph/0004033]. (Cited on page 3.)
- [18] J. Bartels, D. Colferai, G.P. Vacca, *The NLO jet vertex for Mueller-Navelet and forward jets: The Quark part*, Eur. Phys. J. C **24** (2002) 83 doi:[10.1007/s100520200919](https://doi.org/10.1007/s100520200919) [hep-ph/0112283]. (Cited on pages 3 and 11.)
- [19] J. Bartels, D. Colferai, G.P. Vacca, *The NLO jet vertex for Mueller-Navelet and forward jets: The Gluon part*, Eur. Phys. J. C **29** (2003) 235 doi:[10.1140/epjc/s2003-01169-5](https://doi.org/10.1140/epjc/s2003-01169-5) [hep-ph/0206290]. (Cited on page 3.)
- [20] F. Caporale, D.Yu. Ivanov, B. Murdaca, A. Papa, A. Perri, *The next-to-leading order jet vertex for Mueller-Navelet and forward jets revisited*, JHEP **1202** (2012) 101 doi:[10.1007/JHEP02\(2012\)101](https://doi.org/10.1007/JHEP02(2012)101) [arXiv:1112.3752 [hep-ph]]. (Cited on pages 3 and 11.)
- [21] D.Yu. Ivanov, A. Papa, *The next-to-leading order forward jet vertex in the small-cone approximation*, JHEP **1205** (2012) 086 doi:[10.1007/JHEP05\(2012\)086](https://doi.org/10.1007/JHEP05(2012)086) [arXiv:1202.1082 [hep-ph]]. (Cited on pages 3 and 11.)
- [22] D. Colferai, A. Niccoli, *The NLO jet vertex in the small-cone approximation for kt and cone algorithms*, JHEP **1504** (2015) 071 doi:[10.1007/JHEP04\(2015\)071](https://doi.org/10.1007/JHEP04(2015)071) [arXiv:1501.07442 [hep-ph]]. (Cited on pages 3 and 11.)
- [23] D.Yu. Ivanov, A. Papa, *Inclusive production of a pair of hadrons separated by a large interval of rapidity in proton collisions*, JHEP **1207** (2012) 045 doi:[10.1007/JHEP07\(2012\)045](https://doi.org/10.1007/JHEP07(2012)045) [arXiv:1205.6068 [hep-ph]]. (Cited on page 3.)
- [24] D.Yu. Ivanov, M.I. Kotsky, A. Papa, *The Impact factor for the virtual photon to light vector meson transition*, Eur. Phys. J. C **38** (2004) 195 doi:[10.1140/epjc/s2004-02039-4](https://doi.org/10.1140/epjc/s2004-02039-4) [hep-ph/0405297]. (Cited on page 3.)
- [25] J. Bartels, S. Gieseke, C. F. Qiao, *The (γ^* $\rightarrow q \bar{q}$) Reggeon vertex in next-to-leading order QCD*, Phys. Rev. D **63** (2001) 056014 Erratum: [Phys. Rev. D **65** (2002) 079902] doi:[10.1103/PhysRevD.63.056014](https://doi.org/10.1103/PhysRevD.63.056014), doi:[10.1103/PhysRevD.65.079902](https://doi.org/10.1103/PhysRevD.65.079902) [hep-ph/0009102]. (Cited on page 3.)
- [26] J. Bartels, S. Gieseke, A. Kyrieleis, *The Process $\gamma^*(L) + q \rightarrow (q \bar{q}) + q$: Real corrections to the virtual photon impact factor*, Phys. Rev. D **65** (2002) 014006 doi:[10.1103/PhysRevD.65.014006](https://doi.org/10.1103/PhysRevD.65.014006) [hep-ph/0107152]. (Cited on page 3.)
- [27] J. Bartels, D. Colferai, S. Gieseke, A. Kyrieleis, *NLO corrections to the photon impact factor: Combining real and virtual corrections*, Phys. Rev. D **66** (2002) 094017 doi:[10.1103/PhysRevD.66.094017](https://doi.org/10.1103/PhysRevD.66.094017) [hep-ph/0208130]. (Cited on page 3.)
- [28] J. Bartels, *The photon impact factor in next-to-leading order*, Nucl. Phys. Proc. Suppl. **116** (2003) 126. doi:[10.1016/S0920-5632\(03\)80156-1](https://doi.org/10.1016/S0920-5632(03)80156-1) (Cited on page 3.)
- [29] J. Bartels, A. Kyrieleis, *NLO corrections to the γ^* impact factor: First numerical results for the real corrections to $\gamma^*(L)$* , Phys. Rev. D **70** (2004) 114003 doi:[10.1103/PhysRevD.70.114003](https://doi.org/10.1103/PhysRevD.70.114003) [hep-ph/0407051]. (Cited on page 3.)
- [30] V.S. Fadin, D.Yu. Ivanov, M.I. Kotsky, *Photon Reggeon interaction vertices in the NLA*, Phys. Atom. Nucl. **65** (2002) 1513 [Yad. Fiz. **65** (2002) 1551] doi:[10.1134/1.1501664](https://doi.org/10.1134/1.1501664) [hep-ph/0106099]. (Cited on page 3.)
- [31] I. Balitsky, G.A. Chirilli, *Photon impact factor and k_T -factorization for DIS in the next-to-leading order*, Phys. Rev. D **87** (2013) no.1, 014013 doi:[10.1103/PhysRevD.87.014013](https://doi.org/10.1103/PhysRevD.87.014013) [arXiv:1207.3844 [hep-ph]]. (Cited on page 3.)

- [32] F.G. Celiberto, PhD thesis, *High-energy resummation in semi-hard processes at the LHC*, arXiv:1707.04315 [hep-ph]. (Cited on page 3.)
- [33] A.H. Mueller, H. Navelet, *An Inclusive Minijet Cross-Section and the Bare Pomeron in QCD*, Nucl. Phys. B **282** (1987) 727 doi:[10.1016/0550-3213\(87\)90705-X](https://doi.org/10.1016/0550-3213(87)90705-X). (Cited on pages 3 and 28.)
- [34] C. Marquet, C. Royon, *Azimuthal decorrelation of Mueller-Navelet jets at the Tevatron and the LHC*, Phys. Rev. D **79** (2009), 034028 doi:[10.1103/PhysRevD.79.034028](https://doi.org/10.1103/PhysRevD.79.034028) [arXiv:0704.3409 [hep-ph]]. (Cited on page 3.)
- [35] D. Colferai, F. Schwennsen, L. Szymanowski, S. Wallon, *Mueller Navelet jets at LHC - complete NLL BFKL calculation*, JHEP **1012** (2010) 026 doi:[10.1007/JHEP12\(2010\)026](https://doi.org/10.1007/JHEP12(2010)026) [arXiv:1002.1365 [hep-ph]]. (Cited on page 3.)
- [36] F. Caporale, D.Yu. Ivanov, B. Murdaca, A. Papa, *Mueller-Navelet small-cone jets at LHC in next-to-leading BFKL*, Nucl. Phys. B **877** (2013) 73 doi:[10.1016/j.nuclphysb.2013.09.013](https://doi.org/10.1016/j.nuclphysb.2013.09.013) [arXiv:1211.7225 [hep-ph]]. (Cited on pages 3, 7 and 34.)
- [37] B. Ducloué, L. Szymanowski, S. Wallon, *Confronting Mueller-Navelet jets in NLL BFKL with LHC experiments at 7 TeV*, JHEP **1305** (2013) 096 doi:[10.1007/JHEP05\(2013\)096](https://doi.org/10.1007/JHEP05(2013)096) [arXiv:1302.7012 [hep-ph]]. (Cited on pages 3, 11 and 28.)
- [38] B. Ducloué, L. Szymanowski, S. Wallon, *Evidence for high-energy resummation effects in Mueller-Navelet jets at the LHC*, Phys. Rev. Lett. **112** (2014) 082003 doi:[10.1103/PhysRevLett.112.082003](https://doi.org/10.1103/PhysRevLett.112.082003) [arXiv:1309.3229 [hep-ph]]. (Cited on pages 3 and 14.)
- [39] F. Caporale, B. Murdaca, A. Sabio Vera, C. Salas, *Scale choice and collinear contributions to Mueller-Navelet jets at LHC energies*, Nucl. Phys. B **875** (2013) 134 doi:[10.1016/j.nuclphysb.2013.07.005](https://doi.org/10.1016/j.nuclphysb.2013.07.005) [arXiv:1305.4620 [hep-ph]]. (Cited on pages 3 and 14.)
- [40] B. Ducloué, L. Szymanowski, S. Wallon, *Violation of energy-momentum conservation in Mueller-Navelet jets production*, Phys. Lett. B **738** (2014) 311 doi:[10.1016/j.physletb.2014.09.025](https://doi.org/10.1016/j.physletb.2014.09.025) [arXiv:1407.6593 [hep-ph]]. (Cited on pages 3 and 5.)
- [41] F. Caporale, D.Yu. Ivanov, B. Murdaca, A. Papa, *Mueller-Navelet jets in next-to-leading order BFKL: theory versus experiment*, Eur. Phys. J. C **74** (2014) no.10, 3084 Erratum: [Eur. Phys. J. C **75** (2015) no.11, 535] doi:[10.1140/epjc/s10052-014-3084-z](https://doi.org/10.1140/epjc/s10052-014-3084-z), doi:[10.1140/epjc/s10052-015-3754-5](https://doi.org/10.1140/epjc/s10052-015-3754-5) [arXiv:1407.8431 [hep-ph]]. (Cited on pages 3, 7, 11, 13 and 14.)
- [42] B. Ducloué, L. Szymanowski, S. Wallon, *Evaluating the double parton scattering contribution to Mueller-Navelet jets production at the LHC*, Phys. Rev. D **92** (2015) no.7, 076002 doi:[10.1103/PhysRevD.92.076002](https://doi.org/10.1103/PhysRevD.92.076002) [arXiv:1507.04735 [hep-ph]]. (Cited on page 3.)
- [43] F. Caporale, D.Yu. Ivanov, B. Murdaca, A. Papa, *Brodsky-Lepage-Mackenzie optimal renormalization scale setting for semihard processes*, Phys. Rev. D **91** (2015) no.11, 114009 doi:[10.1103/PhysRevD.91.114009](https://doi.org/10.1103/PhysRevD.91.114009) [arXiv:1504.06471 [hep-ph]]. (Cited on pages 3, 15 and 16.)
- [44] F.G. Celiberto, D.Yu. Ivanov, B. Murdaca, A. Papa, *Mueller-Navelet Jets at LHC: BFKL Versus High-Energy DGLAP*, Eur. Phys. J. C **75** (2015) no.6, 292 doi:[10.1140/epjc/s10052-015-3522-6](https://doi.org/10.1140/epjc/s10052-015-3522-6) [arXiv:1504.08233 [hep-ph]]. (Cited on pages 3, 5, 19, 20 and 30.)
- [45] F.G. Celiberto, D.Yu. Ivanov, B. Murdaca, A. Papa, *Mueller-Navelet Jets at the LHC: Discriminating BFKL from DGLAP by Asymmetric Cuts*, Acta Phys. Polon. Supp. **8** (2015) 935 doi:[10.5506/APhysPolBSupp.8.935](https://doi.org/10.5506/APhysPolBSupp.8.935) [arXiv:1510.01626 [hep-ph]]. (Cited on pages 3, 5 and 19.)
- [46] F.G. Celiberto, D.Yu. Ivanov, B. Murdaca, A. Papa, *Mueller-Navelet jets at 13 TeV LHC: dependence on dynamic constraints in the central rapidity region*, Eur. Phys. J. C **76** (2016) no.4, 224 doi:[10.1140/epjc/s10052-016-4053-5](https://doi.org/10.1140/epjc/s10052-016-4053-5) [arXiv:1601.07847 [hep-ph]]. (Cited on page 3.)
- [47] F.G. Celiberto, D.Yu. Ivanov, B. Murdaca, A. Papa, *BFKL effects and central rapidity dependence in Mueller-Navelet jet production at 13 TeV LHC*, PoS DIS **2016** (2016) 176 doi:[10.22323/1.265.0176](https://doi.org/10.22323/1.265.0176) [arXiv:1606.08892 [hep-ph]]. (Cited on page 3.)
- [48] F. Caporale, F.G. Celiberto, G. Chachamis, D. Gordo Gómez, A. Sabio Vera, *Inclusive dijet hadroproduction with a rapidity veto constraint*, Nucl. Phys. B **935** (2018) 412 doi:[10.1016/j.nuclphysb.2018.09.002](https://doi.org/10.1016/j.nuclphysb.2018.09.002) [arXiv:1806.06309 [hep-ph]]. (Cited on pages 3 and 14.)
- [49] G. Chachamis, *BFKL phenomenology*, In: Proceedings of the summer school and workshop on high energy physics at the LHC: New trends in HEP, October 21 - November 6, 2014, Natal, Brazil, arXiv:1512.04430 [hep-ph]. (Cited on page 3.)
- [50] V. Khachatryan *et al.* [CMS Collaboration], *Azimuthal decorrelation of jets widely separated in rapidity in pp collisions at $\sqrt{s} = 7$ TeV*, JHEP **1608** (2016) 139 doi:[10.1007/JHEP08\(2016\)139](https://doi.org/10.1007/JHEP08(2016)139) [arXiv:1601.06713 [hep-ex]]. (Cited on pages 4, 5, 12 and 13.)
- [51] F. Caporale, G. Chachamis, B. Murdaca, A. Sabio Vera, *Balitsky-Fadin-Kuraev-Lipatov Predictions for Inclusive Three Jet Production at the LHC*, Phys. Rev. Lett. **116** (2016) no.1, 012001 doi:[10.1103/PhysRevLett.116.012001](https://doi.org/10.1103/PhysRevLett.116.012001) [arXiv:1508.07711 [hep-ph]]. (Cited on page 4.)

- [52] F. Caporale, F.G. Celiberto, G. Chachamis, A. Sabio Vera, *Multi-Regge kinematics and azimuthal angle observables for inclusive four-jet production*, Eur. Phys. J. C **76** (2016) no.3, 165 doi:[10.1140/epjc/s10052-016-3963-6](https://doi.org/10.1140/epjc/s10052-016-3963-6) [arXiv:1512.03364 [hep-ph]]. (Cited on page 4.)
- [53] F. Caporale, F.G. Celiberto, G. Chachamis, D. Gordo Gómez, A. Sabio Vera, *BFKL Azimuthal Imprints in Inclusive Three-jet Production at 7 and 13 TeV*, Nucl. Phys. B **910** (2016) 374 doi:[10.1016/j.nuclphysb.2016.07.012](https://doi.org/10.1016/j.nuclphysb.2016.07.012) [arXiv:1603.07785 [hep-ph]]. (Cited on page 4.)
- [54] F. Caporale, F.G. Celiberto, G. Chachamis, A. Sabio Vera, *Inclusive four-jet production: a study of Multi-Regge kinematics and BFKL observables*, PoS DIS **2016** (2016) 177 doi:[10.22323/1.265.0177](https://doi.org/10.22323/1.265.0177) [arXiv:1610.01880 [hep-ph]]. (Cited on page 4.)
- [55] F. Caporale, F.G. Celiberto, G. Chachamis, D. Gordo Gómez, A. Sabio Vera, *Inclusive Four-jet Production at 7 and 13 TeV: Azimuthal Profile in Multi-Regge Kinematics*, Eur. Phys. J. C **77** (2017) no.1, 5 doi:[10.1140/epjc/s10052-016-4557-z](https://doi.org/10.1140/epjc/s10052-016-4557-z) arXiv:1606.00574 [hep-ph]. (Cited on page 4.)
- [56] F.G. Celiberto, *BFKL phenomenology: resummation of high-energy logs in semi-hard processes at LHC*, Frascati Phys. Ser. **63** (2016) 43 [arXiv:1606.07327 [hep-ph]]. (Cited on page 4.)
- [57] F. Caporale, F.G. Celiberto, G. Chachamis, D. Gordo Gómez, A. Sabio Vera, *Inclusive three- and four-jet production in multi-Regge kinematics at the LHC*, AIP Conf. Proc. **1819** (2017) no.1, 060009 doi:[10.1063/1.4977165](https://doi.org/10.1063/1.4977165) [arXiv:1611.04813 [hep-ph]]. (Cited on page 4.)
- [58] F. Caporale, F.G. Celiberto, G. Chachamis, D. Gordo Gómez, A. Sabio Vera, *Probing the BFKL dynamics in inclusive three jet production at the LHC*, EPJ Web Conf. **164** (2017) 07027 doi:[10.1051/epjconf/201716407027](https://doi.org/10.1051/epjconf/201716407027) [arXiv:1612.02771 [hep-ph]]. (Cited on page 4.)
- [59] F. Caporale, F.G. Celiberto, G. Chachamis, D. Gordo Gómez, A. Sabio Vera, *Stability of Azimuthal-angle Observables under Higher Order Corrections in Inclusive Three-jet Production*, Phys. Rev. D **95** (2017) no.7, 074007 doi:[10.1103/PhysRevD.95.074007](https://doi.org/10.1103/PhysRevD.95.074007) [arXiv:1612.05428 [hep-ph]]. (Cited on page 4.)
- [60] F.G. Celiberto, D.Yu. Ivanov, B. Murdaca, A. Papa, *High energy resummation in dihadron production at the LHC*, Phys. Rev. D **94** (2016) no.3, 034013 doi:[10.1103/PhysRevD.94.034013](https://doi.org/10.1103/PhysRevD.94.034013) [arXiv:1604.08013 [hep-ph]]. (Cited on pages 4, 10 and 17.)
- [61] F.G. Celiberto, D.Yu. Ivanov, B. Murdaca, A. Papa, *Dihadron Production at LHC: BFKL Predictions for Cross Sections and Azimuthal Correlations*, AIP Conf. Proc. **1819** (2017) no.1, 060005 doi:[10.1063/1.4977161](https://doi.org/10.1063/1.4977161) [arXiv:1611.04811 [hep-ph]]. (Cited on page 4.)
- [62] F.G. Celiberto, D.Yu. Ivanov, B. Murdaca, A. Papa, *Dihadron production at the LHC: full next-to-leading BFKL calculation*, Eur. Phys. J. C **77** (2017) no.6, 382 doi:[10.1140/epjc/s10052-017-4949-8](https://doi.org/10.1140/epjc/s10052-017-4949-8) [arXiv:1701.05077 [hep-ph]]. (Cited on pages 4 and 17.)
- [63] A.D. Bolognino, F.G. Celiberto, D.Yu. Ivanov, M.M.A. Mohammed, A. Papa, *Hadron-jet correlations in high-energy hadronic collisions at the LHC*, Eur. Phys. J. C **78** (2018) no.9, 772 doi:[10.1140/epjc/s10052-018-6253-7](https://doi.org/10.1140/epjc/s10052-018-6253-7) [arXiv:1808.05483 [hep-ph]]. (Cited on pages 4, 6 and 10.)
- [64] A.D. Bolognino, F.G. Celiberto, D.Yu. Ivanov, M.M.A. Mohammed, A. Papa, *Inclusive hadron-jet production at the LHC*, Acta Phys. Polon. Supp. **12** (2019) no.4, 773 doi:[10.5506/APhysPolBSupp.12.773](https://doi.org/10.5506/APhysPolBSupp.12.773) [arXiv:1902.04511 [hep-ph]]. (Cited on page 4.)
- [65] A.D. Bolognino, F.G. Celiberto, D.Yu. Ivanov, M.M.A. Mohammed, A. Papa, *High-energy effects in forward inclusive dijet and hadron-jet production*, PoS DIS **2019** (2019) 049 doi:[10.22323/1.352.0049](https://doi.org/10.22323/1.352.0049) [arXiv:1906.11800 [hep-ph]]. (Cited on page 4.)
- [66] F.G. Celiberto, D.Yu. Ivanov, A. Papa, *Diffractive production of Λ hyperons in the high-energy limit of strong interactions*, Phys. Rev. D **102** (2020) no.9, 094019 doi:[10.1103/PhysRevD.102.094019](https://doi.org/10.1103/PhysRevD.102.094019) [arXiv:2008.10513 [hep-ph]]. (Cited on page 4.)
- [67] S.J. Brodsky, V.S. Fadin, V.T. Kim, L.N. Lipatov, G.B. Pivovarov, *High-energy QCD asymptotics of photon-photon collisions*, JETP Lett. **76** (2002) 249 [Pisma Zh. Eksp. Teor. Fiz. **76** (2002) 306] doi:[10.1134/1.1520615](https://doi.org/10.1134/1.1520615) [hep-ph/0207297]. (Cited on page 4.)
- [68] S.J. Brodsky, V.S. Fadin, V.T. Kim, L.N. Lipatov, G. B. Pivovarov, *The QCD pomeron with optimal renormalization*, JETP Lett. **70** (1999) 155 doi:[10.1134/1.568145](https://doi.org/10.1134/1.568145) [hep-ph/9901229]. (Cited on page 4.)
- [69] F. Caporale, D.Yu. Ivanov, A. Papa, *BFKL resummation effects in the $\gamma^* \gamma^*$ gamma* gamma* total hadronic cross section*, Eur. Phys. J. C **58** (2008) 1 doi:[10.1140/epjc/s10052-008-0732-1](https://doi.org/10.1140/epjc/s10052-008-0732-1) [arXiv:0807.3231 [hep-ph]]. (Cited on page 4.)
- [70] X.C. Zheng, X.G. Wu, S.Q. Wang, J.M. Shen, Q.L. Zhang, *Reanalysis of the BFKL Pomeron at the next-to-leading logarithmic accuracy*, JHEP **1310** (2013) 117 doi:[10.1007/JHEP10\(2013\)117](https://doi.org/10.1007/JHEP10(2013)117) [arXiv:1308.2381 [hep-ph]]. (Cited on page 4.)
- [71] G.A. Chirilli, Y.V. Kovchegov, *$\gamma^* \gamma^*$ Cross Section at NLO and Properties of the BFKL Evolution at Higher Orders*, JHEP **1405** (2014) 099 Erratum: [JHEP **1508** (2015) 075] doi:[10.1007/JHEP05\(2014\)099](https://doi.org/10.1007/JHEP05(2014)099)

- 10.1007/JHEP08(2015)075 [arXiv:1403.3384 [hep-ph]]. (Cited on page 4.)
- [72] D.Yu. Ivanov, B. Murdaca, A. Papa, *The $\gamma^*\gamma^*$ total cross section in next-to-leading order BFKL and LEP2 data*, JHEP **1410** (2014) 058 doi:[10.1007/JHEP10\(2014\)058](https://doi.org/10.1007/JHEP10(2014)058) [arXiv:1407.8447 [hep-ph]]. (Cited on page 4.)
- [73] M. Deak, L. Frankfurt, M. Strikman, A. Stašto, *Taming of preasymptotic small x evolution within resummation framework*, arXiv:2001.01276 [hep-ph]. (Cited on page 4.)
- [74] B.I. Ermolaev, D.Yu. Ivanov, S.I. Troyan, *Elastic scattering of virtual photons via a quark loop in the double-logarithmic approximation*, Phys. Rev. D **97** (2018) no.7, 076007 doi:[10.1103/PhysRevD.97.076007](https://doi.org/10.1103/PhysRevD.97.076007) [arXiv:1708.01437 [hep-ph]]. (Cited on page 4.)
- [75] B. Ermolaev, S. Troyan, *Light-by-light scattering in Double-Logarithmic Approximation*, Eur. Phys. J. C **78** (2018) no.6, 517 doi:[10.1140/epjc/s10052-018-5998-3](https://doi.org/10.1140/epjc/s10052-018-5998-3) [arXiv:1708.02446 [hep-ph]]. (Cited on page 4.)
- [76] J. Bartels, B.I. Ermolaev, M.G. Ryskin, *Nonsinglet contributions to the structure function g_1 at small x* , Z. Phys. C **70** (1996) 273 [hep-ph/9507271]. (Cited on page 4.)
- [77] J. Bartels, B.I. Ermolaev, M.G. Ryskin, *Flavor singlet contribution to the structure function $G(1)$ at small x* , Z. Phys. C **72** (1996) 627 doi:[10.1007/s002880050285](https://doi.org/10.1007/s002880050285), doi:[10.1007/BF02909194](https://doi.org/10.1007/BF02909194) [hep-ph/9603204]. (Cited on page 4.)
- [78] Y.V. Kovchegov, D. Pitonyak, M.D. Sievert, *Helicity Evolution at Small- x* , JHEP **1601** (2016) 072 Erratum: [JHEP **1610** (2016) 148] doi:[10.1007/JHEP01\(2016\)072](https://doi.org/10.1007/JHEP01(2016)072), doi:[10.1007/JHEP10\(2016\)148](https://doi.org/10.1007/JHEP10(2016)148) [arXiv:1511.06737 [hep-ph]]. (Cited on page 4.)
- [79] Y.V. Kovchegov, D. Pitonyak, M.D. Sievert, *Small- x asymptotics of the quark helicity distribution*, Phys. Rev. Lett. **118** (2017) no.5, 052001 doi:[10.1103/PhysRevLett.118.052001](https://doi.org/10.1103/PhysRevLett.118.052001) [arXiv:1610.06188 [hep-ph]]. (Cited on page 4.)
- [80] Y.V. Kovchegov, D. Pitonyak, M.D. Sievert, *Helicity Evolution at Small x : Flavor Singlet and Non-Singlet Observables*, Phys. Rev. D **95** (2017) no.1, 014033 doi:[10.1103/PhysRevD.95.014033](https://doi.org/10.1103/PhysRevD.95.014033) [arXiv:1610.06197 [hep-ph]]. (Cited on page 4.)
- [81] Y.V. Kovchegov, D. Pitonyak, M.D. Sievert, *Small- x Asymptotics of the Quark Helicity Distribution: Analytic Results*, Phys. Lett. B **772** (2017) 136 doi:[10.1016/j.physletb.2017.06.032](https://doi.org/10.1016/j.physletb.2017.06.032) [arXiv:1703.05809 [hep-ph]]. (Cited on page 4.)
- [82] Y.V. Kovchegov, D. Pitonyak, M.D. Sievert, *Small- x Asymptotics of the Gluon Helicity Distribution*, JHEP **1710** (2017) 198 doi:[10.1007/JHEP10\(2017\)198](https://doi.org/10.1007/JHEP10(2017)198) [arXiv:1706.04236 [nucl-th]]. (Cited on page 4.)
- [83] K.G. Wilson, *Confinement of Quarks*, Phys. Rev. D **10** (1974) 2445. doi:[10.1103/PhysRevD.10.2445](https://doi.org/10.1103/PhysRevD.10.2445) (Cited on page 4.)
- [84] Y.V. Kovchegov, M.D. Sievert, *Valence Quark Transversity at Small x* , Phys. Rev. D **99** (2019) no.5, 054033 doi:[10.1103/PhysRevD.99.054033](https://doi.org/10.1103/PhysRevD.99.054033) [arXiv:1808.10354 [hep-ph]]. (Cited on page 4.)
- [85] Y.V. Kovchegov, *Orbital Angular Momentum at Small x* , JHEP **1903** (2019) 174 doi:[10.1007/JHEP03\(2019\)174](https://doi.org/10.1007/JHEP03(2019)174) [arXiv:1901.07453 [hep-ph]]. (Cited on page 4.)
- [86] V.G. Gorshkov, V.N. Gribov, L.N. Lipatov, G.V. Frolov, *Doubly logarithmic asymptotic behavior in quantum electrodynamics*, Sov. J. Nucl. Phys. **6** (1968) 95 [Yad. Fiz. **6** (1967) 129]. (Cited on page 4.)
- [87] V.G. Gorshkov, V.N. Gribov, L.N. Lipatov, G.V. Frolov, *Backward electron - positron scattering at high-energies*, Sov. J. Nucl. Phys. **6** (1968) 262 [Yad. Fiz. **6** (1967) 361]. (Cited on page 4.)
- [88] R. Kirschner, L.N. Lipatov, *Doubly Logarithmic Asymptotic Of The Quark Scattering Amplitude With Nonvacuum Exchange In The T Channel*, Sov. Phys. JETP **56** (1982) 266 [Zh. Eksp. Teor. Fiz. **83** (1982) 488]. (Cited on page 4.)
- [89] R. Kirschner, L.N. Lipatov, *Double Logarithmic Asymptotics and Regge Singularities of Quark Amplitudes with Flavor Exchange*, Nucl. Phys. B **213** (1983) 122. doi:[10.1016/0550-3213\(83\)90178-5](https://doi.org/10.1016/0550-3213(83)90178-5) (Cited on page 4.)
- [90] J. Bartels, M. Lublinsky, *Quark anti-quark exchange in $\gamma^*\gamma^*$ scattering*, JHEP **0309** (2003) 076 doi:[10.1088/1126-6708/2003/09/076](https://doi.org/10.1088/1126-6708/2003/09/076) [hep-ph/0308181]. (Cited on page 4.)
- [91] J. Bartels, M. Lublinsky, *$\gamma^*\gamma^*$ scattering via secondary Reggeon exchange in QCD*, Mod. Phys. Lett. A **19** (2004) 19691982 doi:[10.1142/S021773230415191](https://doi.org/10.1142/S021773230415191) [hep-ph/0406273]. (Cited on page 4.)
- [92] B. Pire, L. Szymanowski, S. Wallon, *Double diffractive rho-production in $\gamma^*\gamma^*$ collisions*, Eur. Phys. J. C **44** (2005), 545-558 doi:[10.1140/epjc/s2005-02386-6](https://doi.org/10.1140/epjc/s2005-02386-6) [arXiv:hep-ph/0507038 [hep-ph]]. (Cited on page 4.)
- [93] M. Segond, L. Szymanowski, S. Wallon, Eur. Phys. J. C **52** (2007), 93-112 doi:[10.1140/epjc/s10052-007-0365-9](https://doi.org/10.1140/epjc/s10052-007-0365-9) [arXiv:hep-ph/0703166 [hep-ph]]. (Cited on page 4.)
- [94] R. Enberg, B. Pire, L. Szymanowski, S. Wallon, *BFKL resummation effects in $\gamma^*\gamma^* \rightarrow \rho \rho$* , Eur. Phys. J. C **45** (2006) 759 Erratum: [Eur. Phys. J. C **51** (2007) 1015] doi:[10.1140/epjc/s10052-007-0375-7](https://doi.org/10.1140/epjc/s10052-007-0375-7), doi:[10.1140/epjc/s2005-02451-2](https://doi.org/10.1140/epjc/s2005-02451-2) [hep-ph/0508134]. (Cited on page 4.)
- [95] D.Yu. Ivanov, A. Papa, *Electroproduction of two light vector mesons in the next-to-leading approximation*, Nucl. Phys. B **732** (2006) 183 doi:[10.1016/j.nuclphysb.2005.10.028](https://doi.org/10.1016/j.nuclphysb.2005.10.028) [hep-ph/0508162]. (Cited on pages 4 and 8.)

- [96] D.Yu. Ivanov, A. Papa, *Electroproduction of two light vector mesons in next-to-leading BFKL: Study of systematic effects*, Eur. Phys. J. C **49** (2007) 947 doi:[10.1140/epjc/s10052-006-0180-8](https://doi.org/10.1140/epjc/s10052-006-0180-8) [hep-ph/0610042]. (Cited on pages 4 and 8.)
- [97] I.F. Ginzburg, D.Yu. Ivanov, *The Q^{**2} dependence of the hard diffractive photoproduction of vector meson or photon and the range of pQCD validity*, Phys. Rev. D **54**, 5523 (1996) doi:[10.1103/PhysRevD.54.5523](https://doi.org/10.1103/PhysRevD.54.5523) [hep-ph/9604437]. (Cited on page 4.)
- [98] A.D. Bolognino, F.G. Celiberto, M. Fucilla, D.Yu. Ivanov, A. Papa, *High-energy resummation in heavy-quark pair hadroproduction*, Eur. Phys. J. C **79** (2019) no.11, 939 doi:[10.1140/epjc/s10052-019-7392-1](https://doi.org/10.1140/epjc/s10052-019-7392-1) [arXiv:1909.03068 [hep-ph]]. (Cited on pages 4 and 31.)
- [99] F.G. Celiberto, D.Yu. Ivanov, B. Murdaca, A. Papa, *High-energy resummation in heavy-quark pair photoproduction*, Phys. Lett. B **777** (2018) 141 doi:[10.1016/j.physletb.2017.12.020](https://doi.org/10.1016/j.physletb.2017.12.020) [arXiv:1709.10032 [hep-ph]]. (Cited on pages 4 and 31.)
- [100] A.D. Bolognino, F.G. Celiberto, M. Fucilla, D.Yu. Ivanov, B. Murdaca, A. Papa, *Inclusive production of two rapidity-separated heavy quarks as a probe of BFKL dynamics*, PoS DIS **2019** (2019) 067 doi:[10.22323/1.352.0067](https://doi.org/10.22323/1.352.0067) [arXiv:1906.05940 [hep-ph]]. (Cited on pages 4 and 31.)
- [101] R. Boussarie, B. Ducloué, L. Szymanowski, S. Wallon, *Forward J/ψ and very backward jet inclusive production at the LHC*, Phys. Rev. D **97** (2018) no.1, 014008 doi:[10.1103/PhysRevD.97.014008](https://doi.org/10.1103/PhysRevD.97.014008) [arXiv:1709.01380 [hep-ph]]. (Cited on pages 4 and 31.)
- [102] F.G. Celiberto, D.Yu. Ivanov, M.M.A. Mohammed, A. Papa, *High-energy resummed distributions for the inclusive Higgs-plus-jet production at the LHC*, Eur. Phys. J. C **81** (2021) no.4, 293 doi:[10.1140/epjc/s10052-021-09063-2](https://doi.org/10.1140/epjc/s10052-021-09063-2) [arXiv:2008.00501 [hep-ph]]. (Cited on pages 4 and 31.)
- [103] A.D. Bolognino, F.G. Celiberto, M. Fucilla, D.Yu. Ivanov, A. Papa, *Inclusive production of a heavy-light dijet system in hybrid high-energy and collinear factorization*, Phys. Rev. D **103** (2021) no.9, 094004 doi:[10.1103/PhysRevD.103.094004](https://doi.org/10.1103/PhysRevD.103.094004) [arXiv:2103.07396 [hep-ph]]. (Cited on page 4.)
- [104] J. Kwieciński, A.D. Martin, P.J. Sutton, *Constraints on gluon evolution at small x* , Z. Phys. C **71** (1996) 585 doi:[10.1007/BF02907019](https://doi.org/10.1007/BF02907019), doi:[10.1007/s002880050206](https://doi.org/10.1007/s002880050206) [hep-ph/9602320]. (Cited on pages 4 and 14.)
- [105] K.J. Golec-Biernat, L. Motyka, T. Stebel, *Forward Drell-Yan and backward jet production as a probe of the BFKL dynamics*, JHEP **1812** (2018) 091 doi:[10.1007/JHEP12\(2018\)091](https://doi.org/10.1007/JHEP12(2018)091) [arXiv:1811.04361 [hep-ph]]. (Cited on page 4.)
- [106] S. Catani, M. Ciafaloni, F. Hautmann, *High-energy factorization and small x heavy flavor production*, Nucl. Phys. B **366** (1991) 135. doi:[10.1016/0550-3213\(91\)90055-3](https://doi.org/10.1016/0550-3213(91)90055-3) (Cited on page 5.)
- [107] E.M. Levin, M.G. Ryskin, Y.M. Shabelski, A.G. Shuvaev, *Heavy quark production in semihard nucleon interactions*, Sov. J. Nucl. Phys. **53** (1991), 657 [Yad. Fiz. **53** (1991) 1059-1076] (Cited on page 5.)
- [108] J. Blumlein, *On the $k(T)$ dependent gluon density of the proton*, [arXiv:hep-ph/9506403 [hep-ph]]. (Cited on page 5.)
- [109] M. Ryskin, Y. Shabelski, *The Role of screening corrections in small x behavior of structure functions*, Phys. Atom. Nucl. **58** (1995), 1782-1787 doi:[10.1007/BF01496590](https://doi.org/10.1007/BF01496590) (Cited on page 5.)
- [110] J. Kwieciński, A.D. Martin, A. Stasto, *A Unified BFKL and GLAP description of F_2 data*, Phys. Rev. D **56** (1997), 3991-4006 doi:[10.1103/PhysRevD.56.3991](https://doi.org/10.1103/PhysRevD.56.3991) [arXiv:hep-ph/9703445 [hep-ph]]. (Cited on page 5.)
- [111] K.J. Golec-Biernat, M. Wüsthoff, *Saturation effects in deep inelastic scattering at low Q^{**2} and its implications on diffraction*, Phys. Rev. D **59** (1998), 014017 doi:[10.1103/PhysRevD.59.014017](https://doi.org/10.1103/PhysRevD.59.014017) [arXiv:hep-ph/9807513 [hep-ph]]. (Cited on page 5.)
- [112] K.J. Golec-Biernat, M. Wüsthoff, *Saturation in diffractive deep inelastic scattering*, Phys. Rev. D **60** (1999), 114023 doi:[10.1103/PhysRevD.60.114023](https://doi.org/10.1103/PhysRevD.60.114023) [arXiv:hep-ph/9903358 [hep-ph]]. (Cited on page 5.)
- [113] J. Bartels, K.J. Golec-Biernat, K. Peters, *An Estimate of higher twist at small $x(B)$ and low Q^{**2} based upon a saturation model*, Eur. Phys. J. C **17** (2000), 121-128 doi:[10.1007/s100520000429](https://doi.org/10.1007/s100520000429) [arXiv:hep-ph/0003042 [hep-ph]]. (Cited on page 5.)
- [114] H. Jung, *CCFM prediction on forward jets and $F(2)$: Parton level predictions and a new hadron level Monte Carlo generator CASCADE*, [arXiv:hep-ph/9908497 [hep-ph]]. (Cited on page 5.)
- [115] H. Jung, G. Salam, *Hadronic final state predictions from CCFM: The Hadron level Monte Carlo generator CASCADE*, Eur. Phys. J. C **19** (2001), 351-360 doi:[10.1007/s100520100604](https://doi.org/10.1007/s100520100604) [arXiv:hep-ph/0012143 [hep-ph]]. (Cited on page 5.)
- [116] I.P. Ivanov, N.N. Nikolaev, *Anatomy of the differential gluon structure function of the proton from the experimental data on $F(2p)$ (x, Q^{**2})*, Phys. Rev. D **65** (2002), 054004 doi:[10.1103/PhysRevD.65.054004](https://doi.org/10.1103/PhysRevD.65.054004) [arXiv:hep-ph/0004206 [hep-ph]]. (Cited on page 5.)
- [117] I.P. Ivanov, PhD thesis, *Diffractive production of vector mesons in deep inelastic scattering within $k(t)$ factorization approach*, [arXiv:hep-ph/0303053 [hep-ph]]. (Cited on page 5.)

- [118] M. Kimber, A.D. Martin, M. Ryskin, *Unintegrated parton distributions*, Phys. Rev. D **63** (2001), 114027 doi:[10.1103/PhysRevD.63.114027](https://doi.org/10.1103/PhysRevD.63.114027) [arXiv:hep-ph/0101348 [hep-ph]]. (Cited on page 5.)
- [119] G. Watt, A.D. Martin, M. Ryskin, *Unintegrated parton distributions and inclusive jet production at HERA*, Eur. Phys. J. C **31** (2003), 73-89 doi:[10.1140/epjc/s2003-01320-4](https://doi.org/10.1140/epjc/s2003-01320-4) [arXiv:hep-ph/0306169 [hep-ph]]. (Cited on page 5.)
- [120] K. Kutak, S. Sapeta, *Gluon saturation in dijet production in $p\text{-}Pb$ collisions at Large Hadron Collider*, Phys. Rev. D **86** (2012), 094043 doi:[10.1103/PhysRevD.86.094043](https://doi.org/10.1103/PhysRevD.86.094043) [arXiv:1205.5035 [hep-ph]]. (Cited on page 5.)
- [121] M. Hentschinski, A. Sabio Vera, C. Salas, *Hard to Soft Pomeron Transition in Small- x Deep Inelastic Scattering Data Using Optimal Renormalization*, Phys. Rev. Lett. **110** (2013) no.4, 041601 doi:[10.1103/PhysRevLett.110.041601](https://doi.org/10.1103/PhysRevLett.110.041601) [arXiv:1209.1353 [hep-ph]]. (Cited on page 5.)
- [122] F. Hautmann, H. Jung, *Transverse momentum dependent gluon density from DIS precision data*, Nucl. Phys. B **883** (2014), 1-19 doi:[10.1016/j.nuclphysb.2014.03.014](https://doi.org/10.1016/j.nuclphysb.2014.03.014) [arXiv:1312.7875 [hep-ph]]. (Cited on page 5.)
- [123] F. Hautmann, H. Jung, A. Lelek, V. Radescu, R. Žlebčík, *Soft-gluon resolution scale in QCD evolution equations*, Phys. Lett. B **772** (2017), 446-451 doi:[10.1016/j.physletb.2017.07.005](https://doi.org/10.1016/j.physletb.2017.07.005) [arXiv:1704.01757 [hep-ph]]. (Cited on page 5.)
- [124] F. Hautmann, H. Jung, A. Lelek, V. Radescu, R. Žlebčík, *Collinear and TMD Quark and Gluon Densities from Parton Branching Solution of QCD Evolution Equations*, JHEP **01** (2018), 070 doi:[10.1007/JHEP01\(2018\)070](https://doi.org/10.1007/JHEP01(2018)070) [arXiv:1708.03279 [hep-ph]]. (Cited on page 5.)
- [125] A. Bermudez Martinez, P. Connor, H. Jung, A. Lelek, R. Žlebčík, F. Hautmann, V. Radescu, *Collinear and TMD parton densities from fits to precision DIS measurements in the parton branching method*, Phys. Rev. D **99** (2019) no.7, 074008 doi:[10.1103/PhysRevD.99.074008](https://doi.org/10.1103/PhysRevD.99.074008) [arXiv:1804.11152 [hep-ph]]. (Cited on page 5.)
- [126] J.R. Andersen *et al.* [Small x Collaboration], *Small x phenomenology: Summary and status*, Eur. Phys. J. C **35** (2004) 67 doi:[10.1140/epjc/s2004-01775-7](https://doi.org/10.1140/epjc/s2004-01775-7) [hep-ph/0312333]. (Cited on page 5.)
- [127] J.R. Andersen *et al.* [Small x Collaboration], *Small x Phenomenology: Summary of the 3rd Lund Small x Workshop in 2004*, Eur. Phys. J. C **48** (2006) 53 doi:[10.1140/epjc/s2006-02615-6](https://doi.org/10.1140/epjc/s2006-02615-6) [hep-ph/0604189]. (Cited on page 5.)
- [128] B. Andersson *et al.* [Small x Collaboration], *Small x phenomenology: Summary and status*, Eur. Phys. J. C **25** (2002) 77 doi:[10.1007/s10052-002-0998-7](https://doi.org/10.1007/s10052-002-0998-7) [hep-ph/0204115]. (Cited on page 5.)
- [129] R. Angeles-Martinez *et al.*, *Transverse Momentum Dependent (TMD) parton distribution functions: status and prospects*, Acta Phys. Polon. B **46** (2015) no.12, 2501 doi:[10.5506/APhysPolB.46.2501](https://doi.org/10.5506/APhysPolB.46.2501) [arXiv:1507.05267 [hep-ph]]. (Cited on pages 5 and 31.)
- [130] G. Chachamis, M. Deák, M. Hentschinski, G. Rodrigo, A. Sabio Vera, *Single bottom quark production in k_T -factorisation*, JHEP **1509** (2015) 123 doi:[10.1007/JHEP09\(2015\)123](https://doi.org/10.1007/JHEP09(2015)123) [arXiv:1507.05778 [hep-ph]]. (Cited on page 5.)
- [131] I. Bautista, A. Fernandez Tellez, M. Hentschinski, *BFKL evolution and the growth with energy of exclusive J/ψ and Υ photoproduction cross sections*, Phys. Rev. D **94** (2016) no.5, 054002 doi:[10.1103/PhysRevD.94.054002](https://doi.org/10.1103/PhysRevD.94.054002) [arXiv:1607.05203 [hep-ph]]. (Cited on page 5.)
- [132] A. Arroyo Garcia, M. Hentschinski, K. Kutak, *QCD evolution based evidence for the onset of gluon saturation in exclusive photo-production of vector mesons*, Phys. Lett. B **795** (2019) 569 doi:[10.1016/j.physletb.2019.06.061](https://doi.org/10.1016/j.physletb.2019.06.061) [arXiv:1904.04394 [hep-ph]]. (Cited on page 5.)
- [133] F.G. Celiberto, D. Gordo Gómez, A. Sabio Vera, *Forward Drell-Yan production at the LHC in the BFKL formalism with collinear corrections*, Phys. Lett. B **786** (2018) 201 doi:[10.1016/j.physletb.2018.09.045](https://doi.org/10.1016/j.physletb.2018.09.045) [arXiv:1808.09511 [hep-ph]]. (Cited on page 5.)
- [134] K.J. Golec-Biernat, E. Lewandowska, A.M. Staśto, *Drell-Yan process at forward rapidity at the LHC*, Phys. Rev. D **82** (2010) 094010 doi:[10.1103/PhysRevD.82.094010](https://doi.org/10.1103/PhysRevD.82.094010) [arXiv:1008.2652 [hep-ph]]. (Cited on page 5.)
- [135] L. Motyka, M. Sadzikowski, T. Stebel, *Twist expansion of Drell-Yan structure functions in color dipole approach*, JHEP **1505** (2015) 087 doi:[10.1007/JHEP05\(2015\)087](https://doi.org/10.1007/JHEP05(2015)087) [arXiv:1412.4675 [hep-ph]]. (Cited on page 5.)
- [136] E. Basso, V.P. Goncalves, J. Nemchik, R. Pasechnik, M. Sumner, *Drell-Yan phenomenology in the color dipole picture revisited*, Phys. Rev. D **93** (2016) no.3, 034023 doi:[10.1103/PhysRevD.93.034023](https://doi.org/10.1103/PhysRevD.93.034023) [arXiv:1510.00650 [hep-ph]]. (Cited on page 5.)
- [137] W. Schäfer, A. Szczurek, *Low mass Drell-Yan production of lepton pairs at forward directions at the LHC: a hybrid approach*, Phys. Rev. D **93** (2016) no.7, 074014 doi:[10.1103/PhysRevD.93.074014](https://doi.org/10.1103/PhysRevD.93.074014) [arXiv:1602.06740 [hep-ph]]. (Cited on page 5.)
- [138] D. Brzemiński, L. Motyka, M. Sadzikowski, T. Stebel, *Twist decomposition of Drell-Yan structure functions: phenomenological implications*, JHEP **1701** (2017) 005 doi:[10.1007/JHEP01\(2017\)005](https://doi.org/10.1007/JHEP01(2017)005) [arXiv:1611.04449 [hep-ph]]. (Cited on page 5.)
- [139] L. Motyka, M. Sadzikowski, T. Stebel, *Lam-Tung relation breaking in Z^0 hadroproduction as a probe of parton transverse momentum*, Phys. Rev. D **95** (2017) no.11, 114025 doi:[10.1103/PhysRevD.95.114025](https://doi.org/10.1103/PhysRevD.95.114025) [arXiv:1609.04300

- [hep-ph]]. (Cited on page 5.)
- [140] A.D. Bolognino, F.G. Celiberto, D.Yu. Ivanov, A. Papa, *Unintegrated gluon distribution from forward polarized ρ -electroproduction*, Eur. Phys. J. C **78** (2018) no.12, 1023 doi:[10.1140/epjc/s10052-018-6493-6](https://doi.org/10.1140/epjc/s10052-018-6493-6) [arXiv:1808.02395 [hep-ph]]. (Cited on page 5.)
- [141] A.D. Bolognino, F.G. Celiberto, D.Yu. Ivanov, A. Papa, *ρ -meson leptoproduction as testfield for the unintegrated gluon distribution in the proton*, Frascati Phys. Ser. **67** (2018) 76 [arXiv:1808.02958 [hep-ph]]. (Cited on page 5.)
- [142] A.D. Bolognino, F.G. Celiberto, D.Yu. Ivanov, A. Papa, *Leptoproduction of ρ -mesons as discriminator for the unintegrated gluon distribution in the proton*, Acta Phys. Polon. Supp. **12** (2019) no.4, 891 doi:[10.5506/APhysPolBSupp.12.891](https://doi.org/10.5506/APhysPolBSupp.12.891) [arXiv:1902.04520 [hep-ph]]. (Cited on page 5.)
- [143] F.G. Celiberto, *Unraveling the unintegrated gluon distribution in the proton via ρ -meson leptoproduction*, Nuovo Cim. C **42** (2019) 220 doi:[10.1393/ncc/i2019-19220-9](https://doi.org/10.1393/ncc/i2019-19220-9) [arXiv:1912.11313 [hep-ph]]. (Cited on page 5.)
- [144] I.V. Anikin, D.Yu. Ivanov, B. Pire, L. Szymanowski, S. Wallon, *QCD factorization of exclusive processes beyond leading twist: $\gamma^* T \rightarrow \rho(T)$ impact factor with twist three accuracy*, Nucl. Phys. B **828** (2010) 1 doi:[10.1016/j.nuclphysb.2009.10.022](https://doi.org/10.1016/j.nuclphysb.2009.10.022) [arXiv:0909.4090 [hep-ph]]. (Cited on page 5.)
- [145] I.V. Anikin, A. Besse, D.Yu. Ivanov, B. Pire, L. Szymanowski, S. Wallon, *A phenomenological study of helicity amplitudes of high energy exclusive leptoproduction of the rho meson*, Phys. Rev. D **84** (2011) 054004 doi:[10.1103/PhysRevD.84.054004](https://doi.org/10.1103/PhysRevD.84.054004) [arXiv:1105.1761 [hep-ph]]. (Cited on page 5.)
- [146] A. Besse, L. Szymanowski, S. Wallon, *The Dipole Representation of Vector Meson Electroproduction Beyond Leading Twist*, Nucl. Phys. B **867** (2013) 19 doi:[10.1016/j.nuclphysb.2012.09.011](https://doi.org/10.1016/j.nuclphysb.2012.09.011) [arXiv:1204.2281 [hep-ph]]. (Cited on page 5.)
- [147] A. Besse, L. Szymanowski, S. Wallon, *Saturation effects in exclusive $\rho(T)$, $\rho(L)$ meson electroproduction*, JHEP **1311** (2013) 062 doi:[10.1007/JHEP11\(2013\)062](https://doi.org/10.1007/JHEP11(2013)062) [arXiv:1302.1766 [hep-ph]]. (Cited on page 5.)
- [148] A.D. Bolognino, A. Szczurek, W. Schäfer, *Exclusive production of ϕ meson in the $\gamma^* p \rightarrow \phi p$ reaction at large photon virtualities within k_T -factorization approach*, Phys. Rev. D **101** (2020) no.5, 054041 doi:[10.1103/PhysRevD.101.054041](https://doi.org/10.1103/PhysRevD.101.054041) arXiv:1912.06507 [hep-ph]. (Cited on page 5.)
- [149] A. Cisek, W. Schafer, A. Szczurek, *Exclusive photoproduction of ϕ meson in $\gamma p \rightarrow \phi p$ and $pp \rightarrow p\phi p$ reactions*, Phys. Lett. B **690** (2010) 168 doi:[10.1016/j.physletb.2010.05.019](https://doi.org/10.1016/j.physletb.2010.05.019) [arXiv:1004.0070 [hep-ph]]. (Cited on page 5.)
- [150] M.V. Terentev, *On the Structure of Wave Functions of Mesons as Bound States of Relativistic Quarks*, Sov. J. Nucl. Phys. **24** (1976) 106 [Yad. Fiz. **24** (1976) 207]. (Cited on page 5.)
- [151] V.B. Berestetsky, M.V. Terentev, *Nucleon Form-Factors and Dynamics of the Light Front*, Sov. J. Nucl. Phys. **25** (1977) 347 [Yad. Fiz. **25** (1977) 653]. (Cited on page 5.)
- [152] L.A. Kondratyuk, M.V. Terentev, *The Scattering Problem For Relativistic Systems With Fixed Number Of Particles*, Sov. J. Nucl. Phys. **31** (1980) 561 [Yad. Fiz. **31** (1980) 1087]. (Cited on page 5.)
- [153] J.D. Bjorken, J.B. Kogut, D.E. Soper, *Quantum Electrodynamics at Infinite Momentum: Scattering from an External Field*, Phys. Rev. D **3** (1971) 1382. doi:[10.1103/PhysRevD.3.1382](https://doi.org/10.1103/PhysRevD.3.1382) (Cited on page 5.)
- [154] G.P. Lepage, S.J. Brodsky, *Exclusive Processes in Perturbative Quantum Chromodynamics*, Phys. Rev. D **22** (1980) 2157. doi:[10.1103/PhysRevD.22.2157](https://doi.org/10.1103/PhysRevD.22.2157) (Cited on page 5.)
- [155] S.J. Brodsky, H.C. Pauli, S.S. Pinsky, *Quantum chromodynamics and other field theories on the light cone*, Phys. Rept. **301** (1998) 299 doi:[10.1016/S0370-1573\(97\)00089-6](https://doi.org/10.1016/S0370-1573(97)00089-6) [hep-ph/9705477]. (Cited on page 5.)
- [156] T. Heinzl, PhD thesis, *Light cone dynamics of particles and fields*, hep-th/9812190. (Cited on page 5.)
- [157] M. Hentschinski, A. Sabio Vera, C. Salas, *Description of F_2 and F_L at small x using a collinearly-improved BFKL resummation*, Phys. Rev. D **87** (2013) 076005 doi:[10.1103/PhysRevD.87.076005](https://doi.org/10.1103/PhysRevD.87.076005) [arXiv:1301.5283 [hep-ph]]. (Cited on page 5.)
- [158] R.D. Ball, V. Bertone, M. Bonvini, S. Marzani, J. Rojo, L. Rottoli, *Parton distributions with small- x resummation: evidence for BFKL dynamics in HERA data*, Eur. Phys. J. C **78** (2018) no.4, 321 doi:[10.1140/epjc/s10052-018-5774-4](https://doi.org/10.1140/epjc/s10052-018-5774-4) [arXiv:1710.05935 [hep-ph]]. (Cited on pages 5 and 32.)
- [159] V.N. Gribov, L.N. Lipatov, *Deep inelastic e p scattering in perturbation theory*, Sov. J. Nucl. Phys. **15** (1972) 438. (Cited on page 5.)
- [160] V.N. Gribov, L.N. Lipatov, *e^+e^- pair annihilation and deep inelastic e p scattering in perturbation theory*, Sov. J. Nucl. Phys. **15** (1972) 675 [Yad. Fiz. **15** (1972) 1218]. (Cited on page 5.)
- [161] L.N. Lipatov, *The parton model and perturbation theory*, Sov. J. Nucl. Phys. **20** (1975) 94 [Yad. Fiz. **20** (1974) 181]. (Cited on page 5.)
- [162] G. Altarelli, G. Parisi, *Asymptotic Freedom in Parton Language*, Nucl. Phys. B **126** (1977) 298 doi:[10.1016/0550-3213\(77\)90384-4](https://doi.org/10.1016/0550-3213(77)90384-4). (Cited on page 5.)
- [163] Y.L. Dokshitzer, *Calculation of the Structure Functions for Deep Inelastic Scattering and e^+e^- Annihilation by*

- Perturbation Theory in Quantum Chromodynamics*, Sov. Phys. JETP **46** (1977) 641. (Cited on page 5.)
- [164] J.R. Andersen, V. Del Duca, S. Frixione, C.R. Schmidt, W.J. Stirling, *Mueller-Navelet jets at hadron colliders*, JHEP **0102** (2001) 007 doi:[10.1088/1126-6708/2001/02/007](https://doi.org/10.1088/1126-6708/2001/02/007) [hep-ph/0101180]. (Cited on page 5.)
- [165] M. Fontannaz, J.P. Guillet, G. Heinrich, *Is a large intrinsic $k(T)$ needed to describe photon + jet photoproduction at HERA?*, Eur. Phys. J. C **22** (2001) 303 doi:[10.1007/s100520100797](https://doi.org/10.1007/s100520100797) [hep-ph/0107262]. (Cited on page 5.)
- [166] A.V. Kotikov, L.N. Lipatov, *NLO corrections to the BFKL equation in QCD and in supersymmetric gauge theories*, Nucl. Phys. B **582** (2000) 19 doi:[10.1016/S0550-3213\(00\)00329-1](https://doi.org/10.1016/S0550-3213(00)00329-1), [hep-ph/0004008]. (Cited on page 8.)
- [167] A.V. Kotikov, L.N. Lipatov, *DGLAP and BFKL equations in the $N = 4$ supersymmetric gauge theory*, Nucl. Phys. B **661** (2003) 19 [Erratum: Nucl. Phys. B **685** (2004) 405] doi:[10.1016/S0550-3213\(03\)00264-5](https://doi.org/10.1016/S0550-3213(03)00264-5), doi:[10.1016/j.nuclphysb.2004.02.032](https://doi.org/10.1016/j.nuclphysb.2004.02.032) [hep-ph/0208220]. (Cited on page 8.)
- [168] B.R. Webber, *QCD power corrections from a simple model for the running coupling*, JHEP **10** (1998), 012 doi:[10.1088/1126-6708/1998/10/012](https://doi.org/10.1088/1126-6708/1998/10/012) [arXiv:hep-ph/9805484 [hep-ph]]. (Cited on page 10.)
- [169] J. Bartels, H. Lotter, *A Note on the BFKL pomeron and the 'hot spot' cross-section*, Phys. Lett. B **309** (1993), 400-408 doi:[10.1016/0370-2693\(93\)90953-F](https://doi.org/10.1016/0370-2693(93)90953-F) (Cited on page 10.)
- [170] F. Caporale, G. Chachamis, J.D. Madrigal, B. Murdaca, A. Sabio Vera, *A study of the diffusion pattern in $N = 4$ SYM at high energies*, Phys. Lett. B **724** (2013), 127-132 doi:[10.1016/j.physletb.2013.05.058](https://doi.org/10.1016/j.physletb.2013.05.058) [arXiv:1305.1474 [hep-th]]. (Cited on page 10.)
- [171] D.A. Ross, A. Sabio Vera, *The Effect of the Infrared Phase of the Discrete BFKL Pomeron on Transverse Momentum Diffusion*, JHEP **08** (2016), 071 doi:[10.1007/JHEP08\(2016\)071](https://doi.org/10.1007/JHEP08(2016)071) [arXiv:1605.08265 [hep-ph]]. (Cited on page 10.)
- [172] L.A. Harland-Lang, A.D. Martin, P. Motylinski, R.S. Thorne, *Parton distributions in the LHC era: MMHT 2014 PDFs*, Eur. Phys. J. C **75** (2015) no.5, 204 doi:[10.1140/epjc/s10052-015-3397-6](https://doi.org/10.1140/epjc/s10052-015-3397-6) [arXiv:1412.3989 [hep-ph]]. (Cited on pages 10 and 13.)
- [173] S. Dulat *et al.* *New parton distribution functions from a global analysis of quantum chromodynamics*, Phys. Rev. D **93** (2016) no.3, 033006 doi:[10.1103/PhysRevD.93.033006](https://doi.org/10.1103/PhysRevD.93.033006) [arXiv:1506.07443 [hep-ph]]. (Cited on page 10.)
- [174] R.D. Ball *et al.* [NNPDF Collaboration], *Parton distributions for the LHC Run II*, JHEP **1504** (2015) 040 doi:[10.1007/JHEP04\(2015\)040](https://doi.org/10.1007/JHEP04(2015)040) [arXiv:1410.8849 [hep-ph]]. (Cited on page 10.)
- [175] V. Bertone *et al.* [NNPDF Collaboration], *A determination of the fragmentation functions of pions, kaons, and protons with faithful uncertainties*, Eur. Phys. J. C **77** (2017) no.8, 516 doi:[10.1140/epjc/s10052-017-5088-y](https://doi.org/10.1140/epjc/s10052-017-5088-y) [arXiv:1706.07049 [hep-ph]]. (Cited on pages 10, 16, 17 and 18.)
- [176] J. Butterworth *et al.*, *PDF4LHC recommendations for LHC Run II*, J. Phys. G **43** (2016) 023001 doi:[10.1088/0954-3899/43/2/023001](https://doi.org/10.1088/0954-3899/43/2/023001) [arXiv:1510.03865 [hep-ph]]. (Cited on pages 10 and 13.)
- [177] S. Albino, B.A. Kniehl, G. Kramer, *AKK Update: Improvements from New Theoretical Input and Experimental Data*, Nucl. Phys. B **803**, (2008) 42 doi:[10.1016/j.nuclphysb.2008.05.017](https://doi.org/10.1016/j.nuclphysb.2008.05.017) [arXiv:0803.2768 [hep-ph]]. (Cited on page 10.)
- [178] D. de Florian, R. Sassot, M. Stratmann, *Global analysis of fragmentation functions for pions and kaons and their uncertainties*, Phys. Rev. D **75** (2007) 114010 doi:[10.1103/PhysRevD.75.114010](https://doi.org/10.1103/PhysRevD.75.114010) [hep-ph/0703242 [hep-ph]]. (Cited on page 10.)
- [179] D. de Florian, R. Sassot, M. Stratmann, *Global analysis of fragmentation functions for protons and charged hadrons*, Phys. Rev. D **76** (2007) 074033 doi:[10.1103/PhysRevD.76.074033](https://doi.org/10.1103/PhysRevD.76.074033) [arXiv:0707.1506 [hep-ph]]. (Cited on page 10.)
- [180] M. Hirai, S. Kumano, T.-H. Nagai, K. Sudoh, *Determination of fragmentation functions and their uncertainties*, Phys. Rev. D **75**, (2007) 094009 doi:[10.1103/PhysRevD.75.094009](https://doi.org/10.1103/PhysRevD.75.094009) [hep-ph/0702250]. (Cited on page 10.)
- [181] S. Forte, L. Garrido, J.I. Latorre, A. Piccione, *Neural network parametrization of deep inelastic structure functions*, JHEP **0205** (2002) 062 doi:[10.1088/1126-6708/2002/05/062](https://doi.org/10.1088/1126-6708/2002/05/062) [hep-ph/0204232]. (Cited on pages 11 and 31.)
- [182] S.V. Chekanov, *Jet algorithms: A Minireview*, hep-ph/0211298. (Cited on page 11.)
- [183] G.P. Salam, *Towards Jetography*, Eur. Phys. J. C **67** (2010) 637 doi:[10.1140/epjc/s10052-010-1314-6](https://doi.org/10.1140/epjc/s10052-010-1314-6) [arXiv:0906.1833 [hep-ph]]. (Cited on page 11.)
- [184] S. Catani, Y.L. Dokshitzer, M.H. Seymour, B.R. Webber, *Longitudinally invariant K_t clustering algorithms for hadron hadron collisions*, Nucl. Phys. B **406** (1993) 187. doi:[10.1016/0550-3213\(93\)90166-M](https://doi.org/10.1016/0550-3213(93)90166-M) (Cited on page 11.)
- [185] M. Cacciari, G.P. Salam, G. Soyez, *The anti- k_t jet clustering algorithm*, JHEP **0804** (2008) 063 doi:[10.1088/1126-6708/2008/04/063](https://doi.org/10.1088/1126-6708/2008/04/063) [arXiv:0802.1189 [hep-ph]]. (Cited on page 11.)
- [186] M. Furman, *Study of a Nonleading QCD Correction to Hadron Calorimeter Reactions*, Nucl. Phys. B **197** (1982) 413. doi:[10.1016/0550-3213\(82\)90452-7](https://doi.org/10.1016/0550-3213(82)90452-7) (Cited on page 11.)
- [187] F. Aversa, P. Chiappetta, M. Greco, J.P. Guillet, *QCD Corrections to Parton-Parton Scattering Processes*, Nucl. Phys. B **327** (1989) 105. doi:[10.1016/0550-3213\(89\)90288-5](https://doi.org/10.1016/0550-3213(89)90288-5) (Cited on page 11.)

- [188] D. Colferai, A. Niccoli, F. Deganutti, *Improved theoretical description of Mueller-Navelet jets at LHC*, PoS QCDEV **2016** (2017) 031 doi:[10.22323/1.284.0031](https://doi.org/10.22323/1.284.0031) (Cited on page 11.)
- [189] CMS Collaboration, *Measurement of the very forward inclusive jet cross section in pp collisions at $\sqrt{s} = 13$ TeV with CMS*, CMS-PAS-FSQ-16-003. (Cited on page 12.)
- [190] A.D. Martin, W.J. Stirling, R.S. Thorne, G. Watt, *Parton distributions for the LHC*, Eur. Phys. J. C **63** (2009) 189 doi:[10.1140/epjc/s10052-009-1072-5](https://doi.org/10.1140/epjc/s10052-009-1072-5) [arXiv:0901.0002 [hep-ph]]. (Cited on page 13.)
- [191] A. Sabio Vera, F. Schwennsen, *The Azimuthal decorrelation of jets widely separated in rapidity as a test of the BFKL kernel*, Nucl. Phys. B **776** (2007) 170 doi:[10.1103/PhysRevLett.77.595](https://doi.org/10.1103/PhysRevLett.77.595) [hep-ph/0702158 [hep-ph]]. (Cited on page 14.)
- [192] G.P. Salam, *A Resummation of large subleading corrections at small x*, JHEP **9807** (1998) 019 doi:[10.1088/1126-6708/1998/07/019](https://doi.org/10.1088/1126-6708/1998/07/019) [hep-ph/9806482]. (Cited on page 14.)
- [193] M. Ciafaloni, D. Colferai, *The BFKL equation at next-to-leading level and beyond*, Phys. Lett. B **452** (1999) 372 doi:[10.1016/S0370-2693\(99\)00281-6](https://doi.org/10.1016/S0370-2693(99)00281-6) [hep-ph/9812366]. (Cited on page 14.)
- [194] M. Ciafaloni, D. Colferai, G.P. Salam, *renormalization group improved small x equation*, Phys. Rev. D **60** (1999) 114036 doi:[10.1103/PhysRevD.60.114036](https://doi.org/10.1103/PhysRevD.60.114036) [hep-ph/9905566]. (Cited on page 14.)
- [195] M. Ciafaloni, D. Colferai, G.P. Salam, *A collinear model for small x physics*, JHEP **9910** (1999) 017 doi:[10.1088/1126-6708/1999/10/017](https://doi.org/10.1088/1126-6708/1999/10/017) [hep-ph/9907409]. (Cited on page 14.)
- [196] M. Ciafaloni, D. Colferai, G.P. Salam, *On factorization at small x*, JHEP **0007** (2000) 054 doi:[10.1088/1126-6708/2000/07/054](https://doi.org/10.1088/1126-6708/2000/07/054) [hep-ph/0007240]. (Cited on page 14.)
- [197] M. Ciafaloni, D. Colferai, G.P. Salam, A.M. Staśto, *Tunneling transition to the pomeron regime*, Phys. Lett. B **541** (2002) 314 doi:[10.1016/S0370-2693\(02\)02271-2](https://doi.org/10.1016/S0370-2693(02)02271-2) [hep-ph/0204287]. (Cited on page 14.)
- [198] M. Ciafaloni, D. Colferai, G.P. Salam, A.M. Staśto, *Expanding running coupling effects in the hard pomeron*, Phys. Rev. D **66** (2002) 054014 doi:[10.1103/PhysRevD.66.054014](https://doi.org/10.1103/PhysRevD.66.054014) [hep-ph/0204282]. (Cited on page 14.)
- [199] M. Ciafaloni, D. Colferai, D. Colferai, G.P. Salam, A.M. Staśto, *Extending QCD perturbation theory to higher energies*, Phys. Lett. B **576** (2003) 143 doi:[10.1016/j.physletb.2003.09.078](https://doi.org/10.1016/j.physletb.2003.09.078) [hep-ph/0305254]. (Cited on page 14.)
- [200] M. Ciafaloni, D. Colferai, G.P. Salam, A.M. Staśto, *renormalization group improved small x Green's function*, Phys. Rev. D **68** (2003) 114003 doi:[10.1103/PhysRevD.68.114003](https://doi.org/10.1103/PhysRevD.68.114003) [hep-ph/0307188]. (Cited on page 14.)
- [201] M. Ciafaloni, D. Colferai, G.P. Salam, A.M. Staśto, Phys. Lett. B **587** (2004) 87 doi:[10.1016/j.physletb.2004.02.054](https://doi.org/10.1016/j.physletb.2004.02.054) [hep-ph/0311325]. (Cited on page 14.)
- [202] A. Sabio Vera, *An 'All-poles' approximation to collinear resummations in the Regge limit of perturbative QCD*, Nucl. Phys. B **722** (2005) 65 doi:[10.1016/j.nuclphysb.2005.06.003](https://doi.org/10.1016/j.nuclphysb.2005.06.003) [hep-ph/0505128]. (Cited on page 14.)
- [203] F. Caporale, A. Papa, A. Sabio Vera, *Collinear improvement of the BFKL kernel in the electroproduction of two light vector mesons*, Eur. Phys. J. C **53** (2008) 525 doi:[10.1140/epjc/s10052-007-0481-6](https://doi.org/10.1140/epjc/s10052-007-0481-6) [arXiv:0707.4100 [hep-ph]]. (Cited on page 14.)
- [204] J. Kwieciński, L. Motyka, *Probing the QCD pomeron in doubly tagged e^+e^- collisions*, Phys. Lett. B **462** (1999) 203 doi:[10.1016/S0370-2693\(99\)00866-7](https://doi.org/10.1016/S0370-2693(99)00866-7) [hep-ph/9905567]. (Cited on page 14.)
- [205] C.R. Schmidt, *Rapidity separation dependence and the large next-to-leading corrections to the BFKL equation*, Phys. Rev. D **60** (1999) 074003 doi:[10.1103/PhysRevD.60.074003](https://doi.org/10.1103/PhysRevD.60.074003) [hep-ph/9901397]. (Cited on page 14.)
- [206] J.R. Forshaw, D.A. Ross, A. Sabio Vera, *Rapidity veto effects in the NLO BFKL equation*, Phys. Lett. B **455** (1999) 273 doi:[10.1016/S0370-2693\(99\)00451-7](https://doi.org/10.1016/S0370-2693(99)00451-7) [hep-ph/9903390]. (Cited on page 14.)
- [207] P.M. Stevenson, *Resolution of the renormalization Scheme Ambiguity in Perturbative QCD*, Phys. Lett. **100B** (1981) 61 doi:[10.1016/0370-2693\(81\)90287-2](https://doi.org/10.1016/0370-2693(81)90287-2). (Cited on page 14.)
- [208] P.M. Stevenson, *Optimized Perturbation Theory*, Phys. Rev. D **23** (1981) 2916 doi:[10.1103/PhysRevD.23.2916](https://doi.org/10.1103/PhysRevD.23.2916). (Cited on page 14.)
- [209] G. Grunberg, *Renormalization Group Improved Perturbative QCD*, Phys. Lett. **95B** (1980) 70 [Erratum: Phys. Lett. **110B** (1982) 501] doi:[10.1016/0370-2693\(80\)90402-5](https://doi.org/10.1016/0370-2693(80)90402-5). (Cited on page 14.)
- [210] G. Grunberg, *Renormalization Group Improved Predictions for Quarkonium Decay*, Phys. Lett. **114B** (1982) 271 doi:[10.1016/0370-2693\(82\)90494-4](https://doi.org/10.1016/0370-2693(82)90494-4). (Cited on page 14.)
- [211] G. Grunberg, *Renormalization Scheme Independent QCD and QED: The Method of Effective Charges*, Phys. Rev. D **29** (1984) 2315 doi:[10.1103/PhysRevD.29.2315](https://doi.org/10.1103/PhysRevD.29.2315). (Cited on page 14.)
- [212] *On the elimination of scale ambiguities in perturbative quantum chromodynamics*, S.J. Brodsky, G.P. Lepage, P.B. Mackenzie, Phys. Rev. D **28**, (1983) 228 doi:[10.1103/PhysRevD.28.228](https://doi.org/10.1103/PhysRevD.28.228) (Cited on page 14.)
- [213] S.J. Brodsky, F. Hautmann, D.E. Soper, *Probing the QCD Pomeron in e^+e^- collisions*, Phys. Rev. Lett. **78**, (1997) 803 [Erratum: Phys. Rev. Lett. **79**, (1997) 3544] doi:[10.1103/PhysRevLett.78.803](https://doi.org/10.1103/PhysRevLett.78.803) [hep-ph/9610260]. (Cited on page 14.)

- [214] S.J. Brodsky, F. Hautmann, D.E. Soper, *Virtual photon scattering at high-energies as a probe of the short distance Pomeron*, Phys. Rev. D **56**, (1997) 6957 doi:[10.1103/PhysRevD.56.6957](https://doi.org/10.1103/PhysRevD.56.6957) [hep-ph/9706427]. (Cited on page 14.)
- [215] S.J. Brodsky, V.S. Fadin, V.T. Kim, L.N. Lipatov, G.B. Pivovarov, *The QCD Pomeron with optimal renormalization*, JETP Lett. **70**, (1999) 155 doi:[10.1134/1.568145](https://doi.org/10.1134/1.568145). (Cited on page 14.)
- [216] S.J. Brodsky, V.S. Fadin, V.T. Kim, L.N. Lipatov, G.B. Pivovarov, *High-energy QCD asymptotic behavior of photon-photon collisions*, JETP Lett. **76**, (2002) 249 doi:[10.1134/1.1520615](https://doi.org/10.1134/1.1520615). (Cited on page 14.)
- [217] F. G. Celiberto, M. Fucilla, D.Yu. Ivanov, A. Papa, *High-energy resummation in Λ_c baryon production*, Eur. Phys. J. C **81** (2021) no.8, 780 doi:[10.1140/epjc/s10052-021-09448-3](https://doi.org/10.1140/epjc/s10052-021-09448-3) [arXiv:2105.06432 [hep-ph]]. (Cited on page 17.)
- [218] B.A. Kniehl, G. Kramer, I. Schienbein, H. Spiesberger, Λ_c^\pm *production in pp collisions with a new fragmentation function*, Phys. Rev. D **101** (2020) no.11, 114021 doi:[10.1103/PhysRevD.101.114021](https://doi.org/10.1103/PhysRevD.101.114021) [arXiv:2004.04213 [hep-ph]]. (Cited on page 17.)
- [219] T. Kneesch, B.A. Kniehl, G. Kramer, I. Schienbein, Nucl. Phys. B **799** (2008), 34-59 doi:[10.1016/j.nuclphysb.2008.02.015](https://doi.org/10.1016/j.nuclphysb.2008.02.015) [arXiv:0712.0481 [hep-ph]]. (Cited on page 17.)
- [220] D.P. Anderle, T. Kaufmann, M. Stratmann, F. Ringer, I. Vitev, *Using hadron-in-jet data in a global analysis of D^* fragmentation functions*, Phys. Rev. D **96** (2017) no.3, 034028 doi:[10.1103/PhysRevD.96.034028](https://doi.org/10.1103/PhysRevD.96.034028) [arXiv:1706.09857 [hep-ph]]. (Cited on page 17.)
- [221] M. Soleimaniinia, H. Khanpour, S.M. Moosavi Nejad, *First determination of D^{*+} -meson fragmentation functions and their uncertainties at next-to-next-to-leading order*, Phys. Rev. D **97** (2018) no.7, 074014 doi:[10.1103/PhysRevD.97.074014](https://doi.org/10.1103/PhysRevD.97.074014) [arXiv:1711.11344 [hep-ph]]. (Cited on page 17.)
- [222] B.A. Kniehl, G. Kramer, I. Schienbein, H. Spiesberger, *Finite-mass effects on inclusive B meson hadroproduction*, Phys. Rev. D **77** (2008), 014011 doi:[10.1103/PhysRevD.77.014011](https://doi.org/10.1103/PhysRevD.77.014011) [arXiv:0705.4392 [hep-ph]]. (Cited on page 17.)
- [223] G. Kramer, H. Spiesberger, *b-hadron production in the general-mass variable-flavour-number scheme and LHC data*, Phys. Rev. D **98** (2018) no.11, 114010 doi:[10.1103/PhysRevD.98.114010](https://doi.org/10.1103/PhysRevD.98.114010), [arXiv:1809.04297 [hep-ph]]. (Cited on page 17.)
- [224] O. Nachtmann, *Positivity constraints for anomalous dimensions*, Nucl. Phys. B **63** (1973) 237. doi:[10.1016/0550-3213\(73\)90144-2](https://doi.org/10.1016/0550-3213(73)90144-2) (Cited on page 20.)
- [225] H. Georgi, H.D. Politzer, *Freedom at Moderate Energies: Masses in Color Dynamics*, Phys. Rev. D **14** (1976) 1829. doi:[10.1103/PhysRevD.14.1829](https://doi.org/10.1103/PhysRevD.14.1829) (Cited on page 20.)
- [226] R. Barbieri, J.R. Ellis, M.K. Gaillard, G.G. Ross, *Mass Corrections to Scaling in Deep Inelastic Processes*, Nucl. Phys. B **117** (1976) 50. doi:[10.1016/0550-3213\(76\)90563-0](https://doi.org/10.1016/0550-3213(76)90563-0) (Cited on page 20.)
- [227] R. Barbieri, J.R. Ellis, M.K. Gaillard, G.G. Ross, *A Quest for a Wholly Scaling Variable*, Phys. Lett. **64B** (1976) 171. doi:[10.1016/0370-2693\(76\)90323-3](https://doi.org/10.1016/0370-2693(76)90323-3) (Cited on page 20.)
- [228] R.K. Ellis, W. Furmanski, R. Petronzio, *Power Corrections to the Parton Model in QCD*, Nucl. Phys. B **207** (1982) 1. doi:[10.1016/0550-3213\(82\)90132-8](https://doi.org/10.1016/0550-3213(82)90132-8) (Cited on page 20.)
- [229] R. K. Ellis, W. Furmanski, R. Petronzio, *Unraveling Higher Twists*, Nucl. Phys. B **212** (1983) 29. doi:[10.1016/0550-3213\(83\)90597-7](https://doi.org/10.1016/0550-3213(83)90597-7) (Cited on page 20.)
- [230] A. De Rujula, H. Georgi, H.D. Politzer, *Trouble with xi Scaling?*, Phys. Rev. D **15** (1977) 2495. doi:[10.1103/PhysRevD.15.2495](https://doi.org/10.1103/PhysRevD.15.2495) (Cited on page 20.)
- [231] A. De Rujula, H. Georgi, H.D. Politzer, *Demythification of Electroproduction, Local Duality and Precocious Scaling*, Annals Phys. **103** (1977) 315. doi:[10.1016/S0003-4916\(97\)90003-8](https://doi.org/10.1016/S0003-4916(97)90003-8) (Cited on page 20.)
- [232] I. Schienbein *et al.*, *A Review of Target Mass Corrections*, J. Phys. G **35** (2008) 053101 doi:[10.1088/0954-3899/35/5/053101](https://doi.org/10.1088/0954-3899/35/5/053101) [arXiv:0709.1775 [hep-ph]]. (Cited on page 20.)
- [233] A. Accardi, J.W. Qiu, *Collinear factorization for deep inelastic scattering structure functions at large Bjorken $x(B)$* , JHEP **0807** (2008) 090 doi:[10.1088/1126-6708/2008/07/090](https://doi.org/10.1088/1126-6708/2008/07/090) [arXiv:0805.1496 [hep-ph]]. (Cited on page 20.)
- [234] A. Accardi, W. Melnitchouk, *Target mass corrections for spin-dependent structure functions in collinear factorization*, Phys. Lett. B **670** (2008) 114 doi:[10.1016/j.physletb.2008.10.036](https://doi.org/10.1016/j.physletb.2008.10.036) [arXiv:0808.2397 [hep-ph]]. (Cited on page 20.)
- [235] G. P. Lepage, *A New Algorithm for Adaptive Multidimensional Integration*, J. Comput. Phys. **27** (1978) 192. (Cited on page 29.)
- [236] T. Hahn, *A Library for multidimensional numerical integration*, Comput. Phys. Commun. **168** (2005) 78 doi:[10.1016/j.cpc.2005.01.010](https://doi.org/10.1016/j.cpc.2005.01.010) [hep-ph/0404043]. (Cited on page 29.)
- [237] T. Hahn, *Concurrent Cuba*, J. Phys. Conf. Ser. **608** (2015) no.1, 012066 doi:[10.1088/1742-6596/608/1/012066](https://doi.org/10.1088/1742-6596/608/1/012066) [arXiv:1408.6373 [physics.comp-ph]]. (Cited on page 29.)
- [238] CERNLIB Homepage: <http://cernlib.web.cern.ch/cernlib>. Accessed 31 May 2019 (Cited on page 30.)
- [239] A. Buckley, J. Ferrando, S. Lloyd, K. Nordström, B. Page, M. Rüfenacht, M. Schönherr, G. Watt, *LHAPDF6*:

- parton density access in the LHC precision era*, Eur. Phys. J. C **75** (2015) 132 doi:[10.1140/epjc/s10052-015-3318-8](https://doi.org/10.1140/epjc/s10052-015-3318-8) [arXiv:1412.7420 [hep-ph]]. (Cited on page 30.)
- [240] F. Chevallier, O. Kepka, C. Marquet, C. Royon, *Gaps between jets at hadron colliders in the next-to-leading BFKL framework*, Phys. Rev. D **79** (2009), 094019 doi:[10.1103/PhysRevD.79.094019](https://doi.org/10.1103/PhysRevD.79.094019) [arXiv:0903.4598 [hep-ph]]. (Cited on page 30.)
- [241] M. Hentschinski, J.D. Madrigal Martínez, B. Murdaca, A. Sabio Vera, *The next-to-leading order vertex for a forward jet plus a rapidity gap at high energies*, Phys. Lett. B **735** (2014), 168-172 doi:[10.1016/j.physletb.2014.06.022](https://doi.org/10.1016/j.physletb.2014.06.022) [arXiv:1404.2937 [hep-ph]]. (Cited on page 30.)
- [242] M. Hentschinski, J.D. Madrigal Martínez, B. Murdaca, A. Sabio Vera, *The gluon-induced Mueller-Tang jet impact factor at next-to-leading order*, Nucl. Phys. B **889** (2014), 549-579 doi:[10.1016/j.nuclphysb.2014.10.026](https://doi.org/10.1016/j.nuclphysb.2014.10.026) [arXiv:1409.6704 [hep-ph]]. (Cited on page 30.)
- [243] C. Royon, F. Deganutti, *Probing BFKL dynamics at hadronic colliders in jet gap jet events*, EPJ Web Conf. **235** (2020), 05003 doi:[10.1051/epjconf/202023505003](https://doi.org/10.1051/epjconf/202023505003) (Cited on page 30.)
- [244] A.H. Mueller, W.K. Tang, *High-energy parton-parton elastic scattering in QCD*, Phys. Lett. B **284** (1992), 123-126 doi:[10.1016/0370-2693\(92\)91936-4](https://doi.org/10.1016/0370-2693(92)91936-4) (Cited on page 30.)
- [245] G. Chachamis, A. Sabio Vera, *The Colour Octet Representation of the Non-Forward BFKL Green Function*, Phys. Lett. B **709** (2012), 301-308 doi:[10.1016/j.physletb.2012.02.036](https://doi.org/10.1016/j.physletb.2012.02.036) [arXiv:1112.4162 [hep-th]]. (Cited on page 30.)
- [246] G. Chachamis, A. Sabio Vera, C. Salas, *Bootstrap and momentum transfer dependence in small x evolution equations*, Phys. Rev. D **87** (2013) no.1, 016007 doi:[10.1103/PhysRevD.87.016007](https://doi.org/10.1103/PhysRevD.87.016007) [arXiv:1211.6332 [hep-ph]]. (Cited on page 30.)
- [247] G. Chachamis, A. Sabio Vera, *Solution of the Bartels-Kwiecinski-Praszalowicz equation via Monte Carlo integration*, Phys. Rev. D **94** (2016) no.3, 034019 doi:[10.1103/PhysRevD.94.034019](https://doi.org/10.1103/PhysRevD.94.034019) [arXiv:1606.07349 [hep-ph]]. (Cited on page 30.)
- [248] A. van Hameren, *KaTie: For parton-level event generation with k_T -dependent initial states*, Comput. Phys. Commun. **224** (2018), 371-380 doi:[10.1016/j.cpc.2017.11.005](https://doi.org/10.1016/j.cpc.2017.11.005) [arXiv:1611.00680 [hep-ph]]. (Cited on page 30.)
- [249] F. Hautmann, H. Jung, M. Krämer, P.J. Mulders, E.R. Nocera, T.C. Rogers, A. Signori, *TMDlib and TMDplotter: library and plotting tools for transverse-momentum-dependent parton distributions*, Eur. Phys. J. C **74** (2014), 3220 doi:[10.1140/epjc/s10052-014-3220-9](https://doi.org/10.1140/epjc/s10052-014-3220-9) [arXiv:1408.3015 [hep-ph]]. (Cited on page 30.)
- [250] N. Brambilla *et al.*, *Heavy Quarkonium: Progress, Puzzles, and Opportunities*, Eur. Phys. J. C **71** (2011) 1534 doi:[10.1140/epjc/s10052-010-1534-9](https://doi.org/10.1140/epjc/s10052-010-1534-9) [arXiv:1010.5827 [hep-ph]]. (Cited on page 31.)
- [251] G.T. Bodwin, E. Braaten, E. Eichten, S.L. Olsen, T.K. Pedlar, J. Russ, *Quarkonium at the Frontiers of High Energy Physics: A Snowmass White Paper*, arXiv:1307.7425 [hep-ph]. (Cited on page 31.)
- [252] A. Andronic *et al.*, *Heavy-flavour and quarkonium production in the LHC era: from proton-proton to heavy-ion collisions*, Eur. Phys. J. C **76** (2016) no.3, 107 doi:[10.1140/epjc/s10052-015-3819-5](https://doi.org/10.1140/epjc/s10052-015-3819-5) [arXiv:1506.03981 [nucl-ex]]. (Cited on page 31.)
- [253] H. Fritzsch, *Producing Heavy Quark Flavors in Hadronic Collisions: A Test of Quantum Chromodynamics*, Phys. Lett. **67B** (1977) 217. doi:[10.1016/0370-2693\(77\)90108-3](https://doi.org/10.1016/0370-2693(77)90108-3) (Cited on page 31.)
- [254] F. Halzen, *Cvc for Gluons and Hadroproduction of Quark Flavors* Phys. Lett. **69B** (1977) 105. doi:[10.1016/0370-2693\(77\)90144-7](https://doi.org/10.1016/0370-2693(77)90144-7) (Cited on page 31.)
- [255] G. T. Bodwin, E. Braaten, G.P. Lepage, *Rigorous QCD analysis of inclusive annihilation and production of heavy quarkonium* Phys. Rev. D **51** (1995) 1125 Erratum: [Phys. Rev. D **55** (1997) 5853] doi:[10.1103/PhysRevD.55.5853](https://doi.org/10.1103/PhysRevD.55.5853), doi:[10.1103/PhysRevD.51.1125](https://doi.org/10.1103/PhysRevD.51.1125) [hep-ph/9407339]. (Cited on page 31.)
- [256] A. Bacchetta, F.G. Celiberto, M. Radici, P. Taels, *Transverse-momentum-dependent gluon distribution functions in a spectator model*, Eur. Phys. J. C **80** (2020) no.8, 733 doi:[10.1140/epjc/s10052-020-8327-6](https://doi.org/10.1140/epjc/s10052-020-8327-6) [arXiv:2005.02288 [hep-ph]]. (Cited on page 31.)
- [257] F.G. Celiberto, *3D tomography of the nucleon: transverse-momentum-dependent gluon distributions*, Nuovo Cim. C **44** (2021) 36 doi:[10.1393/ncc/i2021-21036-3](https://doi.org/10.1393/ncc/i2021-21036-3) [arXiv:2101.04630 [hep-ph]]. (Cited on page 31.)
- [258] T.C. Rogers, *An overview of transverse-momentum-dependent factorization and evolution* Eur. Phys. J. A **52** (2016) no.6, 153 doi:[10.1140/epja/i2016-16153-7](https://doi.org/10.1140/epja/i2016-16153-7) [arXiv:1509.04766 [hep-ph]]. (Cited on page 31.)
- [259] M. Diehl, *Introduction to GPDs and TMDs*, Eur. Phys. J. A **52** (2016) no.6, 149 doi:[10.1140/epja/i2016-16149-3](https://doi.org/10.1140/epja/i2016-16149-3) [arXiv:1512.01328 [hep-ph]]. (Cited on page 31.)
- [260] S. Boffi, A.V. Efremov, B. Pasquini, P. Schweitzer, *Azimuthal spin asymmetries in light-cone constituent quark models*, Phys. Rev. D **79** (2009), 094012 doi:[10.1103/PhysRevD.79.094012](https://doi.org/10.1103/PhysRevD.79.094012) [arXiv:0903.1271 [hep-ph]]. (Cited on page 31.)
- [261] B. Pasquini, P. Schweitzer, *Naive time-reversal odd phenomena in semi-inclusive deep-inelastic scattering from light-cone constituent quark models*, Phys. Rev. D **83** (2011), 114044 doi:[10.1103/PhysRevD.83.114044](https://doi.org/10.1103/PhysRevD.83.114044) [arXiv:1103.5977

- [hep-ph]]. (Cited on page 31.)
- [262] B. Pasquini, P. Schweitzer, *Pion transverse momentum dependent parton distributions in a light-front constituent approach, and the Boer-Mulders effect in the pion-induced Drell-Yan process*, Phys. Rev. D **90** (2014) no.1, 014050 doi:[10.1103/PhysRevD.90.014050](https://doi.org/10.1103/PhysRevD.90.014050) [arXiv:1406.2056 [hep-ph]]. (Cited on page 31.)
- [263] L.Y. Dai, Z.B. Kang, A. Prokudin, I. Vitev, *Next-to-leading order transverse momentum-weighted Sivers asymmetry in semi-inclusive deep inelastic scattering: the role of the three-gluon correlator*, Phys. Rev. D **92** (2015) no.11, 114024 doi:[10.1103/PhysRevD.92.114024](https://doi.org/10.1103/PhysRevD.92.114024) [arXiv:1409.5851 [hep-ph]]. (Cited on page 31.)
- [264] M.G. Echevarria, T. Kasemets, P.J. Mulders, C. Pisano, *QCD evolution of (un)polarized gluon TMDPDFs and the Higgs q_T -distribution*, JHEP **07** (2015), 158 doi:[10.1007/JHEP07\(2015\)158](https://doi.org/10.1007/JHEP07(2015)158) [arXiv:1502.05354 [hep-ph]]. (Cited on page 31.)
- [265] D. Boer, S. Cotogno, T. van Daal, P.J. Mulders, A. Signori, Y.J. Zhou, *Gluon and Wilson loop TMDs for hadrons of spin ≤ 1* , JHEP **10** (2016), 013 doi:[10.1007/JHEP10\(2016\)013](https://doi.org/10.1007/JHEP10(2016)013) [arXiv:1607.01654 [hep-ph]]. (Cited on page 31.)
- [266] J.P. Lansberg, C. Pisano, M. Schlegel, *Associated production of a dilepton and a $\Upsilon(J/\psi)$ at the LHC as a probe of gluon transverse momentum dependent distributions*, Nucl. Phys. B **920** (2017), 192-210 doi:[10.1016/j.nuclphysb.2017.04.011](https://doi.org/10.1016/j.nuclphysb.2017.04.011) [arXiv:1702.00305 [hep-ph]]. (Cited on page 31.)
- [267] A. Bacchetta, F. Delcarro, C. Pisano, M. Radici, A. Signori, *Extraction of partonic transverse momentum distributions from semi-inclusive deep-inelastic scattering, Drell-Yan and Z-boson production*, JHEP **06** (2017), 081 doi:[10.1007/JHEP06\(2017\)081](https://doi.org/10.1007/JHEP06(2017)081) [arXiv:1703.10157 [hep-ph]]. (Cited on page 31.)
- [268] M. Radici, A. Bacchetta, *First Extraction of Transversity from a Global Analysis of Electron-Proton and Proton-Proton Data*, Phys. Rev. Lett. **120** (2018) no.19, 192001 doi:[10.1103/PhysRevLett.120.192001](https://doi.org/10.1103/PhysRevLett.120.192001) [arXiv:1802.05212 [hep-ph]]. (Cited on page 31.)
- [269] M. Boglione, U. D'Alesio, C. Flore, J. Gonzalez-Hernandez, *Assessing signals of TMD physics in SIDIS azimuthal asymmetries and in the extraction of the Sivers function*, JHEP **07** (2018), 148 doi:[10.1007/JHEP07\(2018\)148](https://doi.org/10.1007/JHEP07(2018)148) [arXiv:1806.10645 [hep-ph]]. (Cited on page 31.)
- [270] M. Anselmino, M. Boglione, U. D'Alesio, F. Murgia, A. Prokudin, *Role of transverse momentum dependence of unpolarized parton distribution and fragmentation functions in the analysis of azimuthal spin asymmetries*, Phys. Rev. D **98** (2018) no.9, 094023 doi:[10.1103/PhysRevD.98.094023](https://doi.org/10.1103/PhysRevD.98.094023) [arXiv:1809.09500 [hep-ph]]. (Cited on page 31.)
- [271] M.G. Buffing, Z.B. Kang, K.Lee, X. Liu, *A transverse momentum dependent framework for back-to-back photon+jet production*, [arXiv:1812.07549 [hep-ph]]. (Cited on page 31.)
- [272] M. Boglione, A. Dotson, L. Gamberg, S. Gordon, J.O. Gonzalez-Hernandez, A. Prokudin, T.C. Rogers, N. Sato, *Mapping the Kinematical Regimes of Semi-Inclusive Deep Inelastic Scattering*, JHEP **10** (2019), 122 doi:[10.1007/JHEP10\(2019\)122](https://doi.org/10.1007/JHEP10(2019)122) [arXiv:1904.12882 [hep-ph]]. (Cited on page 31.)
- [273] V. Bertone, I. Scimemi, A. Vladimirov, *Extraction of unpolarized quark transverse momentum dependent parton distributions from Drell-Yan/Z-boson production*, JHEP **06** (2019), 028 doi:[10.1007/JHEP06\(2019\)028](https://doi.org/10.1007/JHEP06(2019)028) [arXiv:1902.08474 [hep-ph]]. (Cited on page 31.)
- [274] D. Gutierrez-Reyes, I. Scimemi, W.J. Waalewijn, L. Zoppi, *Transverse momentum dependent distributions in e^+e^- and semi-inclusive deep-inelastic scattering using jets*, JHEP **10** (2019), 031 doi:[10.1007/JHEP10\(2019\)031](https://doi.org/10.1007/JHEP10(2019)031) [arXiv:1904.04259 [hep-ph]]. (Cited on page 31.)
- [275] D. Gutierrez-Reyes, S. Leal-Gomez, I. Scimemi, A. Vladimirov, *Linearly polarized gluons at next-to-next-to leading order and the Higgs transverse momentum distribution*, JHEP **11** (2019), 121 doi:[10.1007/JHEP11\(2019\)121](https://doi.org/10.1007/JHEP11(2019)121) [arXiv:1907.03780 [hep-ph]]. (Cited on page 31.)
- [276] M.G. Echevarria, *Proper TMD factorization for quarkonia production: $pp \rightarrow \eta_{c,b}$ as a study case*, JHEP **10** (2019), 144 doi:[10.1007/JHEP10\(2019\)144](https://doi.org/10.1007/JHEP10(2019)144) [arXiv:1907.06494 [hep-ph]]. (Cited on page 31.)
- [277] B. Pasquini, S. Rodini, A. Bacchetta, *Revisiting model relations between T-odd transverse-momentum dependent parton distributions and generalized parton distributions*, Phys. Rev. D **100** (2019) no.5, 054039 doi:[10.1103/PhysRevD.100.054039](https://doi.org/10.1103/PhysRevD.100.054039) [arXiv:1907.06960 [hep-ph]]. (Cited on page 31.)
- [278] U. D'Alesio, F. Murgia, C. Pisano, P. Taels, *Azimuthal asymmetries in semi-inclusive $J/\psi +$ jet production at an EIC* Phys. Rev. D **100** (2019) no.9, 094016 doi:[10.1103/PhysRevD.100.094016](https://doi.org/10.1103/PhysRevD.100.094016) [arXiv:1908.00446 [hep-ph]]. (Cited on page 31.)
- [279] F. Scarpa, D. Boer, M.G. Echevarria, J.P. Lansberg, C. Pisano, M. Schlegel, *Studies of gluon TMDs and their evolution using quarkonium-pair production at the LHC*, Eur. Phys. J. C **80** (2020) no.2, 87 doi:[10.1140/epjc/s10052-020-7619-1](https://doi.org/10.1140/epjc/s10052-020-7619-1) [arXiv:1909.05769 [hep-ph]]. (Cited on page 31.)
- [280] U. D'Alesio, F. Murgia, C. Pisano, S. Rajesh, *Single-spin asymmetries in $p^\uparrow p \rightarrow J/\psi + X$ within a TMD approach: role of the color octet mechanism*, Eur. Phys. J. C **79** (2019) no.12, 1029 doi:[10.1140/epjc/s10052-019-7551-4](https://doi.org/10.1140/epjc/s10052-019-7551-4) [arXiv:1910.09640 [hep-ph]]. (Cited on page 31.)
- [281] S. Fleming, Y. Makris, T. Mehen, *An effective field theory approach to quarkonium at small transverse momentum*,

- JHEP **04** (2020), 122 doi:[10.1007/JHEP04\(2020\)122](https://doi.org/10.1007/JHEP04(2020)122) [arXiv:1910.03586 [hep-ph]]. (Cited on page 31.)
- [282] I. Scimemi, A. Vladimirov, *Non-perturbative structure of semi-inclusive deep-inelastic and Drell-Yan scattering at small transverse momentum*, JHEP **06** (2020), 137 doi:[10.1007/JHEP06\(2020\)137](https://doi.org/10.1007/JHEP06(2020)137) [arXiv:1912.06532 [hep-ph]]. (Cited on page 31.)
- [283] A. Bacchetta, V. Bertone, C. Bissolotti, G. Bozzi, F. Delcarro, F. Piacenza, M. Radici, *Transverse-momentum-dependent parton distributions up to N^3LL from Drell-Yan data*, JHEP **07** (2020), 117 doi:[10.1007/JHEP07\(2020\)117](https://doi.org/10.1007/JHEP07(2020)117) [arXiv:1912.07550 [hep-ph]]. (Cited on page 31.)
- [284] X. Luo, H. Sun, *Transverse single spin asymmetry $A_{UT}^{\sin(\phi_h - \phi_S)}$ for single hadron production in SIDIS*, Phys. Rev. D **101** (2020) no.7, 074016 doi:[10.1103/PhysRevD.101.074016](https://doi.org/10.1103/PhysRevD.101.074016) [arXiv:2004.03764 [hep-ph]]. (Cited on page 31.)
- [285] D. Boer, U. D'Alesio, F. Murgia, C. Pisano, P. Taels, *J/ψ meson production in SIDIS: matching high and low transverse momentum*, [arXiv:2004.06740 [hep-ph]]. (Cited on page 31.)
- [286] A. Bacchetta, F. Delcarro, C. Pisano, M. Radici, *The three-dimensional distribution of quarks in momentum space*, [arXiv:2004.14278 [hep-ph]]. (Cited on page 31.)
- [287] S. Bastami, L. Gamberg, B. Parsamyan, B. Pasquini, A. Prokudin, P. Schweitzer, *The Drell-Yan process with pions and polarized nucleons*, [arXiv:2005.14322 [hep-ph]]. (Cited on page 31.)
- [288] R.D. Ball, S. Forte, *Summation of leading logarithms at small x* , Phys. Lett. B **351** (1995) 313 doi:[10.1016/0370-2693\(95\)00395-2](https://doi.org/10.1016/0370-2693(95)00395-2) [hep-ph/9501231]. (Cited on page 31.)
- [289] R.D. Ball, S. Forte, *Asymptotically free partons at high-energy*, Phys. Lett. B **405** (1997) 317 doi:[10.1016/S0370-2693\(97\)00625-4](https://doi.org/10.1016/S0370-2693(97)00625-4) [hep-ph/9703417]. (Cited on page 31.)
- [290] G. Altarelli, R.D. Ball, S. Forte, *Factorization and resummation of small x scaling violations with running coupling*, Nucl. Phys. B **621** (2002) 359 doi:[10.1016/S0550-3213\(01\)00563-6](https://doi.org/10.1016/S0550-3213(01)00563-6) [hep-ph/0109178]. (Cited on page 31.)
- [291] G. Altarelli, R.D. Ball, S. Forte, *An Anomalous dimension for small x evolution*, Nucl. Phys. B **674** (2003) 459 doi:[10.1016/j.nuclphysb.2003.09.040](https://doi.org/10.1016/j.nuclphysb.2003.09.040) [hep-ph/0306156]. (Cited on page 31.)
- [292] G. Altarelli, R.D. Ball, S. Forte, *Perturbatively stable resummed small x evolution kernels*, Nucl. Phys. B **742** (2006) 1 doi:[10.1016/j.nuclphysb.2006.01.046](https://doi.org/10.1016/j.nuclphysb.2006.01.046) [hep-ph/0512237]. (Cited on page 31.)
- [293] G. Altarelli, R.D. Ball, S. Forte, *Small x Resummation with Quarks: Deep-Inelastic Scattering*, Nucl. Phys. B **799** (2008) 199 doi:[10.1016/j.nuclphysb.2008.03.003](https://doi.org/10.1016/j.nuclphysb.2008.03.003) [arXiv:0802.0032 [hep-ph]]. (Cited on page 31.)
- [294] C. White, R. Thorne, *A Global Fit to Scattering Data with NLL BFKL Resummations*, Phys. Rev. D **75** (2007), 034005 doi:[10.1103/PhysRevD.75.034005](https://doi.org/10.1103/PhysRevD.75.034005) [arXiv:hep-ph/0611204 [hep-ph]]. (Cited on page 31.)
- [295] H. Abdolmaleki *et al.* [xFitter Developers' Team], *Impact of low- x resummation on QCD analysis of HERA data*, Eur. Phys. J. C **78** (2018) no.8, 621 doi:[10.1140/epjc/s10052-018-6090-8](https://doi.org/10.1140/epjc/s10052-018-6090-8) [arXiv:1802.00064 [hep-ph]]. (Cited on page 32.)
- [296] M. Bonvini, F. Giulini, *A new simple PDF parametrization: improved description of the HERA data*, Eur. Phys. J. Plus **134** (2019) no.10, 531 doi:[10.1140/epjp/i2019-12872-x](https://doi.org/10.1140/epjp/i2019-12872-x) [arXiv:1902.11125 [hep-ph]]. (Cited on page 32.)
- [297] M. Bonvini, S. Marzani, T. Peraro, *Small- x resummation from HELL*, Eur. Phys. J. C **76** (2016) no.11, 597 doi:[10.1140/epjc/s10052-016-4445-6](https://doi.org/10.1140/epjc/s10052-016-4445-6) [arXiv:1607.02153 [hep-ph]]. (Cited on page 32.)
- [298] M. Bonvini, S. Marzani, C. Muselli, *Towards parton distribution functions with small- x resummation: HELL 2.0*, JHEP **1712** (2017) 117 doi:[10.1007/JHEP12\(2017\)117](https://doi.org/10.1007/JHEP12(2017)117) [arXiv:1708.07510 [hep-ph]]. (Cited on page 32.)
- [299] V. Bertone, S. Carrazza, J. Rojo, *APFEL: A PDF Evolution Library with QED corrections*, Comput. Phys. Commun. **185** (2014) 1647 doi:[10.1016/j.cpc.2014.03.007](https://doi.org/10.1016/j.cpc.2014.03.007) [arXiv:1310.1394 [hep-ph]]. (Cited on page 32.)
- [300] S. Carrazza, A. Ferrara, D. Palazzo, J. Rojo, *APFEL Web : a web-based application for the graphical visualization of parton distribution functions*, J. Phys. G **42** (2015) no.5, 057001 doi:[10.1088/0954-3899/42/5/057001](https://doi.org/10.1088/0954-3899/42/5/057001) [arXiv:1410.5456 [hep-ph]]. (Cited on page 32.)
- [301] V. Bertone, *APFEL++: A new PDF evolution library in C++*, PoS DIS **2017** (2018) 201 doi:[10.22323/1.297.0201](https://doi.org/10.22323/1.297.0201) [arXiv:1708.00911 [hep-ph]]. (Cited on page 32.)
- [302] M. Ciafaloni, *Coherence Effects in Initial Jets at Small q^{**2} / s* , Nucl. Phys. B **296** (1988) 49. doi:[10.1016/0550-3213\(88\)90380-X](https://doi.org/10.1016/0550-3213(88)90380-X) (Cited on page 32.)
- [303] S. Catani, F. Fiorani, G. Marchesini, *Small x Behavior of Initial State Radiation in Perturbative QCD*, Nucl. Phys. B **336** (1990) 18. doi:[10.1016/0550-3213\(90\)90342-B](https://doi.org/10.1016/0550-3213(90)90342-B) (Cited on page 32.)
- [304] S. Catani, F. Fiorani, G. Marchesini, *QCD Coherence in Initial State Radiation*, Phys. Lett. B **234** (1990) 339. doi:[10.1016/0370-2693\(90\)91938-8](https://doi.org/10.1016/0370-2693(90)91938-8) (Cited on page 32.)
- [305] G. Marchesini, *QCD coherence in the structure function and associated distributions at small x* , Nucl. Phys. B **445** (1995) 49 doi:[10.1016/0550-3213\(95\)00149-M](https://doi.org/10.1016/0550-3213(95)00149-M) [hep-ph/9412327]. (Cited on page 32.)
- [306] J.R. Forshaw, A. Sabio Vera, *QCD coherence and jet rates in small x deep inelastic scattering*, Phys. Lett. B **440** (1998) 141 doi:[10.1016/S0370-2693\(98\)01090-9](https://doi.org/10.1016/S0370-2693(98)01090-9) [hep-ph/9806394]. (Cited on page 32.)

- [307] B.R. Webber, *Jet rates in deep inelastic scattering at small x* , Phys. Lett. B **444** (1998) 81 doi:[10.1016/S0370-2693\(98\)01349-5](https://doi.org/10.1016/S0370-2693(98)01349-5) [hep-ph/9810286]. (Cited on page 32.)
- [308] G.P. Salam, *Soft emissions and the equivalence of BFKL and CCFM final states*, JHEP **9903** (1999) 009 doi:[10.1088/1126-6708/1999/03/009](https://doi.org/10.1088/1126-6708/1999/03/009) [hep-ph/9902324]. (Cited on page 32.)
- [309] J. Kwieciński, *Unintegrated gluon distributions from the transverse coordinate representation of the CCFM equation in the single loop approximation*, Acta Phys. Polon. B **33** (2002) 1809 [hep-ph/0203172]. (Cited on page 32.)
- [310] K. Kutak, K.J. Golec-Biernat, S. Jadach, M. Skrzypek, *Nonlinear equation for coherent gluon emission*, JHEP **1202** (2012) 117 doi:[10.1007/JHEP02\(2012\)117](https://doi.org/10.1007/JHEP02(2012)117) [arXiv:1111.6928 [hep-ph]]. (Cited on page 32.)
- [311] K.J. Golec-Biernat, T. Stebel, *Drell-Yan production with the CCFM-K evolution*, arXiv:1911.10103 [hep-ph]. (Cited on page 32.)
- [312] R. Bonciani, S. Catani, M.L. Mangano, P. Nason, *Sudakov resummation of multiparton QCD cross-sections*, Phys. Lett. B **575** (2003) 268 doi:[10.1016/j.physletb.2003.09.068](https://doi.org/10.1016/j.physletb.2003.09.068) [hep-ph/0307035]. (Cited on page 32.)
- [313] D. de Florian, A. Kulesza, W. Vogelsang, *Threshold resummation for high-transverse-momentum Higgs production at the LHC*, JHEP **0602** (2006) 047 doi:[10.1088/1126-6708/2006/02/047](https://doi.org/10.1088/1126-6708/2006/02/047) [hep-ph/0511205]. (Cited on page 32.)
- [314] C. Muselli, S. Forte, G. Ridolfi, *Combined threshold and transverse momentum resummation for inclusive observables*, JHEP **1703** (2017) 106 doi:[10.1007/JHEP03\(2017\)106](https://doi.org/10.1007/JHEP03(2017)106) [arXiv:1701.01464 [hep-ph]]. (Cited on page 32.)
- [315] Y.L. Dokshitzer, D. Diakonov, S.I. Troian, *On the Transverse Momentum Distribution of Massive Lepton Pairs*, Phys. Lett. **79B** (1978) 269. doi:[10.1016/0370-2693\(78\)90240-X](https://doi.org/10.1016/0370-2693(78)90240-X) (Cited on page 32.)
- [316] Y.L. Dokshitzer, D. Diakonov, S.I. Troian, *Hard Processes in Quantum Chromodynamics*, Phys. Rept. **58** (1980) 269. doi:[10.1016/0370-1573\(80\)90043-5](https://doi.org/10.1016/0370-1573(80)90043-5) (Cited on page 32.)
- [317] G. Parisi, R. Petronzio, *Small Transverse Momentum Distributions in Hard Processes* Nucl. Phys. B **154** (1979) 427. doi:[10.1016/0550-3213\(79\)90040-3](https://doi.org/10.1016/0550-3213(79)90040-3) (Cited on page 32.)
- [318] G. Curci, M. Greco, Y. Srivastava, *QCD Jets From Coherent States*, Nucl. Phys. B **159** (1979) 451. doi:[10.1016/0550-3213\(79\)90345-6](https://doi.org/10.1016/0550-3213(79)90345-6) (Cited on page 32.)
- [319] J.C. Collins, D.E. Soper, *Back-To-Back Jets in QCD*, Nucl. Phys. B **193** (1981) 381 Erratum: [Nucl. Phys. B **213** (1983) 545]. doi:[10.1016/0550-3213\(81\)90339-4](https://doi.org/10.1016/0550-3213(81)90339-4) (Cited on page 32.)
- [320] J.C. Collins, D.E. Soper, *Back-To-Back Jets: Fourier Transform from B to K-Transverse*, Nucl. Phys. B **197** (1982) 446. doi:[10.1016/0550-3213\(82\)90453-9](https://doi.org/10.1016/0550-3213(82)90453-9) (Cited on page 32.)
- [321] J.C. Collins, D.E. Soper, G.F. Sterman, *Transverse Momentum Distribution in Drell-Yan Pair and W and Z Boson Production*, Nucl. Phys. B **250** (1985) 199. doi:[10.1016/0550-3213\(85\)90479-1](https://doi.org/10.1016/0550-3213(85)90479-1) (Cited on page 32.)
- [322] J. Kodaira, L. Trentadue, *Summing Soft Emission in QCD*, Phys. Lett. **112B** (1982) 66. doi:[10.1016/0370-2693\(82\)90907-8](https://doi.org/10.1016/0370-2693(82)90907-8) (Cited on page 32.)
- [323] J. Kodaira, L. Trentadue, *Soft Gluon Effects In Perturbative Quantum Chromodynamics*. (Cited on page 32.)
- [324] J. Kodaira, L. Trentadue, *Single Logarithm Effects in electron-Positron Annihilation*, Phys. Lett. **123B** (1983) 335. doi:[10.1016/0370-2693\(83\)91213-3](https://doi.org/10.1016/0370-2693(83)91213-3) (Cited on page 32.)
- [325] S. Catani, D. de Florian, M. Grazzini, *Universality of nonleading logarithmic contributions in transverse momentum distributions*, Nucl. Phys. B **596** (2001) 299 doi:[10.1016/S0550-3213\(00\)00617-9](https://doi.org/10.1016/S0550-3213(00)00617-9) [hep-ph/0008184]. (Cited on page 32.)
- [326] G. Bozzi, S. Catani, D. de Florian, M. Grazzini, *Transverse-momentum resummation and the spectrum of the Higgs boson at the LHC*, Nucl. Phys. B **737** (2006) 73 doi:[10.1016/j.nuclphysb.2005.12.022](https://doi.org/10.1016/j.nuclphysb.2005.12.022) [hep-ph/0508068]. (Cited on page 32.)
- [327] G. Bozzi, S. Catani, G. Ferrera, D. de Florian, M. Grazzini, *Transverse-momentum resummation: A Perturbative study of Z production at the Tevatron*, Nucl. Phys. B **815** (2009) 174 doi:[10.1016/j.nuclphysb.2009.02.014](https://doi.org/10.1016/j.nuclphysb.2009.02.014) [arXiv:0812.2862 [hep-ph]]. (Cited on page 32.)
- [328] S. Catani, M. Grazzini, *QCD transverse-momentum resummation in gluon fusion processes*, Nucl. Phys. B **845** (2011) 297 doi:[10.1016/j.nuclphysb.2010.12.007](https://doi.org/10.1016/j.nuclphysb.2010.12.007) [arXiv:1011.3918 [hep-ph]]. (Cited on page 32.)
- [329] S. Catani, M. Grazzini, *Higgs Boson Production at Hadron Colliders: Hard-Collinear Coefficients at the NNLO*, Eur. Phys. J. C **72** (2012) 2013 Erratum: [Eur. Phys. J. C **72** (2012) 2132] doi:[10.1140/epjc/s10052-012-2013-2](https://doi.org/10.1140/epjc/s10052-012-2013-2), doi:[10.1140/epjc/s10052-012-2132-9](https://doi.org/10.1140/epjc/s10052-012-2132-9) [arXiv:1106.4652 [hep-ph]]. (Cited on page 32.)
- [330] S. Catani, L. Cieri, D. de Florian, G. Ferrera, M. Grazzini, *Universality of transverse-momentum resummation and hard factors at the NNLO*, Nucl. Phys. B **881** (2014) 414 doi:[10.1016/j.nuclphysb.2014.02.011](https://doi.org/10.1016/j.nuclphysb.2014.02.011) [arXiv:1311.1654 [hep-ph]]. (Cited on page 32.)
- [331] S. Catani, D. de Florian, G. Ferrera, M. Grazzini, *Vector boson production at hadron colliders: transverse-momentum resummation and leptonic decay*, JHEP **1512** (2015) 047 doi:[10.1007/JHEP12\(2015\)047](https://doi.org/10.1007/JHEP12(2015)047) [arXiv:1507.06937 [hep-ph]]. (Cited on page 32.)

- [332] A.H. Mueller, B.W. Xiao, F. Yuan, *Sudakov Resummation in Small- x Saturation Formalism*, Phys. Rev. Lett. **110** (2013) no.8, 082301 doi:[10.1103/PhysRevLett.110.082301](https://doi.org/10.1103/PhysRevLett.110.082301) [arXiv:1210.5792 [hep-ph]]. (Cited on page 32.)
- [333] A.H. Mueller, B. W. Xiao, F. Yuan, *Sudakov double logarithms resummation in hard processes in the small- x saturation formalism*, Phys. Rev. D **88** (2013) no.11, 114010 doi:[10.1103/PhysRevD.88.114010](https://doi.org/10.1103/PhysRevD.88.114010) [arXiv:1308.2993 [hep-ph]]. (Cited on page 32.)
- [334] I. Balitsky, A. Tarasov, *Rapidity evolution of gluon TMD from low to moderate x* , JHEP **1510** (2015) 017 doi:[10.1007/JHEP10\(2015\)017](https://doi.org/10.1007/JHEP10(2015)017) [arXiv:1505.02151 [hep-ph]]. (Cited on page 32.)
- [335] S. Marzani, *Combining Q_T and small- x resummations*, Phys. Rev. D **93** (2016) no.5, 054047 doi:[10.1103/PhysRevD.93.054047](https://doi.org/10.1103/PhysRevD.93.054047) [arXiv:1511.06039 [hep-ph]]. (Cited on page 32.)
- [336] A.H. Mueller, L. Szymanowski, S. Wallon, B.W. Xiao, F. Yuan, *Sudakov Resummations in Mueller-Navelet Dijet Production*, JHEP **1603** (2016) 096 doi:[10.1007/JHEP03\(2016\)096](https://doi.org/10.1007/JHEP03(2016)096) [arXiv:1512.07127 [hep-ph]]. (Cited on page 32.)
- [337] B.W. Xiao, F. Yuan, *BFKL and Sudakov Resummation in Higgs Boson Plus Jet Production with Large Rapidity Separation*, Phys. Lett. B **782** (2018) 28 doi:[10.1016/j.physletb.2018.04.070](https://doi.org/10.1016/j.physletb.2018.04.070) [arXiv:1801.05478 [hep-ph]]. (Cited on page 32.)
- [338] A. Arbuzov, A. Bacchetta, M. Butenschoen, F.G. Celiberto, U. D'Alesio, M. Deka, I. Denisenko, M.G. Echevarria, A. Efremov, N.Y. Ivanov, et al. *On the physics potential to study the gluon content of proton and deuteron at NICA SPD*, Prog. Part. Nucl. Phys. **119** (2021), 103858 doi:[10.1016/j.ppnp.2021.103858](https://doi.org/10.1016/j.ppnp.2021.103858) [arXiv:2011.15005 [hep-ex]]. (Cited on page 32.)
- [339] E. Chapon, D. d'Enterria, B. Ducloue, M.G. Echevarria, P.B. Gossiaux, V. Kartvelishvili, T. Kasemets, J.P. Lansberg, R. McNulty, D.D. Price, et al. *Prospects for quarkonium studies at the high-luminosity LHC*, Prog. Part. Nucl. Phys., in press doi:[10.1016/j.ppnp.2021.103906](https://doi.org/10.1016/j.ppnp.2021.103906) [arXiv:2012.14161 [hep-ph]]. (Cited on page 32.)
- [340] R. Abdul Khalek, A. Accardi, J. Adam, D. Adamiak, W. Akers, M. Albaladejo, A. Al-bataineh, M.G. Alexeev, F. Ameli, P. Antonioli, et al. *Science Requirements and Detector Concepts for the Electron-Ion Collider: EIC Yellow Report*, [arXiv:2103.05419 [physics.ins-det]]. (Cited on page 32.)
- [341] D. Binosi, J. Collins, C. Kaufhold, L. Theussl, *JaxoDraw: A Graphical user interface for drawing Feynman diagrams. Version 2.0 release notes*, Comput. Phys. Commun. **180** (2009), 1709-1715 doi:[10.1016/j.cpc.2009.02.020](https://doi.org/10.1016/j.cpc.2009.02.020) [arXiv:0811.4113 [hep-ph]]. (Cited on page 32.)